COMSAT

Technical Review

Volume 18 Number 1, Spring 1988

COMSAT TECHNICAL REVIEW is published twice a year by Communications Satellite Corporation (COMSAT). Subscriptions, which include the two issues published within a calendar year, are: one year, $15 U.S.; two years, $25; three years, $35; single copies, $10; article reprints, $2.50. Overseas air mail delivery is available at an additional cost of $18 per year. Make checks payable to COMSAT and address to Records Department, Communications Satellite Corporation, 22300 Comsat Drive, Clarksburg, MD 20871-9475, U.S.A.

ISSN 0095-9669

COMSAT TECHNICAL REVIEW

Volume 18 Number 1, Spring 1988

1 ION-IMPLANTED HYPERABRUPT VARACTOR DIODES FOR GaAs MMICs 330
P. J. McNally AND **B. B. Cregger**

21 SIMULATION OF A RANDOM-ACCESS-WITH-NOTIFICATION PROTOCOL FOR VSAT APPLICATIONS **L. C. Palmer** AND **P. Y. Chang** 331

CTR NOTES

55 DEPENDENCE OF MEAN OPINION SCORES ON DIFFERENCES IN LINGUAL INTERPRETATION **H. G. Suyderhoud** 332

65 GEOSTATIONARY SATELLITE LOG FOR YEAR END 1987 333
C. H. Schmitt

135 TRANSLATIONS OF ABSTRACTS
FRENCH 135 SPANISH 137

139 AUTHOR INDEX, CTR 1987

141 INDEX OF 1987 PUBLICATIONS BY COMSAT AUTHORS

Index: solid-state devices, oscillators, integrated circuits, diodes, ion implantation

Ion-implanted hyperabrupt varactor diodes for GaAs MMICs

P. J. McNally and B. B. Cregger

(Manuscript received November 12, 1987)

Abstract

The design, fabrication, and characterization of monolithically compatible varactor GaAs diodes are described. An all ion-implantation process was used to fabricate hyperabrupt varactor diodes with large (>10:1) tuning ratios, and high-energy (4- and 6-MeV) implantation was employed to form a buried n^+ layer below the active portion of the device. Additional implantations were performed to provide surface contact to the buried layer and to form the hyperabrupt capacitor profile. Nearly ideal Schottky barriers with an integral high-resistivity guard ring for depletion of the hyperabrupt profile were fabricated. These barriers show an ideality factor of 1.0, low reverse leakage current, and high reverse avalanche breakdown voltage (>30 V). The varactor diodes were characterized at frequencies between 2 and 10 GHz. Data on measured performance in this frequency range, and correlation with the device structure, are presented, and details of the device design, ion-implantation experimental data, and diode electrical characterization are discussed.

Introduction

This paper describes the design, fabrication, and RF characterization of a fully ion-implanted hyperabrupt varactor diode monolithically compatible with GaAs monolithic microwave integrated circuits (MMICs). This diode exhibits a capacitance-voltage (C-V) characteristic given by $C \propto V^{-n}$, with $n > 0.5$.

The design is a planar structure containing a buried n^+ layer produced by MeV ion implantation, and a Schottky barrier with an integral high-resistivity guard ring that exhibits low leakage and high avalanche breakdown voltage characteristics. The planar configuration is realized by an n^- implanted region extending from the chip surface to the buried layer, and an ion-implanted hyperabrupt carrier profile which exhibits capacitance tuning ratios (C_o/C_{min}) of 10:1 over the usable voltage range. The high-resistivity ($>10^7$ Ω-cm) starting substrate provides the necessary isolation between the active regions of the device.

The device fabrication process demonstrates compatibility with MMIC manufacturing technology. RF characterization at 10 GHz shows that this device is attractive for insertion into monolithic GaAs circuits such as voltage-controlled oscillators (VCOs). An improved design in which geometry and doping levels are optimized is discussed in detail. Calculated performance characteristics for the device, including capacitance-voltage, series resistance, and quality factor (Q), are also presented.

Varactor diode design considerations

Hyperabrupt varactor diodes are characterized by a rapid decrease in depletion layer capacitance with applied reverse voltage. This C-V relationship arises from the non-uniform distribution of charge carriers at the junction, or at the potential barrier depletion layer edge. Desirable non-uniform carrier distributions can be produced by an ion-implanted Gaussian dopant profile or by a retrograded (exponential) epitaxial layer profile. Both types of dopant profiles have features which yield specific varactor characteristics, in particular, the rate of change of capacitance with voltage, or the γ-value in the equation

$$C = K(V + V_o)^{-\gamma} \tag{1}$$

where K and V_o are constants and V is the applied reverse voltage. A fully ion-implanted structure is the most compatible for integration of a hyperabrupt varactor diode in a GaAs MMIC circuit.

Figure 1 shows a planar varactor diode structure fabricated using ion implantation for all active layer doping processes. Conventional photolithography was employed to define selected areas of the wafer for implantation doping. Important elements of the structure are the n^+ buried layer, the n^+ region connecting the chip surface to the buried layer, the hyperabrupt carrier profile for the capacitor, the Schottky barrier (to vary the capacitance with voltage), and the ohmic contact metalization.

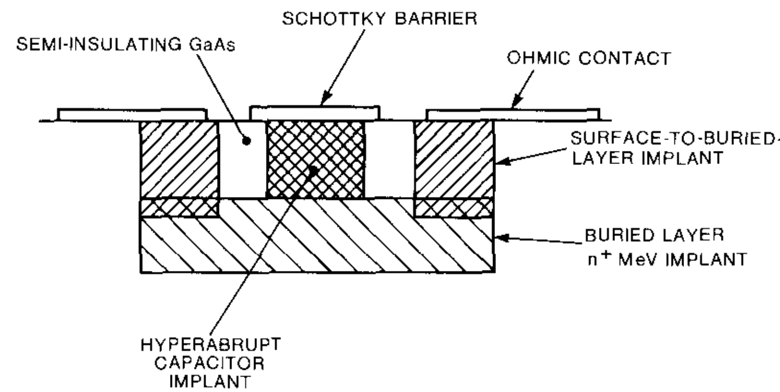

Figure 1. *Cross Section of an Ion-Implanted Hyperabrupt Varactor Diode With a Buried n⁺ Layer for GaAs MMIC*

The figure displays a cross section of a circular device. Recent work on buried-layer n^+ formation by ion implantation has made it possible to implement this structure in a monolithic configuration compatible with other circuit elements. It can be seen that, with the buried n^+ layer in place, the device fabrication requirements are similar to those for implanted GaAs field-effect transistors (FETs) and MMICs. Work by Thompson and Dietrich [1] has shown that the range-energy relationship from n-type dopants in GaAs can be extended into the MeV energy region, and that carrier profiles can be predicted for device design requirements.

The n^+ buried layer in the varactor design provides a high-conductivity layer for minimum device series resistance, and a controlled carrier profile shape between the GaAs surface and the peak of the implanted carrier distribution for minimum capacitance at maximum applied voltage. Figure 2 shows carrier profiles for both the n^+ buried layer (curves labeled 4 MeV and 6 MeV) and the hyperabrupt capacitor. The profiles were constructed assuming Gaussian distributions according to the equation

$$N(x) = N_o \exp\left[\frac{-(X - R_p)^2}{2\sigma^2}\right] \tag{2}$$

where N_o = peak doping concentration

R_p = projected range of implanted ions

σ = standard deviation in the projected range, including the diffusion term $2Dt$, with $D = 1.4 \times 10^{-14}$ cm^{2}s^{-1} and $t = 1{,}200$ s.

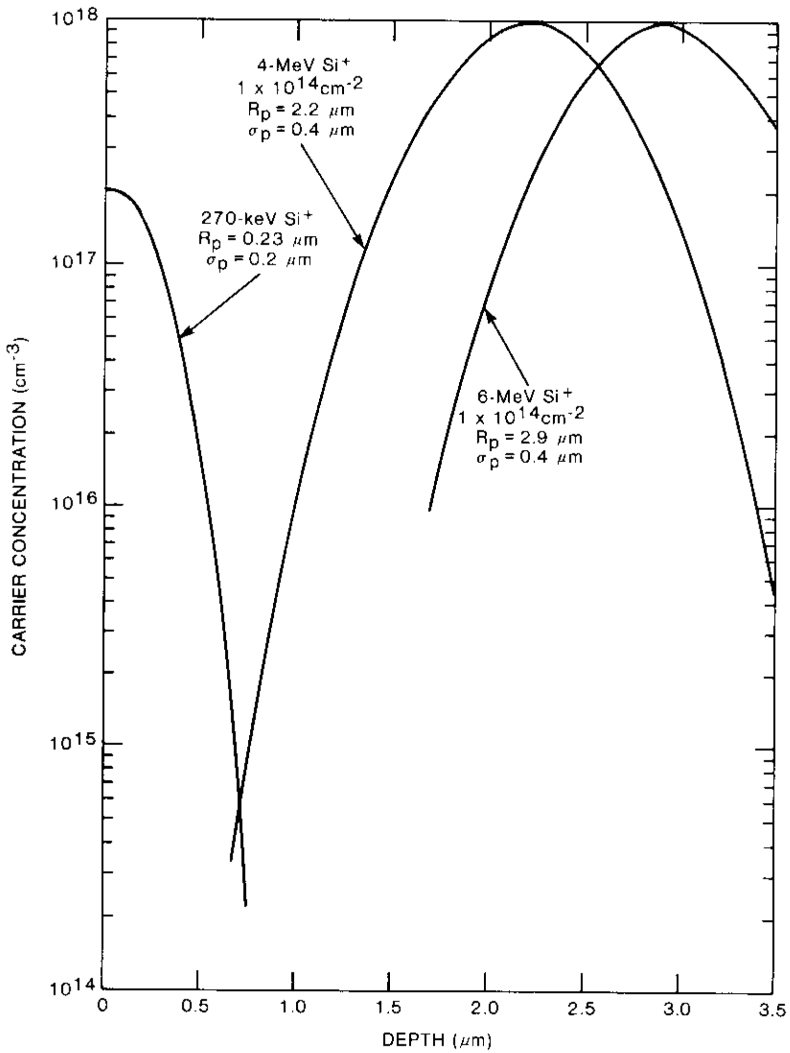

Figure 2. *Theoretical Carrier Profiles of an Ion-Implanted MeV n^+ Buried Layer and a Hyperabrupt Capacitor Profile With Recess Etching*

The 4-MeV, 6-MeV, and 270-keV (capacitor implant energy) R_p and σ values are listed in the figure. The profiles for 4 MeV and 270 keV intersect at about 0.75 µm, thus determining the approximate minimum capacitance (C_{min}) when the capacitor profile is depleted to that depth. The space charge layer will penetrate the n^+ buried region when the avalanche breakdown is greater than the voltage required to fully deplete the capacitor profile, with a corresponding decrease in C_{min}, but at a slower rate of change with applied voltage.

The maximum tuning ratio, C_o/C_{min}, is achieved with a varactor impurity profile that can be fully depleted at a voltage slightly less than the avalanche breakdown voltage, V_{BR}. Since the tuning ratio is directly related to the ratio of the depletion layer widths at zero bias and maximum applied reverse voltage, a peak doping concentration which minimizes the zero bias depletion layer width is desirable. In addition, the carrier concentration at the edge of the n^+ buried layer should be minimal. With an optimized carrier concentration profile, the resistive contribution to the total device series resistance will be minimized, the tuning ratio will be maximized, and the voltage swing will be within the avalanche breakdown voltage constraint.

Device modeling was used to predict the C-V relationship, reverse breakdown voltage, series resistance, carrier profile, and quality factor (Q). The modeling includes equation (1) for the carrier profiles, Poisson's equation

$$\frac{d^2\psi}{dx^2} = -\frac{\rho(x)}{K\epsilon_0} \qquad (3)$$

for calculating the electric field and potential variation with depletion layer depth, and

$$C = (K\epsilon_0 A)/W \qquad (4)$$

where
K = dielectric constant
ϵ_0 = permittivity
A = diode area
W = depletion layer width

which yields capacitance as a function of depletion layer depth. Determination of the lateral resistance contributions to the total device resistance based on the buried n^+ layer and geometry of the hyperabrupt diode follows the methods described by Calviello, Wallace, and Bie [2].

Device fabrication

Undoped liquid-encapsulated Czochralski (LEC) GaAs wafers were prepared and implanted with 4- and 6-MeV Si^+ ions at a dose of 1×10^{14} cm^{-2}. Wafers with 1375J photoresist masking, and others without masking, were processed through the buried-layer implantation step. All wafers yielded a buried n^+ layer in the region shown in Figure 1. The wafers were then masked with 1350J photoresist and implanted with 300- and 100-keV Si^+ ions at doses of 3.3×10^{13} cm^{-2} and 2.3×10^{13} cm^{-2}, respectively, for surface connection to the buried layer. An additional photolithography step was then used to selectively implant the hyperabrupt capacitor profile. The implant schedule of energy and dose were varied for different wafers in order to determine an optimum carrier profile. Device data were obtained on two profile types consisting of a single implant energy of 270 keV and a multiple implant of three energies (100, 200, and 270 keV). Dose levels for both types were selected to achieve a peak doping concentration in the 2.5×10^{17} cm^{-3} range.

After the varactor profile was implanted, the wafers were cleaned and capped with 1,000-Å Si_3N_4 in a plasma-enhanced chemical vapor deposition (PECVD) nitride system. Post-implant annealing was done in an 850°C furnace for 30 minutes in a forming gas atmosphere. Through subsequent photolithographic steps, the nitride was left on the wafer for dielectric-assisted lift-off of ohmic and Schottky barrier metalizations. After each photolithography step, the Si_3N_4 was plasma-etched to expose the GaAs surface. Ohmic contacts consisting of Au-Ge-Ni-Ag-Au were deposited by e-beam evaporation and alloyed in a heat-pulse rapid thermal alloy system at 540°C for 3 seconds. Schottky barrier metalization of either Cr/Au or Ti-Pt-Au was deposited immediately following recess etching of the GaAs in order to establish the doping concentration at the Schottky barrier interface. After Schottky metal lift-off, the wafers were cleaned and probed for electrical characterization.

Wafer characterization

Electrical characterization of device wafers consisted of measuring carrier profiles, the Schottky barrier current-voltage (I-V) relationship, and capacitance-voltage to obtain the tuning ratio.

Carrier profiles

Capacitance-voltage measurements for carrier profiling of doped layers in GaAs are an integral part of wafer characterization. Both Polaron and Hewlett-Packard (HP)-based automated systems are used to determine impurity profiles in ion-implanted material. A monitor wafer was used for Polaron profiling of the low-energy n and n^+ implants, since the device wafers were processed by selective implantation of the doped regions.

Figure 3 is a Polaron profile of the 100/300-keV implant used to extend the buried n^+ layer to the surface. A constant 1×10^{18} cm^{-3} carrier concentration extends from the wafer surface to about 0.4-μm deep, with a tail extending to greater than 0.8 μm. This depth is sufficient to contact the buried-layer 4-MeV implant profile shown in Figure 2. Diode I-V measurements confirm that the surface implant is connected to the buried layer. A contactless conductivity instrument was used to measure the sheet resistance of both the surface implant and the buried layer; values of 50 and 25 Ω/□, respectively, were obtained.

The carrier concentration profiles of the MeV implants were determined from C-V measurements made on a deeply recessed diode with a metal Schottky barrier. An approximate value was obtained for the carrier concentration in the tail region of the hyperabrupt profile. The profile (Figure 4) indicates a concentration of about 3×10^{15} cm^{-3} at the beginning of the 4-MeV buried layer. The profile appears deeper than predicted, which could

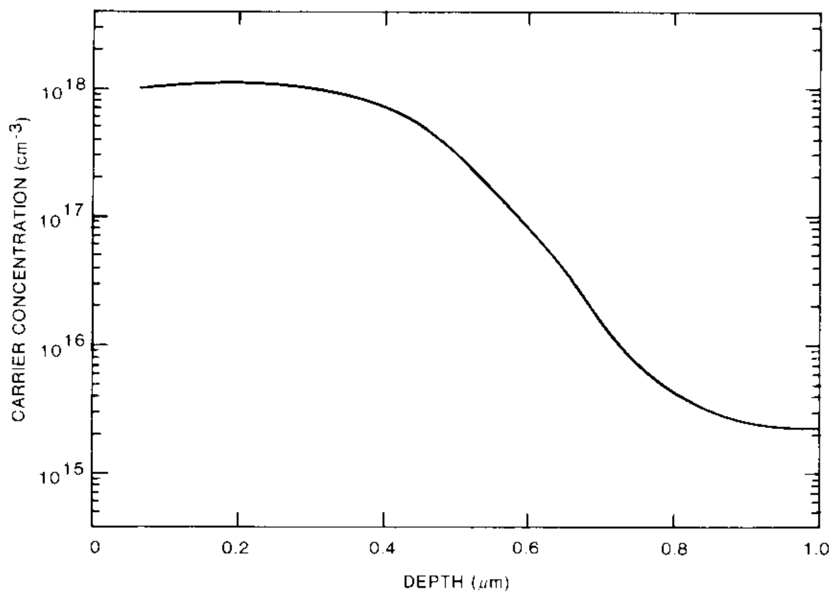

Figure 3. *Polaron Profile of Carrier Concentration vs Depth for the Surface-to-Buried-Layer Implant*

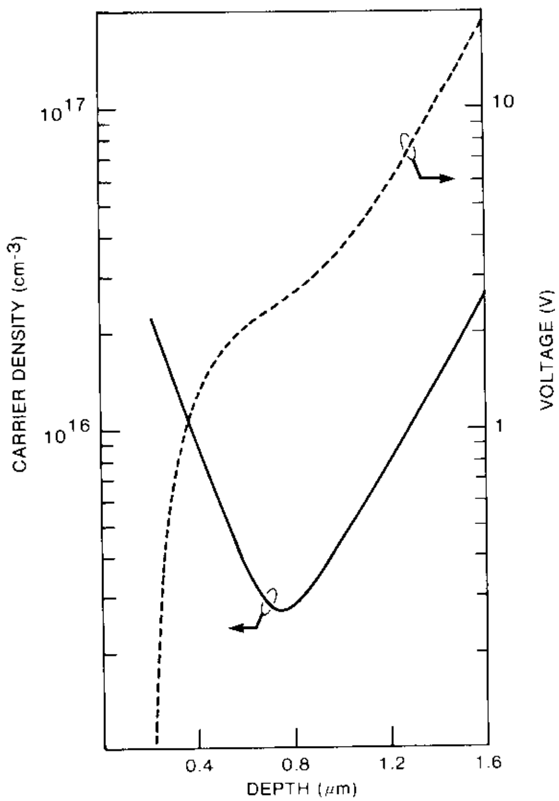

Figure 4. *Carrier Concentration vs Depth Showing the Merging of the Hyperabrupt Capacitor and Buried-Layer Profiles*

be due to the diode area used and the presence of the tail region of the hyperabrupt capacitor profile. Examination of the equation

$$N(x) = \frac{C^3}{q\epsilon A^2(-dC/dV)} \tag{5}$$

where $N(x)$ = carrier concentration *vs* depth
C = junction capacitor
A = junction area
ϵ = GaAs permittivity
q = electronic charge
V = voltage,

which is used to determine carrier concentration *vs* depth, shows that small errors in C/A and dC/dV can cause significant distortion in the $N(x)$ curve. The actual value of the minimum carrier concentration is probably different from that shown; however, the figure shows the desired profile qualitatively. More precise measurements of the MeV profiles are currently being performed.

Schottky barrier characteristics

The diode design approach, which involves extending the Schottky barrier metal over the semi-insulating GaAs (as shown in Figure 1), results in maximum avalanche breakdown voltage and minimum reverse leakage current. A large effective radius of junction curvature exists in this structure. It is well known [3] that junction radius is an important design consideration for planar diode avalanche breakdown. Schottky barrier breakdown voltage and leakage current depend on carrier concentration, with leakage current being sensitive to the metal-semiconductor interface properties. High-breakdown, low-leakage junctions are especially important in varactor diodes because of the high electric fields generated to achieve large tuning ratios. For the diode structure presented here, the peak carrier concentration, breakdown voltage, and tuning ratio can be optimized with less concern for premature edge breakdown.

Figure 5 shows the I-V characteristics measured on these hyperabrupt diodes. Figures 5a and 5b are plots of log I *vs* V for forward and reverse voltage, respectively. The forward I-V plot shows that the diode conforms to the Schottky equation

$$I = A^{**}T^2 \exp(-q\phi_b/kT)\,[\exp(qV/nkT) - 1] \tag{6}$$

where A^{**} = Richardson's constant
T = diode temperature
ϕ_b = Schottky barrier height
V = applied voltage
k = Boltzmann's constant
n = diode ideality factor.

The value of n is seen to be 1.0 over seven decades of forward current, and a barrier height of approximately 0.75 V is computed from the saturation current. This plot indicates nearly ideal characteristics.

The I-V characteristic in Figure 5b clearly shows an avalanche breakdown voltage of 32 V and a leakage current of 5×10^{-7} A. The peak doping at the Schottky junction was 2.5×10^{17} cm^{-3}. Development work is being conducted to reduce the leakage current by process improvements in surface preparation and Schottky metalization.

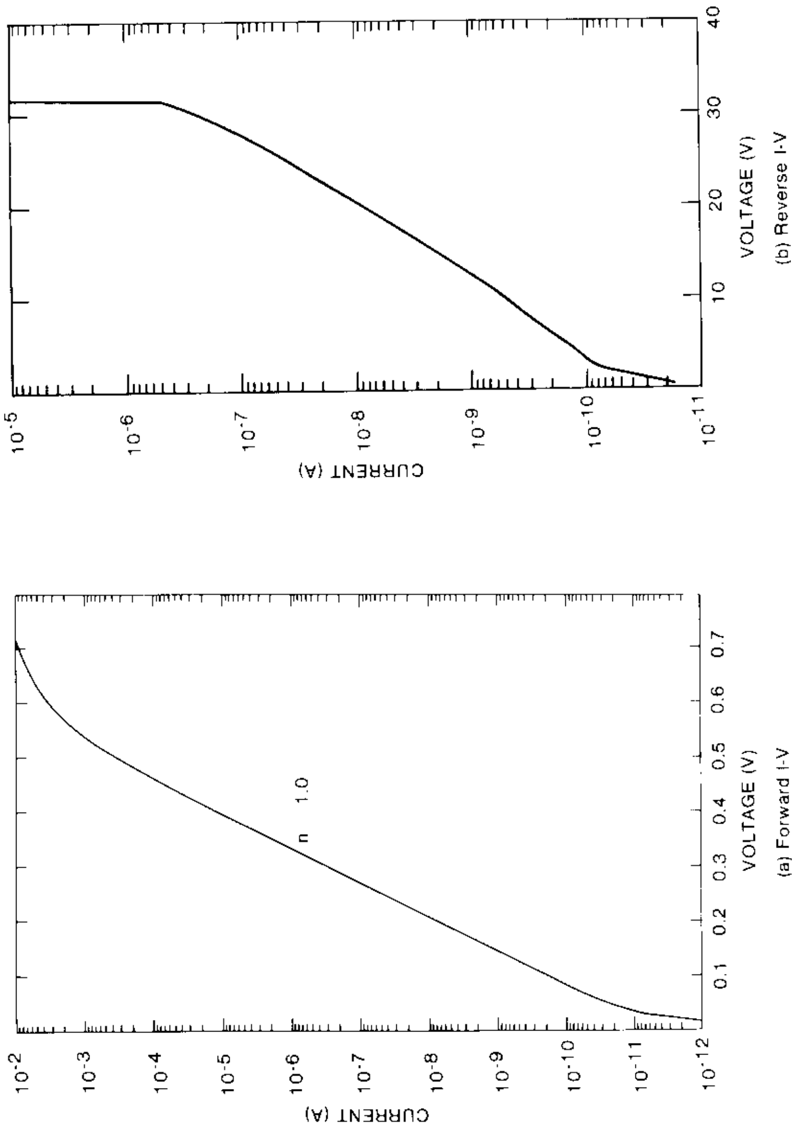

Figure 5. Schottky Barrier I-V Characteristics

Capacitance-voltage relationship

Capacitance-voltage measurements were made on the above fabricated varactor diodes at 1 MHz. Figure 6a shows a C-V curve for a single 270-keV, 7.5×10^{12} cm^{-2}, dose-implanted hyperabrupt profile recessed to a carrier concentration of 2.5×10^{17} cm^{-3}. This device shows depletion to the n^+ buried layer at about 4 V, and a further drop in capacitance as the depletion layer spreads into the n^+ layer. The capacitance tuning ratio for this device is about 9:1. This device, with C_o = 1.4 pF, was mounted in a test fixture for characterization at microwave frequencies.

Figure 6b shows a C-V curve for a multiple-energy implant (100 keV, 5.6×10^{12} cm^{-2}; 200 keV, 1.8×10^{12} cm^{-2}; and 270 keV, 6×10^{11} cm^{-2}) recessed to a carrier concentration of 4×10^{17} cm^{-3}. The hyperabrupt profile is depleted at about 6 V, with the depletion layer spreading into the n^+ layer at higher voltage. The tuning ratio for this device is greater than 10:1.

Varactor diode RF characterization

Upon completion of DC wafer probe measurements, the wafers were thinned to 10 mil and diced into 12 × 12-mil chips. Individual chips were selected for die attach and wire bonding to a chip carrier for characterization at DC and RF.

A broadband test fixture described by Ross and Geller [4] was used to measure the small-signal, one-port S-parameters of each varactor. Each device was epoxy-mounted to the test fixture carrier plate. Prior to the last bondwire attachment, the varactor's I-V and C-V characteristics were measured.

A Tektronix Model 576 curve tracer was used to measure both the forward and reverse I-V data. The forward voltages at current levels of 10 and 110 mA were measured to determine the DC series resistance, given by

$$R_{s(DC)} = \frac{[V(\text{at } 110\text{ mA}) - V(\text{at } 10\text{ mA})]}{110 - 10\text{ mA}} \qquad (7)$$

The parasitic resistance of the probe station was measured to be approximately 1.2 Ω and was subtracted from the device measurement. The reverse breakdown voltage, defined at 10-μA reverse current, was recorded. Typical DC measurements of the varactor diodes designated VVC-4 ($R_{s(DC)}$ = 7 Ω; V_{BR} = −30 V) are

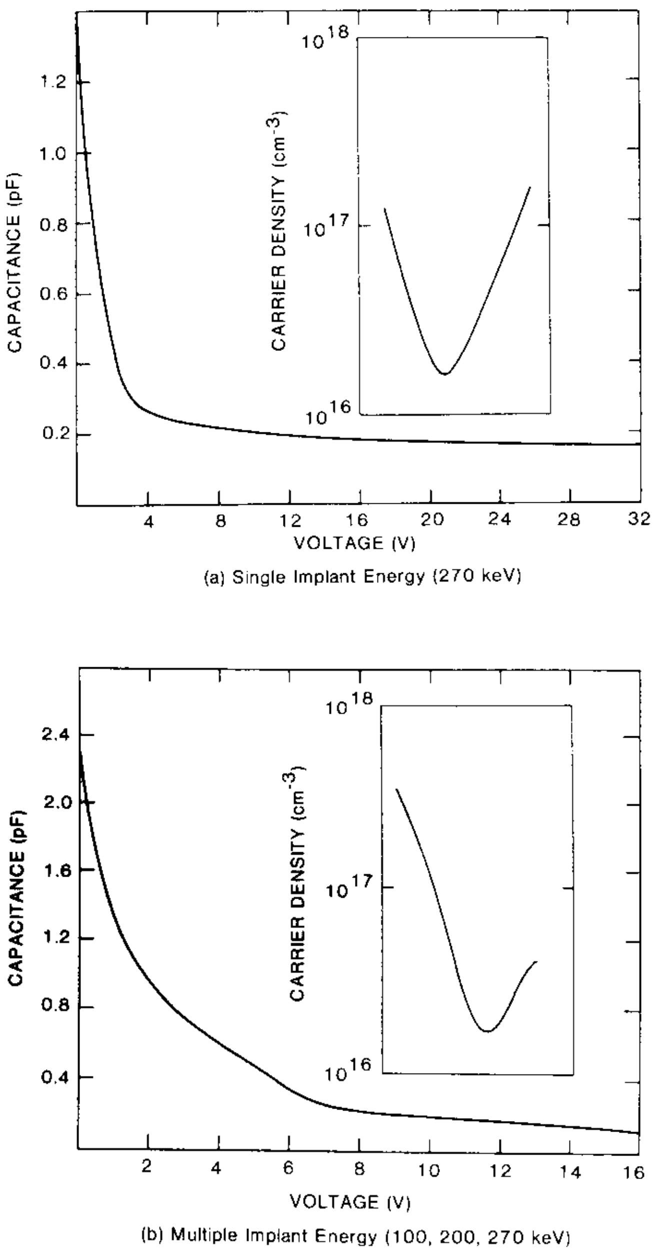

Figure 6. *C-V Characteristic of a Hyperabrupt Profile*

Current (mA)	Voltage (V)
10.0	0.726
110.0	1.5
0.01	−30.0

An HP4275A L-C-R meter was used to measure the capacitance of the varactor diode. Standard measurements are made at a test frequency of 1.0 MHz, with a peak-to-peak AC voltage of 0.10 V. Care was taken to properly zero-out the probe station's parasitic capacitance so that the varactor's true capacitance was measured. Figure 7 shows a typical C-V curve for the VVC-4 varactor. The measured zero-bias capacitance was 1.4 pF. A minimum value of 0.165 pF was measured at −25 V, corresponding to a capacitance ratio (C_o/C_{min}) of 8.48. Furthermore, for approximately 10 devices measured, the capacitance values for any given voltage up to −22 V are within ±0.03 pF of the mean, indicating excellent uniformity from device to device for one wafer.

The last bondwire between the device and the test fixture was added after the I-V and C-V measurements. The varactor diodes were characterized at microwave frequencies by using an HP8510 automatic network analyzer to measure the one-port *S*-parameters. Figure 8 is a simplified block diagram of the test fixture and device under test. Calibration routines were used to compensate for the test fixture and connector path length (essentially a reference plane extension). The fixture and connector losses were included in the measured data and are believed to be insignificant (less than 0.3 dB).

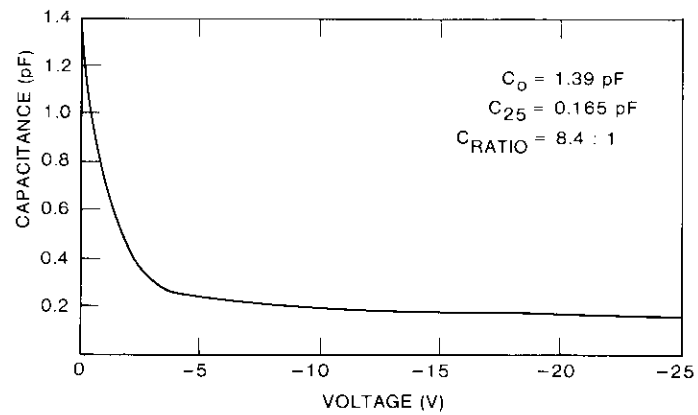

Figure 7. *C-V Curve for a VVC-4 Varactor Diode*

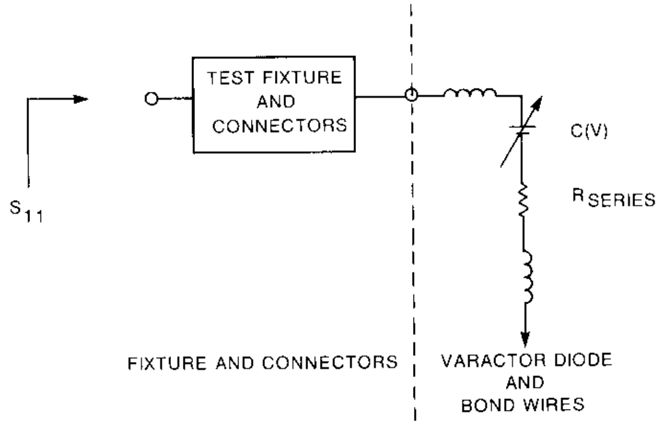

Figure 8. *Block Diagram of Fixture Plus Device Under Test*

The one-port S-parameters of the varactor are measured for a given voltage over the frequency range of 2 to 10 GHz. The voltage is adjusted to a new value, and measurements are again recorded over the same frequency range. This step is repeated for voltages covering the useful voltage range. Measured data may then be rearranged to provide data files of constant-frequency, voltage-variable, one-port S-parameters.

The equivalent resistance and capacitance of the varactor were determined from the S-parameter data. Figure 9 shows a Smith-chart plot of the measured data for the VVC-4 varactor for voltages from 0 to −22 V at 10 GHz. Table 1 gives the 10-GHz measured data of the VVC-4 varactor, and includes the measured resistance (R), measured reactance (X_c), computed capacitance ($C = 1/2\pi f X_c$), and computed quality factor ($Q = X_c/R$). The zero-bias capacitance is 1.32 pF, and decreases to 0.22 pF at −22 V reverse bias. Note also that the quality factor, Q, increases monotonically as the bias is swept from zero to breakdown voltage. This behavior is caused by the decreasing series resistance of the varactor, resulting from the deep implant ohmic contact located directly beneath the varactor's active layer, and from the increasing depletion layer of the hyperabrupt capacitor carrier profiles. The monolithically compatible structure exhibits a large capacitance ratio with a monotonically increasing Q-factor over the entire usable tuning voltage range. These RF characteristics are unique to the device design and can be compared to currently available devices which may exhibit high Q with limited capacitance ratio, or large capacitance ratio with very poor Q-factor performance. Device performance is being improved by refinements in geometry and implant doping levels, as discussed in the next section.

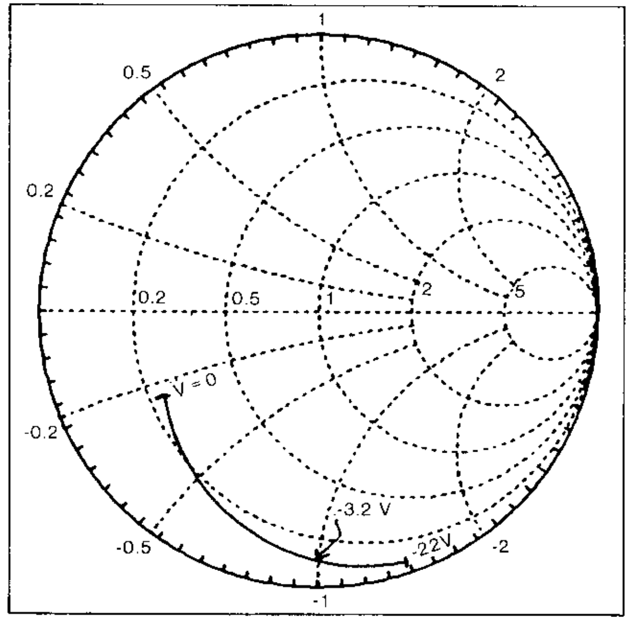

Figure 9. *Smith-Chart Plot of Measured One-Port S-Parameters of VVC-4 Varactor as a Function of Bias (F = 10 GHz)*

Varactor diode optimization

A more optimized hyperabrupt varactor diode (Figure 10) has been designed for insertion into a VCO GaAs MMIC. The basic planar structure of Figure 1 is used, but with changes in device geometry and doping concentration which translate into improved performance compared to present devices. Figure 11 depicts the calculated capacitance, series resistance, and Q *vs* voltage characteristics for the improved device.

The capacitor profile area used a 16-μm-diameter active layer with an 18-μm-diameter Schottky barrier. A 4-μm spacing between the capacitor profile and the surface implant to the buried n^+ layer was assumed. The resistivity of the buried layer was taken to be 1.5×10^{-3} Ω-cm, for an average carrier concentration of about 1.2×10^{18} cm^{-3} and carrier mobility of 3,500 cm^2-V^{-1}s^{-1}, which can be achieved by implanting Si^+ at 4 and 6 MeV and a dose of 3×10^{14} cm^{-2} at each energy. Using a σ of 0.4 μm and 35-percent implant activation after annealing, an average carrier concentration of $\sim 1.2 \times 10^{18}$ cm^{-3} can be achieved.

TABLE 1. 10-GHz MEASUREMENT DATA FOR HYPERABRUPT VARACTOR DIODE

CAPACITANCE (pF)	REVERSE BIAS VOLTAGE (V)	RESISTANCE (Ω)	REACTANCE (Ω)	COMPUTED Q
1.316	0	12.033	12.094	1.0
0.92	0.5	10.888	17.393	1.6
0.71	1	9.869	22.519	2.3
0.57	1.5	8.718	27.943	3.2
0.46	2	7.457	34.959	4.7
0.37	2.5	6.120	42.602	7.0
0.33	3	5.250	48.276	9.2
0.29	4	4.510	54.013	12.0
0.28	5	4.270	56.888	13.3
0.27	6	4.062	59.182	14.4
0.26	8	3.821	62.025	16.2
0.25	10	3.652	64.137	17.6
0.24	12	3.527	65.714	18.6
0.238	14	3.452	66.977	19.4
0.234	16	3.370	68.060	20.2
0.231	18	3.346	69.005	20.6
0.228	20	3.318	69.860	21.0
0.225	22	3.253	70.624	21.7

Figure 11 shows a C_o = 0.52 pF and C_{min} = 0.048 pF at V_R = 9 V, or a tuning ratio of 10.7:1 based on computed values from modeling. The computed Q is greater than 10 over the entire voltage range. The series resistance as a function of bias is also shown in the figure. The resistance is 3.15 Ω at C_o and is nearly constant to about 8 V, which reflects the contribution of the hyperabrupt profile to the total device resistance. Above approximately 8 V, the resistance drops rapidly and reaches a value of 0.68 Ω at C_{min}.

The various contributions to the device series resistance are shown in Figure 10, along with the calculated values for each contribution in this design. The following formulations from Reference 2 were used to determine the resistance contributions:

$$R_1 = \frac{\rho_{n1} X_1}{2\pi a^2} + \frac{\rho_{n1}}{4\pi X_1} \tag{8a}$$

$$R_2 = \frac{\rho_{n1}}{2\pi X_1} \ln \frac{b}{a} \tag{8b}$$

$$R_3 = \rho_{n2} \frac{h}{A} \tag{8c}$$

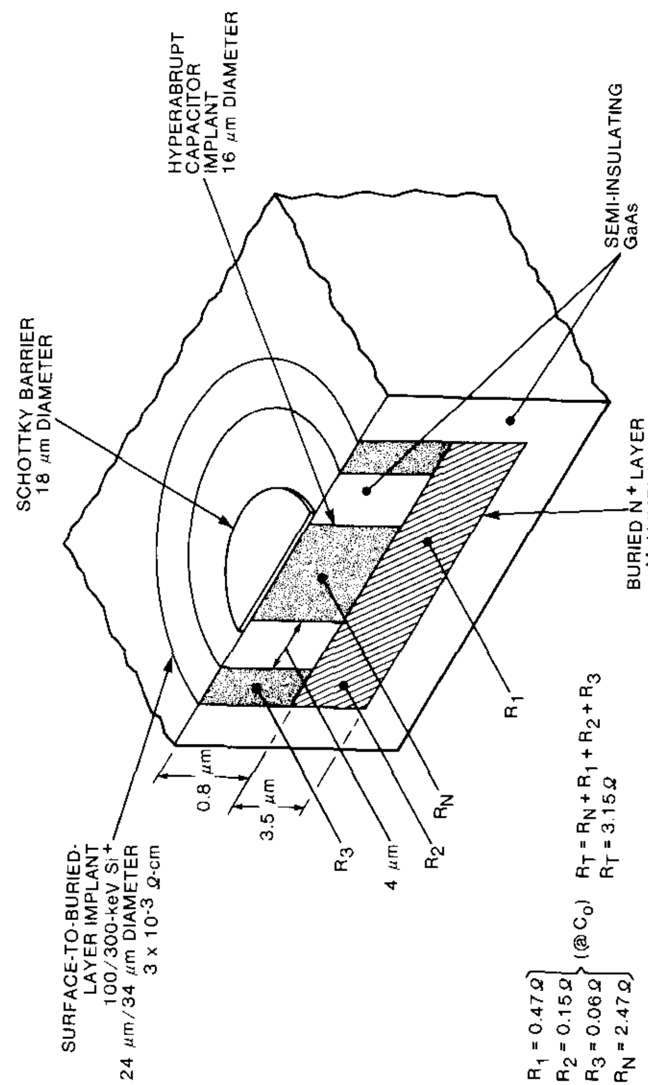

Figure 10. *Cross Section of a Fully Ion-Implanted Varactor Diode Including Series Resistance, Geometry, and Implantation Specifications*

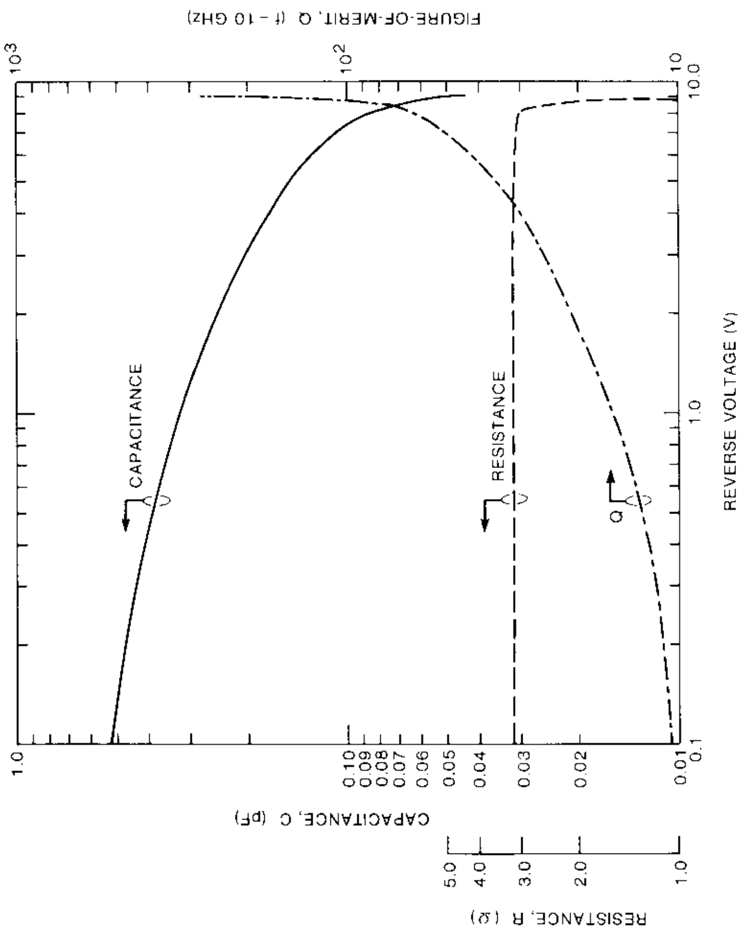

Figure 11. Calculated Values of Capacitance, Series Resistance, and Figure-of-Merit vs Applied Voltage for the Varactor Diode of Figure 10

where
ρ_{n1} = resistivity of n^+ buried layer
ρ_{n2} = resistivity of n^+ surface-to-buried-layer region
a = hyperabrupt profile radius
b = radius of n^+ surface implant ring
X_1 = thickness of n^+ buried layer
h = thickness of surface implant ring
A = area of surface implant ring.

The values of the design inputs are also shown in Figure 10. The hyperabrupt capacitance profile has a peak carrier concentration of 5.7×10^{17} cm^{-3} and a σ of 0.12 μm. The profile is a 270-keV implant recess-etched to 0.3 μm deep. It has a resistance of 2.47 Ω at zero bias (or C_o), and falls to 0.006 Ω at 9-V reverse bias (or C_{min}). Changes in the hyperabrupt capacitor profile can be implemented by varying the implantation energy and dose, thereby changing the C-V characteristics while using the same maskset and other implantation parameters. This permits flexibility in tailoring a specific varactor diode to meet different circuit performance characteristics.

Summary

Experimental results for hyperabrupt varactor diodes fabricated by an ion-implant process demonstrate an approach that is compatible with MMIC circuit manufacture. Selective ion-implantation doping was used to fabricate a planar varactor structure with a buried n^+ layer. Contact to the buried layer was realized by a low-resistance surface implant. A hyperabrupt capacitor profile was implanted in the semi-insulating layer between the wafer surface and the buried layer, and a Schottky barrier with an integral high-resistivity guard ring was fabricated which had nearly ideal characteristics. Capacitance ratios of 6:1 (including microwave fixture parasitics) and a Q greater than 10 over a portion of the voltage swing were demonstrated at 10 GHz.

Experimental data indicate that an improved device geometry and hyperabrupt profile, together with a higher-conductivity buried n^+ layer, can reduce series resistance and improve the Q over the entire voltage range. Such a device has been designed and is being implemented in a GaAs MMIC VCO circuit. The technical approach and implementation procedures have demonstrated flexibility in tailoring C-V characteristics to specific MMIC circuit performance requirements.

References

[1] P. E. Thompson and H. B. Dietrich, "Activation and Characterization of MeV n-Type Dopants in GaAs," Institute of Physics Conference Series, No. 83, Chapter 5, pp. 271–276.

[2] S. A. Calviello, J. L. Wallace, and P. R. Bie, "High Performance GaAs Quasi-Planar Varactors for Millimeter Waves," *IEEE Transactions on Electron Devices*, Vol. ED-21, No. 10, October 1974, pp. 624–630.
[3] S. M. Sze and G. Gibbons, "Effect of Junction Curvature on Breakdown Voltage in Semiconductors," *Solid-State Electronics*, Vol. 9, 1966, pp. 831–845.
[4] P. B. Ross and B. D. Geller, "A Broadband Microwave Test Fixture," *Microwave Journal*, Vol. 30, No. 5, May 1987, pp. 233–248.

Philip J. McNally received a B.S. in Physics from St. Francis College in 1959, and pursued graduate studies at Pennsylvania State University and Northeastern University. Prior to joining COMSAT Laboratories in 1974, he was with Ion Physics Corporation and Honeywell, Inc., where he was an early contributor in the field of ion implantation and its application to semiconductor device technology. These activities included both silicon and compound semiconductor devices, the latter emphasizing photodetector development.

Mr. McNally is currently a Senior Scientist in the Microelectronics Division at COMSAT, where he has been involved in research on IMPATT and varactor diodes, ion-implanted GaAs FETs, and Schottky barrier devices. He has published in the areas of GaAs and InP ion-implantation technology, Si and GaAs devices, compound semiconductor photodetectors, and rapid thermal processing. He holds a patent on an ion-implanted GaAs FET, and is currently responsible for ion-implantation technology development for GaAs integrated circuits. He is a member of IEEE, Sigma Pi Sigma, and Delta Epsilon Sigma.

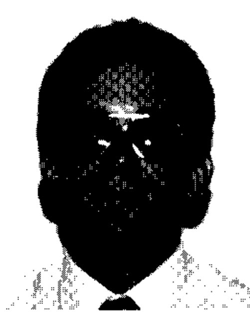

Barton B. Cregger is currently a Product Engineer at Technology Network International in Richardson, Texas, where he is involved in developing a variety of electronic instruments for the petroleum and chemical industries. From September 1986 to October 1987, he was a Member of the Technical Staff in the Microwave Systems Department at COMSAT Laboratories, where his responsibilities included the characterization of microwave oscillators for the NASA Advanced Communications Technology Satellite (ACTS) program and the design of high-bit-rate modems and GaAs voltage-controlled oscillators (VCOs). Prior to joining COMSAT, he worked for the Microwave Technology Products Division of Texas Instruments, Inc., in Dallas, Texas. Mr. Cregger has published several papers on the topics of wideband GaAs VCOs and Schottky barrier varactor diodes used as frequency multipliers. He is a member of IEEE.

Index: computer communications, models, networks, transmission, simulation

Simulation of a random-access-with-notification protocol for VSAT applications

L. C. PALMER and P. Y. CHANG

(Manuscript received February 17, 1988)

Abstract

A simulation program is described which allows delay and throughput performance evaluation of a satellite random-access technique that combines slotted-ALOHA and reservation protocols. Using inbound and outbound control channels, very small aperture terminals (VSATs) in a star network can send packets to a hub station, employing slotted-ALOHA for first attempts and reservation slots for the retransmissions necessitated by contentions or bit errors on the first attempt. This access technique is modeled and simulated to collect statistics on packet delay and throughput *vs* system loading, with emphasis on the transition between random and reservation protocols. Results are given for typical network parameters and bit error rate conditions on the links.

Introduction

Satellite data transmission networks offer considerable flexibility for interconnecting widely dispersed users into networks that allow reliable, rapid exchange of packet data. Early satellite packet data networks [1]–[4] operated in a global-beam broadcast mode designated as *multidestinational half-duplex*. However, with the trend toward small, low-cost earth stations and satellites with spot-beam coverage, these networks are evolving into star configurations with operation emanating from a central hub station [5].

In these satellite packet data networks, very small aperture terminals (VSATs) send packets via satellite to the relatively large hub station, which processes the packets for further dissemination. Outbound links from the hub station back to the VSATs can consist of a single time-division multiplexed (TDM) transmission that is received by all terminals. The terminals continuously monitor the outbound transmission stream and extract from it packets addressed to themselves.

Candidate access techniques for packet data transmission between VSATs and a central hub station range from a variety of random-access techniques (ALOHA [6], slotted-ALOHA [7], and collision resolution [8]), to the more highly structured reservation and time-division multiple-access (TDMA) techniques. These techniques have been examined and compared in many studies [9],[10] over the past 20 years. However, to maintain efficiency on the inbound VSAT-to-hub links, particularly with many (hundreds of) terminals in the network, some type of random-access protocol is needed to allow rapid channel access and delivery of packets to the hub with minimal delay.

When the number of network stations is very large (from 100 to as many as 1,000), random-access techniques such as slotted-ALOHA have a clear advantage in providing rapid access to the channel, particularly in lightly loaded networks. However, unless contentions are extremely rare, the repetitions needed for contention resolution can lead to long delays. Various approaches to this problem have been proposed [11]–[15], and adaptive access protocols such as CPODA [16] have been implemented to provide dynamic allocation of control and data slots in certain network configurations.

For the inbound VSAT-to-hub-station satellite channel, combinations of random-access (slotted-ALOHA) and reservation protocols [5] offer the potential advantages of minimizing delay under lightly loaded network conditions and providing the stable, bounded delay of a full-reservation system when the load increases. One implementation of this type of access is the random-access-with-notification (RAN) [17],[18] technique, which relies on both inbound and outbound control channels. Over the inbound TDMA control channel, VSAT terminals inform the hub station of the number of random-access packets that were sent in the last frame interval. The outbound control channel carries assignments from the hub station to reschedule contentions to be retransmitted in the reserved slots of a future frame. Thus, the division of inbound channel resources between random-access or contention slots and reserved slots constantly varies under control of the hub station via the outbound control channel. This particular protocol has been simulated to examine delay and throughput performance under dynamic conditions as a function of such parameters as frame duration, control and data channel bit rates, packet size, and link bit error rates (BERs).

This paper describes the RAN system, summarizes the approach taken to simulating the system, and presents typical results obtained with the simulation model. A brief description is given of the RAN protocol, as well as approximations of delay performance; theoretical performance predictions have been adequately described elsewhere [17],[18]. The simulation program, which was developed as a practical means to obtain detailed statistics for the distribution of packet delays under conditions of heavy load [19], is also described.

The RAN technique

The RAN concept was initiated based on recent advances in high-speed microprocessors, and on the high throughput performance of packet-switching systems employing slotted-ALOHA techniques. This section presents details of the RAN technique.

RAN frame structure

The RAN access technique uses a frame structure similar to that shown in Figure 1. The inbound channel from the VSATs to the hub is made up of time slots with duration T_p, which are aligned on each of the F frequency channels. One or more separate frequencies serve as control channels. Each user has an assigned control channel slot, so that a frame duration (T_F) consists of a time equal to or greater than $N_u T_c / N_c$, where N_u is the number of users, N_c is the number of control channels, and T_c is the duration of a control slot.

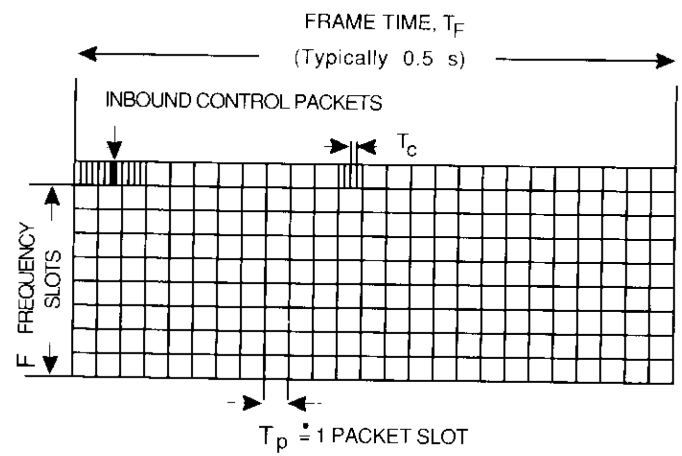

Figure 1. *Typical RAN Frame With Frame Time of 0.5 s*

Finally, control slots are assumed to be some integer submultiple of the data slot duration so that $T_c = T_p/m$, where m is an integer. As an example, with one control channel ($N_c = 1$), if there are $N_u = 200$ users and $m = 4$, there will be 50 traffic slots per frame. If it is further assumed that there are 10 frequency channels, each has 50 traffic slots, for a total of 500. Assuming a 128-kbit/s transmission rate with 1,000 bit/packet, the frame duration is 0.391 s.

Frame lengths will depend on the number of users, the packet size for data and control packets, and the transmission rate over the channel. For $N_u = 200$ users, a typical range of frame lengths can be determined as follows:

- *Typical Minimum Frame Length.* For the case where control slots contain 48 bits and the transmission rate is 256 kbit/s, the frame length is $200 \times 48/256 \times 10^3 = 0.0375$ s. In this case, if data slots contain 48 bytes and the transmission rate is 256 bit/s, the frame contains 25 data slots.
- *Typical Maximum Frame Length.* Where control slots contain 256 bits and the transmission rate is 56 kbit/s, the frame length is $200 \times 256/56 \times 10^3 = 0.914$ s.

In a typical system implementation, a frame length would be selected in the range from 0.25 to 1 s, and a typical nominal frame length would be 0.5 s, as shown in Figure 2.

Defining the path delay from the VSAT to the hub via the satellite as T_{RT} ($\approx$0.25 s), packets that must be repeated will experience minimum, maximum, and expected delays as follows:

$$D_{\min} \cong \left(2T_F + \left\lfloor \frac{2T_{RT}}{T_F} \right\rfloor T_F + T_{RT} \right) \qquad (1)$$

$$D_{\max} \cong \left(4T_F + \left\lfloor \frac{2T_{RT}}{T_F} \right\rfloor T_F + T_{RT} \right) \qquad (2)$$

$$\overline{D} \approx \frac{1}{2}\left(D_{\min} + D_{\max} \right) \qquad (3)$$

where ⌊ ⌋ denotes rounding to the next lower integer. Note that equations (1) and (2) give $3T_{RT}$ for very short frame lengths ($T_F \rightarrow 0$). For a typical frame length of $T_F = 0.51$ s, these expressions give minimum, maximum, and expected delays of 1.27, 2.29, and 1.78 s, respectively, for packets that

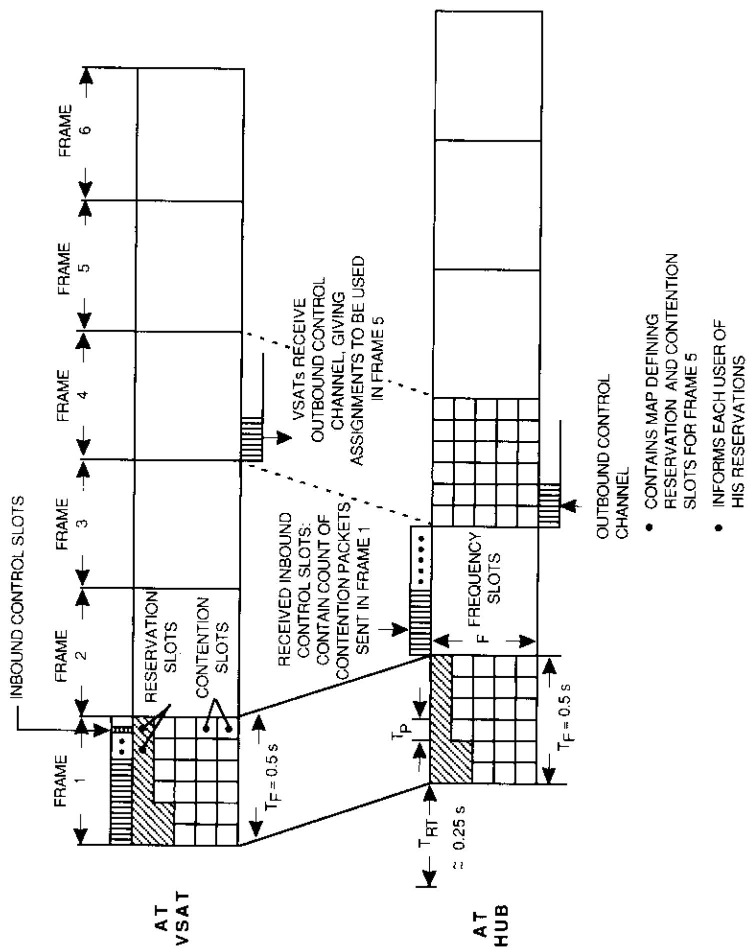

Figure 2. *Approximate Delay Relationship for Frame Length $T_F = 0.5$ s*

must be repeated. Thus, packets are delivered in the hub in 0.25 s if they are delivered successfully on the first attempt, but may require several seconds if they must be retransmitted.

Allocation of reservation slots

The RAN system divides the total number of time slots allocated to the service into C contention slots and R reservation slots, where $C + R = F$. The total (F) is fixed, but C and R can vary as long as their sum is constrained by F. The fraction of the frame devoted to reservation slots can be defined as a ratio $\eta = R/F$. For example, if $\eta = 0.15$ and there are 10 frequency channels each containing 50 packet slots, then the 50 time slots in frequency channel 10 and the first 25 time slots in frequency channel 9 would be devoted to reservation packets. The remaining 25 time slots of channel 9, and all the slots in channels 1 through 8, would be contention slots. This general subdivision of the time slots in the frame is shown in Figure 2.

The fraction of the frame that is reserved (η) is directly related to the fraction of the packets that must be repeated due to contentions. Assuming no bit errors, the average number of packets that must be repeated per packet slot can be estimated as

$$\bar{\eta} = \begin{pmatrix}\text{repeated packets} \\ \text{per slot}\end{pmatrix} = \sum_{k=2}^{\infty} k \Pr \begin{pmatrix}\text{exactly } k \text{ new packets} \\ \text{generated in one slot}\end{pmatrix}$$

$$= \sum_{k=2}^{\infty} k \frac{\lambda^k e^{-\lambda}}{k!} \tag{4}$$

where λ is the input packet intensity in packets per packet slot. This intensity applies in each time slot of the frame, regardless of how the slots are allocated between contention and reservation slots. These new packets compete for the available contention slots, and when most of the slots are reserved, duplications (contentions) become more likely.

Equation (4) can be evaluated using the fact that

$$\sum_{k=0}^{\infty} k \frac{\lambda^k e^{-k}}{k!} = \lambda$$

to give

$$\bar{\eta} = \begin{pmatrix}\text{repeated packets} \\ \text{per slot}\end{pmatrix} = \lambda(1 - e^{-\lambda}) \quad . \tag{5}$$

Estimates of throughput and delay

The delay experienced by a packet can be estimated using the approximate distribution for delay shown in Figure 3. A packet that is transmitted successfully in the contention mode arrives at the hub in exactly one transit time via the satellite (T_{RT}) after it is initiated at the VSAT. The probability that the packet is successfully received on the first attempt is

$$\Pr(\text{success}) = \Pr(\text{no contention}) \Pr(\text{no bit errors}) \tag{6}$$

where the probability of no bit errors in a packet containing N_b bits operating at a BER of P_b is $1 - (1 - P_b)^{N_b}$. The probability that no contention occurs is the probability that no more than one packet is generated and assigned to the frequency channels that correspond to the contention packet slots. This calculation applies when there are F frequency channels that are divided into C contention channels and R reservation channels in a particular time slot.

Given that λ packets are generated in each packet slot, some fraction (r) of these must be repeated, and a fraction ($1 - r$) arrive at the hub on the first attempt. Thus, the expected delay experienced by a packet is

$$\bar{D} \approx T_{RT}(1 - r) + \frac{1}{2} r (D_{min} + D_{max}) \tag{7}$$

where T_{RT} is the round-trip time, and D_{min} and D_{max} are the minimum and maximum delays (given that packets must be repeated) as defined by equations (1) and (2), respectively. The probability that a packet must be repeated is

$$r \doteq \Pr \left(\begin{matrix}\text{packet must} \\ \text{be repeated}\end{matrix} \middle| \begin{matrix}\text{a packet} \\ \text{was generated}\end{matrix} \right)$$

$$= \frac{\Pr \begin{pmatrix}\text{a packet is generated and} \\ \text{must be repeated}\end{pmatrix}}{\Pr(\text{a packet is generated})}$$

$$= \frac{\lambda(1 - e^{-\lambda})}{\lambda} = 1 - e^{-\lambda} \quad . \tag{8}$$

The expected delay becomes

$$\bar{D} \approx T_{RT} e^{-\lambda} + (1 - e^{-\lambda}) \frac{1}{2} D_{min} + D_{max} \quad . \tag{9}$$

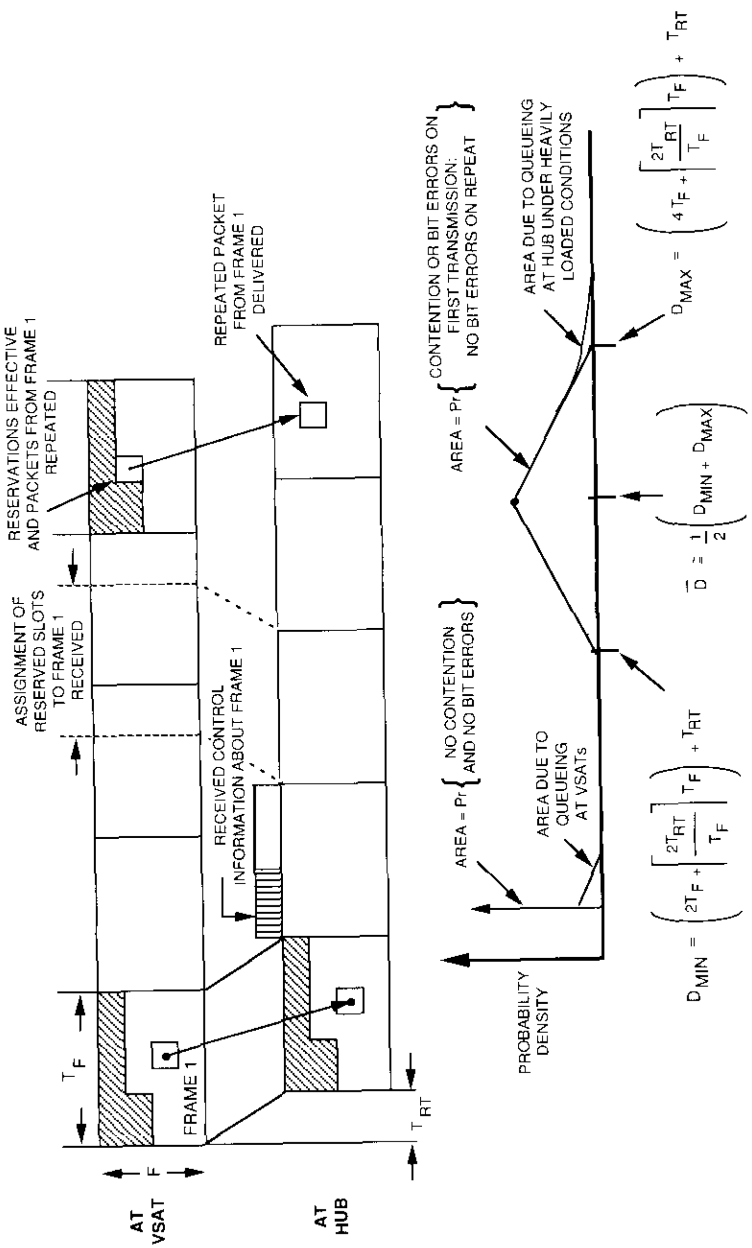

Figure 3. *Approximate Distribution of Packet Delays*

Expected delay is plotted in Figure 4 for a 0.512-s frame time. The figure also shows average delay times taken from the simulation results. Equation (9) gives a reasonable approximation of packet delay, except for the higher values of offered load. In the limit, if the system were completely reservation-oriented, expected delay would be $3T_{RT} + 1/2\ T_F$, or approximately 1.66 s, as noted in Figure 4. The behavior of the system as $\lambda \rightarrow 1$ is discussed in a later section, where the simulation results are also presented.

Although equation (9) gives a rough approximation of mean delay, users of packet transmission networks are generally interested in maximum delays or delay values that are exceeded only rarely. These detailed statistics require information on the distribution of delays, which is obtained from the simulation program described in the next section.

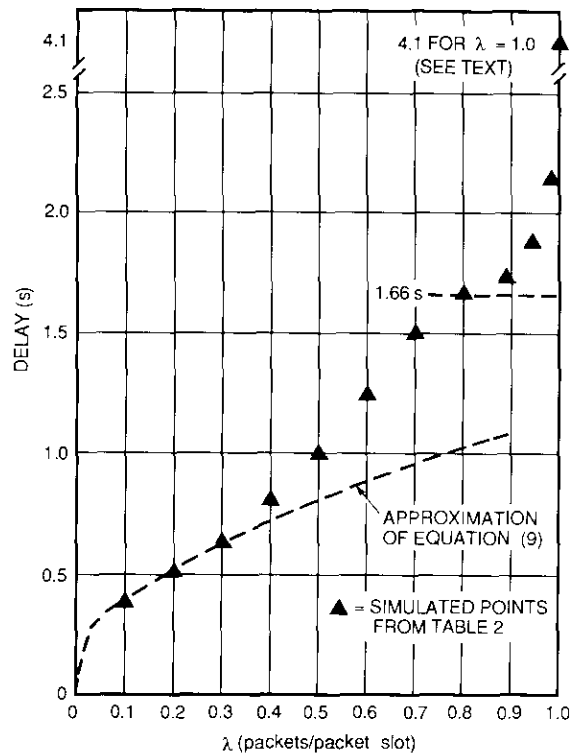

Figure 4. *Bounds on Expected Packet Delay vs λ*

Description of RANSIM

This section summarizes the concept used in the RANSIM program and describes the program features and elements.

General simulation concept

To obtain more detailed performance estimates for the RAN access technique, a simulation program (RANSIM) was developed. RANSIM is a Fortran program that implements time-domain simulation of packet transmission in a network containing a large number of VSATs and a hub station. The transmission channel is divided into inbound time slots of duration T_p, at a transmission rate of R_b bit/s. Multiple frequency channels are available, each with the same time-slotted format. A separate inbound control channel gives each user a short time slot in which to send control information to the hub once per frame.

Packets are generated at an average rate of $F\lambda$ packets per T_p seconds. The convention used here is that $F\lambda$ denotes the total packet transmission rate per time slot. With F frequency slots in each time slot, λ packet/s is the rate per packet slot (which is the conventional nomenclature). These packets are transmitted immediately by the users in a subset of the available inbound traffic slots which is designated for contention slots. The users also transmit to the hub a count of the number of contention packets sent in each frame.

At the hub station, a comparison is made between the number of contention- and error-free packets actually received and the number that were reported sent via the control (or "notification") channel. When this comparison disagrees, the hub makes reservations (via an outbound control channel) in which the VSATs can retransmit packets that either experienced collisions during their first transmission or experienced bit errors upon reception at the hub station.

RANSIM was developed to allow the evaluation of different implementations and extensions of RAN. For example, in addition to the basic results presented here, the simulation can be used in the future to evaluate different algorithms and strategies for measuring system load and for temporarily abandoning the contention mode altogether in favor of a full-reservation mode. This may be a more practical implementation than the one simulated, which basically assumes that perfect control channel information (no bit errors) is available and that the division of the frame between contention and reservation slots can change without constraint from frame to frame.

Another assumption made in the simulation is that an error-free outbound control channel is available from the hub to all VSAT stations, through which individual reservations are sent, as well as a reservation map so that all VSATs know which time slots are reserved in each frame. When the system is so heavily loaded that some time slots are completely reserved, a VSAT with new packets in that slot will queue these until the end of the frame and attempt to transmit the packet in any remaining contention slots. If all slots in the frame are fully reserved, then contention of newly generated packets is certain.

The RANSIM program operates as a time-domain simulation of packet generation, reception, and repetition. After initialization and setup of certain variables, the program steps through the large number of time slots which make up the total simulation run. During the simulation, statistics are collected on such variables as the number of packets generated, the occurrence of contentions in the slotted-ALOHA channels, the number of reserved slots needed (on average), and the delay experienced by the packets from their first initiation at the VSATs until their final delivery to the hub station.

The program is run for a large number of frames, typically several thousand. As an example, for a 0.5-s frame interval, 1 hour of real-time operation corresponds to 7,200 frames. Each of these frames might typically contain 60 packet slots consisting of 20 slots on each of three frequency channels. For an offered load of 0.3 packet/packet slot, a 1-hour simulation will generate more than 10^5 packets, which should be more than adequate to establish statistics at the 0.1-percent exceedance level. In fact, runs one-tenth this length (*i.e.*, generating 10,000 packets resulting in 10 events at the 0.1-percent exceedance level) should suffice for initial program tests. Currently, runs of 10,000 packets take about 100 s of CPU time on an IBM 8032 computer, so the simulation runs at a rate of about 100 packet/s.

The program is set up to simulate continuous operation over a large number of frames. For example, with a typical 0.5-s frame, operation over 10,000 frames corresponds to 1.4 hours of network operation. Within each frame, packets can be generated according to either a Poisson distribution or a uniform distribution in each packet slot, T_p. The Poisson model was used for all of the results reported here. Typically, 50 of these slots constitute a frame, and the frame duration might be between 0.5 and 1.0 s. The program can be run for thousands of frames (hours of simulated network time) to collect statistics on the fraction of packets that require retransmission, and to obtain an average and cumulative distributions of delay times experienced by the packets.

Summary of simulation approach and program features

Inputs to the RANSIM simulation include such variables as the number of VSAT terminals, the bit rates on the inbound data and control channels, the number of frequency channels utilized, the packet lengths, and the channel

BERs. The program simulates the different phases of network operation, including the generation of many packets at the user stations; the transmission of these packets to the hub station; and the scheduled retransmission in reserved slots of packets that do not reach the hub station on the first attempt, due to either contention or bit errors.

The program is organized based on packet slots of duration T_p seconds. These slots are subdivided into control channel slots of duration $T_s = T_p/m$, where for convenience in the simulation m is assumed to be an integer. Transmission is further organized into frames. The frame time is assumed to be at least equal to the product of the number of users (N_u) and the inbound control slot duration, so that $T_F \geqq N_u T_s \geqq N_u T_p/m$.

The mainline of the program contains a sequence of counters that count the number of control slots in a packet slot and the number of control slots in a frame. As new packet slots occur, a subroutine (PACKET) is called that generates the new packets in that time slot. The probability that exactly k new packets are generated in a particular packet slot can be selected either according to the Poisson distribution, with λ packets per packet slot or $F\lambda = sT_p$ packets per time slot,* as

$$\Pr(k \text{ packets in } T_p) = (sT_p)^k/k! \exp(-sT_p) \tag{10a}$$

or according to the uniform distribution

$$\Pr(k \text{ packets in } T_p) = \text{uniform random variable } (0 \rightarrow k_{max}) \tag{10b}$$

where sT_p is the average number of packets generated in each packet slot. During each packet slot of duration T_p seconds, k packets ($k = 0, 1, 2, 3, \ldots k_{max}$) are generated. For each of these new packets, an originating user is selected randomly. Also, a frequency slot is selected randomly from the subset of frequency slots that are available for the transmission of contention packets.

Figure 5 shows inputs and outputs of the simulation program. The methods employed in order to include some of the effects encountered in transmission of the control and data packets can be summarized as follows:

* The program steps through each time slot (T_p) in a frame and generates an average of $F\lambda$ new packets in each time slot for the Poisson model.

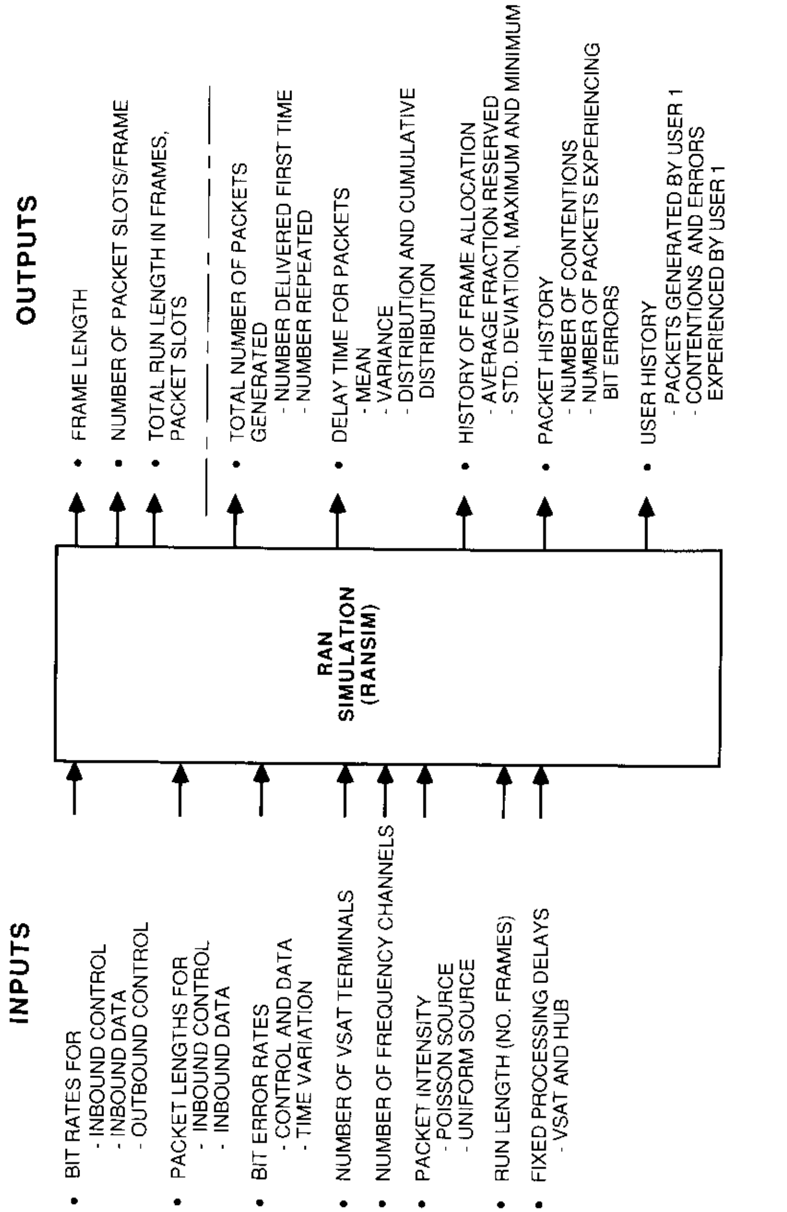

Figure 5. Inputs and Outputs of RAN Simulation

a. *Contention Among Data Packets.* Contentions are detected explicitly, and the hub makes the necessary reservations so that affected VSATs repeat packets.

b. *Bit Errors in Data Packets.* The hub makes reservations so that the VSAT can repeat the packet (the same as for contentions).

c. *Bit Errors in the Inbound Control Channel.* For the affected user in the frame in question, contention-free and error-free packets are delivered, and packets experiencing contention (or with bit errors) are counted as "lost" by the program.

d. *Bit Errors in the Outbound Control Channel.* If the reservation map for a particular frame contains errors at a particular VSAT, any contention (new) packets generated by the user are inhibited and must be repeated (they are counted as contentions immediately, which has the same effect). If VSATs have packets to be repeated in reservation slots, but errors are experienced in the outbound control channel, the affected packets are counted as "lost" by the simulation program.

e. *Time-Varying BER.* This applies to the selected VSAT (usually user 1) only. Two values of BER are used for data packets—BER 1 at first, changing to BER 2 at a user-specified time, and changing back to the original BER at a second user-specified time.

f. *Automatic Switching From Contention to All-Reservation Operation.* The user of the simulation program specifies an averaging interval (in frames) and a threshold (in fraction of frame reserved). The simulation run begins with contention operation; if the fraction of frame reserved, as averaged over the user-specified interval, ever exceeds the user-specified threshold, then operation switches to all-reservation and remains in this mode.

g. *Inbound and Outbound Signal Processing Delay.* The user specifies both. These are added as fixed delays to all packets of all users.

Program elements

The RANSIM program contains the elements shown in Figure 6. The program begins with an initialization section that reads program inputs, zeros certain variables, computes time increments and time frame limits, and initializes time. Following this, the program steps through many time intervals, and at each step events occur at either the VSATs or the hub station (as shown in the lower part of the figure). At the VSATs, packets are randomly generated and assigned a random user ID and a random frequency slot. Contentions are then noted, and packets are marked according to their status, as follows:

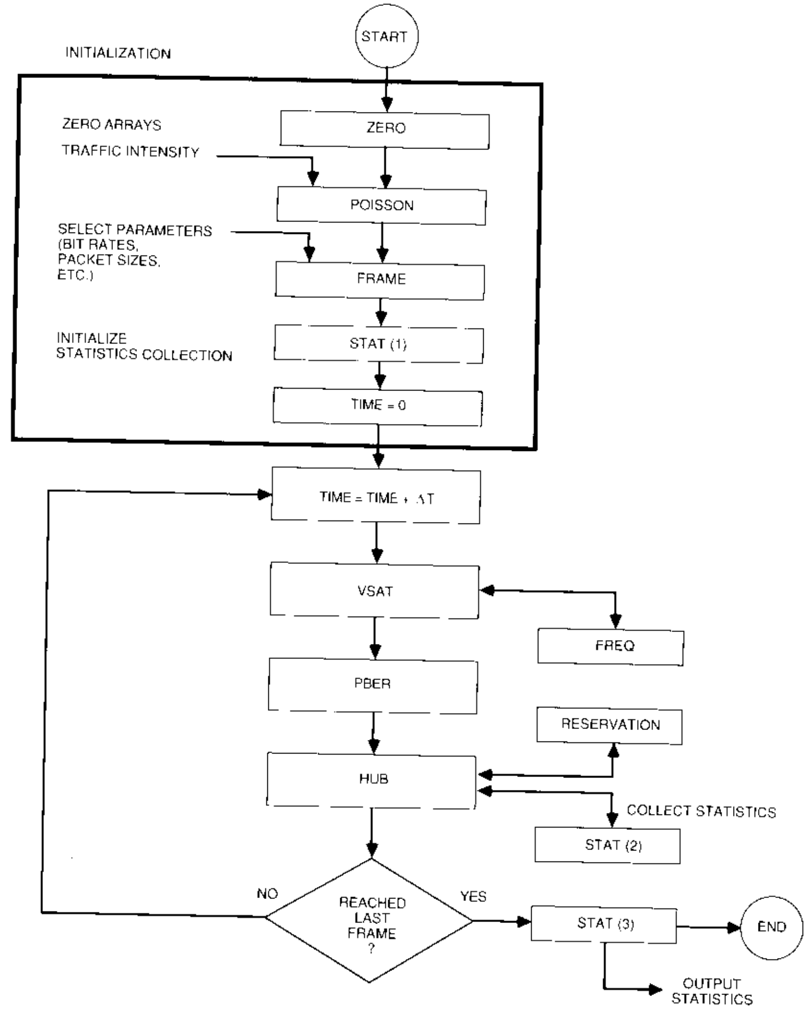

Figure 6. *Elements of RANSIM*

- packet transmitted successfully on the first attempt, with no contention and no bit errors;
- packet experienced contention; or
- packet experienced bit errors.

A final category applies to retransmitted packets which cannot experience collisions on the second transmission attempt because they are assigned a reserved slot.

To implement this processing in the simulation program, packets are generated randomly (using the PACKET subroutine) and a history is kept of all packets generated. This history includes a packet number, an initiating user ID, a time of initiation, a time of retransmission (if applicable), and a status indicator for each packet.

Figure 7 identifies the elements of the array ISTACK, which serves as a storage register for information pertaining to each packet generated in the simulation. New packets at the VSATs are time-stamped and entered into this data file. After the appropriate VSAT-to-hub delay, the packets are processed again in the delayed hub time frame. Packets requiring retransmission must be saved for a longer time and reprocessed to account for retransmissions. Eventually, very old packets are written over in the data file, which has a limited length. A check is made that no packets are lost during this recycling of the data-file pointers. The processing of information at the hub follows the time sequence shown in Figure 8 and uses the logic shown in Figure 9.

Extensions of the RAN system will allow the transmission and processing of packets of various sizes. This capability has been added to the current RAN simulation software to include features for handling longer packets, in addition to the fixed-size packet transmission simulated by RANSIM. To date, this feature has not been used.

Typical simulation results

Simulation runs were made with RANSIM to exercise the program over a representative range of input variables and to gain experience with the program outputs. Several cases were selected to exercise and test the various features of the program. Test case 1 is typical, having a 0.512-s frame length resulting from 256-byte data packets and 56-kbit/s data rates on the control and data channels. For these runs, VSAT and hub processing delays are assumed to be zero. Table 1 summarizes the results for case 1, where the primary variable is the average number of packets presented to the system in each time slot. With three frequency channels, this is three times the average number of packets per packet slot.

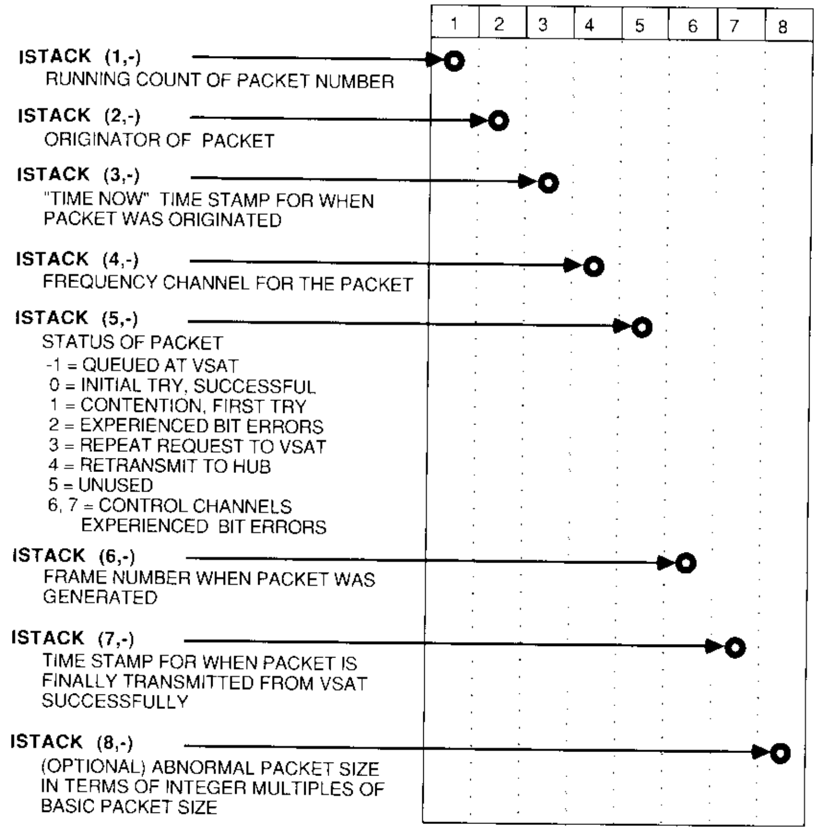

Figure 7. *Definition of Elements of ISTACK (,)*

For most of the simulation runs presented in Table 1, approximately 10,000 packets were generated, with stable statistical results. However, longer runs (10,000 frames yielding over 400,000 packets) were made at channel loads of $\lambda = 0.9$, 0.95, 0.99, and 1.0 to verify steady-state performance at these higher levels. The fraction of packets that are delivered contention-free is indicated in the fourth column in the table. The next four columns give statistics on delay *vs* presented load. The cumulative distribution of packet delay is plotted in Figure 10. At the 0.05 exceedance probability level, delays range from 1.5 to over 2 s for this particular set of frame parameters.

Note that $\lambda = 1.0$ constitutes an unrealistic system load where, even for a pure reservation system, the average packet delay would be expected to

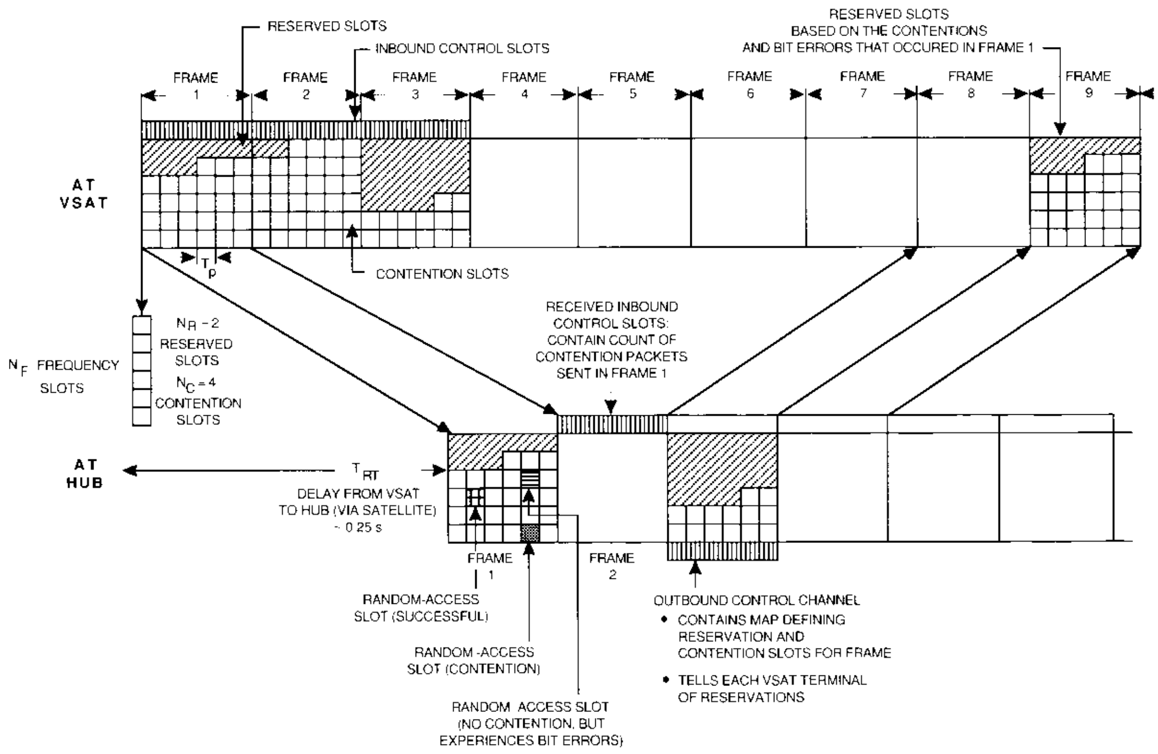

Figure 8. *Example With Frame = 100 ms*

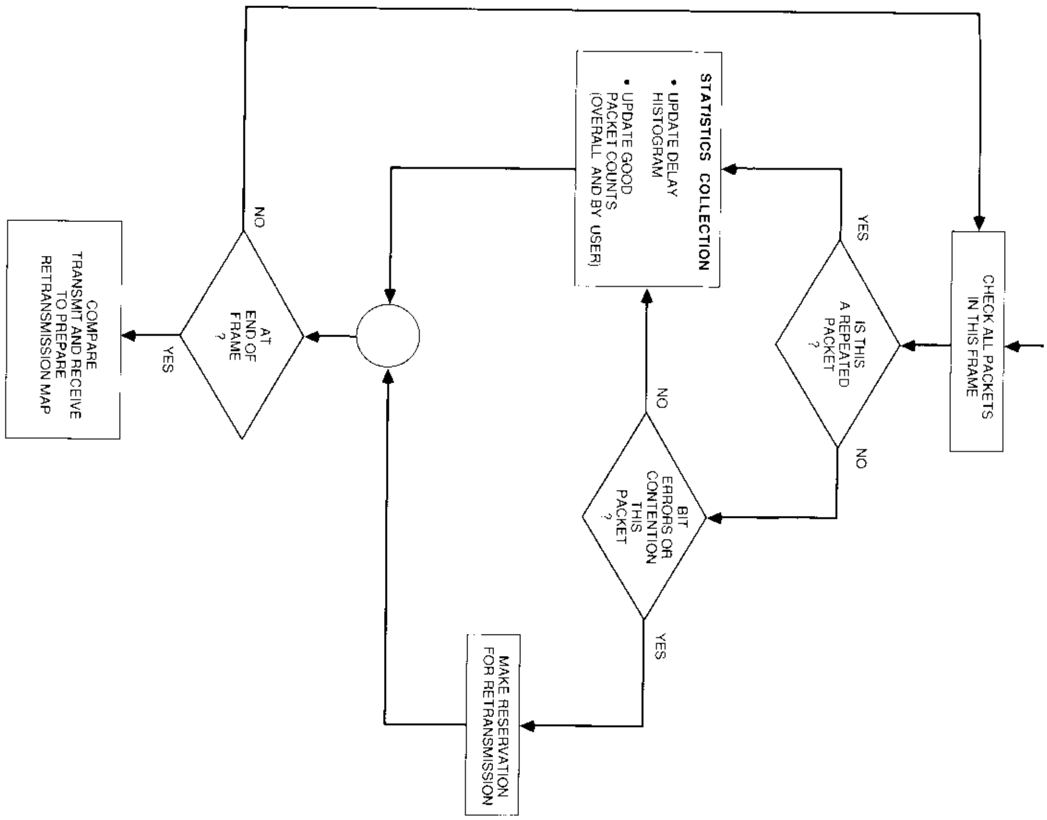

Figure 9. *Logic of Hub Processing*

TABLE 1. TEST CASE 1 SIMULATION RESULTS (200 USERS, 0.512-s FRAME LENGTH, 3 FREQUENCY CHANNELS, 42 PACKET SLOTS/FRAME, BER = 10^{-8})

λ	Packets Generated	Packets Repeated	Received on First Attempt (%)	Mean Delay (s)	Delay Exceeded x% of Time (s)			Average No. of Reserved Slots/Frame		Maximum No. of Reserved Slots/Frame
					5%	1%	0.1%	Number	Fraction	
0.1	10,104	1,010	90.0	0.387	1.53	1.75	1.79	0.42	0.01	6
0.2	9,895	1,852	81.3	0.508	1.68	1.79	1.82	1.54	0.04	8
0.3	10,063	2,805	72.1	0.644	1.75	1.79	1.86	3.50	0.08	14
0.4	10,058	3,814	62.0	0.805	1.79	1.86	1.93	6.3	0.15	26
0.5	10,724	5,435	49.2	1.01	1.86	1.93	2.05	10.8	0.26	27
0.6	10,318	6,802	34.0	1.26	1.93	2.01	2.12	16.8	0.40	37
0.7	10,301	8,377	18.2	1.50	2.01	2.08	2.23	23.8	0.56	42
0.8	10,117	9,310	7.1	1.66	2.00	2.15	2.23	30.0	0.71	42
0.9	10,163	9,818	2.26	1.76	2.08	2.19	2.30	36.2	0.86	42
0.9	377,863	373,068	1.2	1.72	2.08	2.19	2.37	37.3	0.88	42
0.95	399,202	397,266	0.37	1.79	2.19	2.38	2.56	39.8	0.95	42
0.99	416,120	415,762	0.05	2.17	3.10	3.66	4.28	41.5	0.99	42
1.0*	10,400	10,177	0.8	2.14	2.71	2.85	2.99	40.5	0.96	42
1.0*	419,965	419,202	0.02	4.1	8.00	9.73	10.16	41.9	0.99	42

*This represents an unrealistic system load; see text for a discussion of the implications, and Figure 11 for additional simulation results.

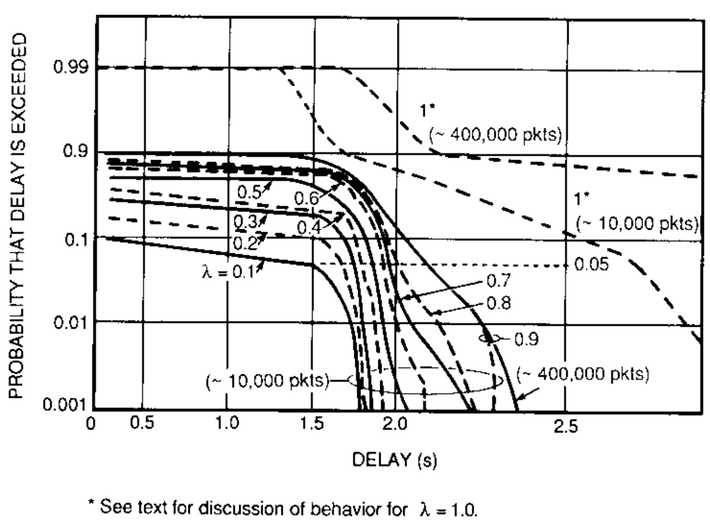

Figure 10. *Exceedance Probability vs Delay for Test Case 1 (0.512-s frame duration)*

increase without limit. It is possible to use $\lambda = 1.0$ in the simulation program, but the results tend to be erratic (as indicated in Table 1) and it is included in some of the results for completeness only.

The primary observation as $\lambda \rightarrow 1$ is an abrupt jump in mean packet delay and a radical change in the cumulative distribution of packet delays (which change in a regular, repeatable way as λ is increased from 0.5 to 0.6, 0.7, and 0.8, as was done in the simulations). A second observation for $\lambda = 1.0$ is that expected packet delay continues to increase (*i.e.*, never converges) as simulation run length increases.

This condition of heavy loading has been investigated by making longer simulation runs for $\lambda = 0.9$, 0.95, and 1.0. The results are shown in Figure 11 for variation in mean delay and 0.05 exceedance delay. Here, the length of the simulation run is extended to 10,000 frames (approximately 1.4 hours of simulated time), and the statistics never stabilize for $\lambda = 1.0$. In contrast, for $\lambda = 0.9$ and 0.95, the statistics stabilize within a few hundred frames (a startup transient must elapse as the system is "filled" with packets).

Results from a second test case are given in Table 2, and delay exceedance probability is plotted in Figure 12. This case is identical to test case 1, except that the BER is varied rather than the load. Also for this case, fixed processing delays of 25 and 45 ms were added at the VSATs and hub, respectively.

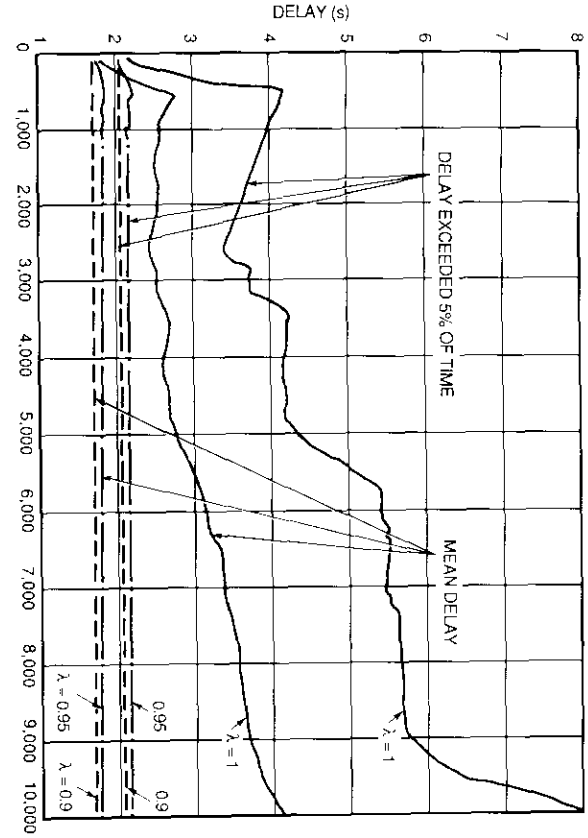

Figure 11. *Detailed Statistics for Case 1 as λ → 1.0*

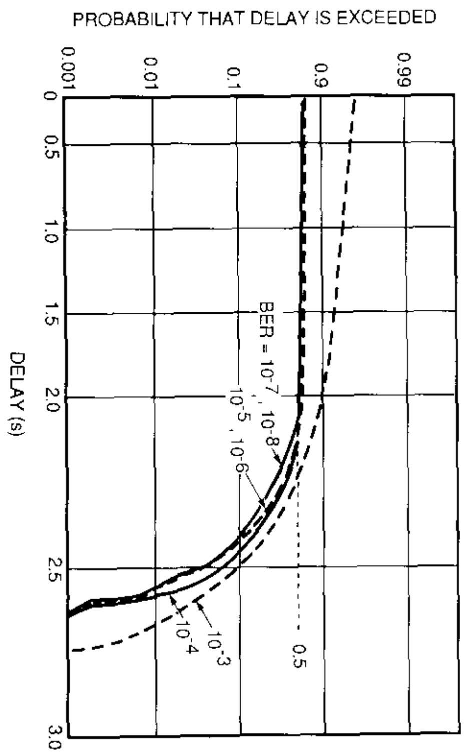

Figure 12. *Exceedance Probability vs Delay for Test Case 2 (0.512-s frame duration, 3 frequency channels, λ = 0.6 packet/packet slot, BER is varied)*

TABLE 2. TEST CASE 2 SIMULATION RESULTS (1,000 USERS, 0.512-S FRAME LENGTH, 3 FREQUENCY CHANNELS, 42 PACKET SLOTS/FRAME, λ = 0.6 PACKET/PACKET SLOT)

Inbound BER	Packets Generated	Packets Repeated	Packets With Bit Errors	Received on First Attempt (%)	Mean Delay (s)	Delay Exceeded x% of Time (s)			Average No. of Reserved Slots/Frame	
						5%	1%	0.1%	Number	Fraction
10^{-8}	10,305	6,616	0	35.4	1.56	2.45	2.52	2.59	16.5	0.39
10^{-7}	10,305	6,623	3	35.4	1.56	2.45	2.52	2.59	16.5	0.39
10^{-6}	10,305	6,819	23	33.5	1.60	2.45	2.52	2.59	17.0	0.40
10^{-5}	10,305	6,967	223	32.0	1.63	2.45	2.56	2.66	17.3	0.41
5×10^{-5}	10,305	7,297	1,014	28.7	1.70	2.45	2.56	2.63	18.2	0.43
10^{-4}	10,305	7,707	1,895	24.7	1.78	2.48	2.56	2.67	19.2	0.46
2×10^{-4}	10,305	8,284	3,402	19.0	1.89	2.48	2.56	2.67	20.6	0.49
5×10^{-4}	10,305	9,308	6,300	8.9	2.07	2.48	2.59	2.70	23.2	0.55
10^{-3}	10,305	9,926	8,435	2.83	2.21	2.48	2.59	2.71	24.7	0.59
10^{-2}	10,305	10,210	9,592	0.0	2.28	2.52	2.59	2.74	25.5	0.61

Table 3 and Figure 13 summarize results from a test of program operation with only a single frequency channel. In this case, contention packets generated early in the frame must be queued for transmission later in the remaining contention slots. The results show the effect of BER on single-frequency channel operation (see Table 4 and Figure 14). Note that the mean and 0.05 delay exceedance levels increase as BER becomes poorer than 10^{-4}.

Additional simulation runs were made with 1,000 users and 10 frequency channels. These results are summarized with variable λ in Figure 15, and with BER varied and λ fixed at 0.6 in Figure 16.

A final series of simulations was performed to exercise the program over the range of bit rates and frame times stored in the program. These seven systems cover a range of data packet sizes (in bytes), data transmission rates (56, 128, and 256 kbit/s), and control channel packet sizes. The results are summarized in Table 5. The distribution of delay times in Figure 17 corresponds to a moderate level of channel loading (λ = 0.6).

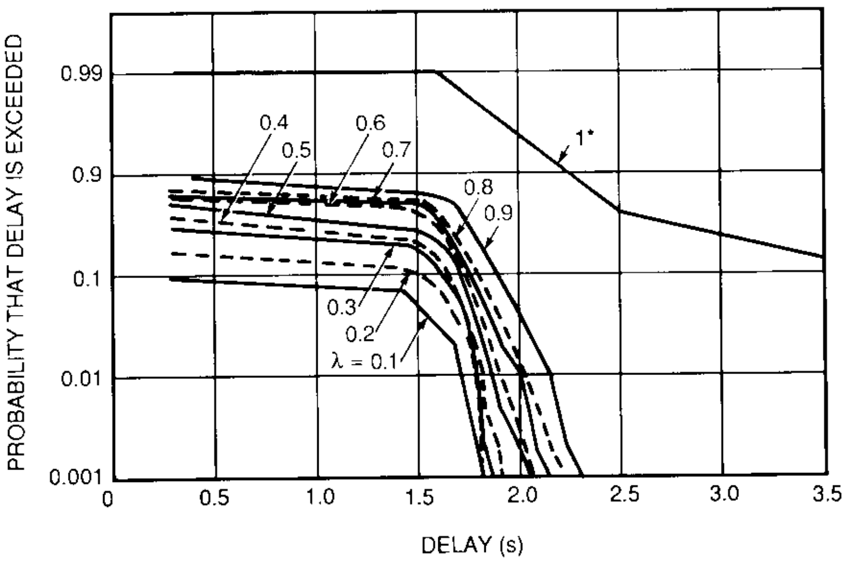

* See text for discussion of behavior for λ = 1.0.

Figure 13. *Exceedance Probability vs Delay for Test Case 3 (0.512-s frame duration, 1 frequency channel)*

Table 3. Test Case 3 Simulation Results (200 Users, 0.512-s Frame Length, 1 Frequency Channel, 14 Slots/Frame, BER = 10^{-8})

Offered Load λ Packets/Packet Slot	Packets Generated	Packets Repeated	Received on First Attempt (%)	Mean Delay (s)	Delay Exceeded x% of Time (s)			Average No. of Reserved Slots/Frame		Maximum No. of Reserved Slots/Frame
					5%	1%	0.1%	Number	Fraction	
0.1	9,871	932	90.5	0.381	1.49	1.71	1.79	0.13	0.09	5
0.2	9,900	1,802	81.8	0.505	1.64	1.75	1.82	0.50	0.036	7
0.3	10,104	2,849	71.8	0.646	1.72	1.79	1.86	1.18	0.084	10
0.4	10,096	3,930	61.1	0.806	1.75	1.82	1.93	2.18	0.155	11
0.5	10,430	5,237	49.7	0.978	1.79	1.86	2.04	3.49	0.249	14
0.6	9,895	6,131	37.9	1.15	1.82	1.97	2.12	5.10	0.36	14
0.7	9,972	7,804	21.6	1.42	1.93	2.08	2.23	7.57	0.54	14
0.8	10,029	8,983	10.0	1.62	1.97	2.12	2.26	9.97	0.71	14
0.9	10,063	9,727	2.88	1.81	2.12	2.23	2.37	12.14	0.87	14
1.0*	9,968	9,806	0.31	2.84	4.46	5.19	5.41	13.70	0.98	14

* See text for discussion of λ = 1.0.

TABLE 4. TEST CASE 4 SIMULATION RESULTS (200 USERS, 0.512-S FRAME LENGTH, 1 FREQUENCY CHANNEL, 14 PACKET SLOTS/FRAME, λ = 0.5 PACKET/PACKET SLOT)

INBOUND BER	PACKETS GENERATED	PACKETS REPEATED	PACKETS WITH BIT ERRORS	RECEIVED ON FIRST ATTEMPT (%)	MEAN DELAY (s)	DELAY EXCEEDED x% OF TIME (s)			AVERAGE NO. OF RESERVED SLOTS/FRAME		MAXIMUM NO. OF RESERVED SLOTS/ FRAME
						5%	1%	0.1%	NUMBER	FRACTION	
10^{-8}	10,430	5,237	0	49.7	0.98	1.79	1.90	2.05	3.49	0.25	14
10^{-7}	10,430	5,228	3	49.8	0.98	1.79	1.90	2.01	3.48	0.25	14
10^{-6}	10,430	5,248	22	49.6	0.98	1.79	1.90	2.05	3.49	0.25	14
10^{-5}	10,430	5,441	211	47.8	1.00	1.79	1.90	2.08	3.62	0.26	14
5×10^{-5}	10,430	5,979	902	42.6	1.07	1.79	1.94	2.08	3.98	0.28	14
10^{-4}	10,430	6,413	1,653	38.4	1.13	1.83	1.94	2.08	4.3	0.30	14
2×10^{-4}	10,430	7,326	2,885	29.6	1.26	1.83	1.93	2.08	4.9	0.35	14
5×10^{-4}	10,430	8,879	5,212	14.7	1.47	1.86	1.97	2.12	5.9	0.42	14
10^{-3}	10,430	9,917	6,806	4.7	1.62	1.90	2.01	2.15	6.6	0.47	14
10^{-2}	10,430	10,408	7,599	0.0	1.68	1.90	2.01	2.12	6.9	0.49	14

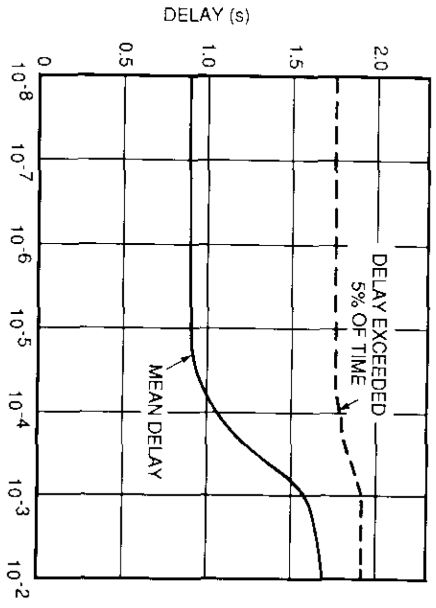

Figure 14. *Effect of Inbound Data Channel BER on Delay for Test Case 4*

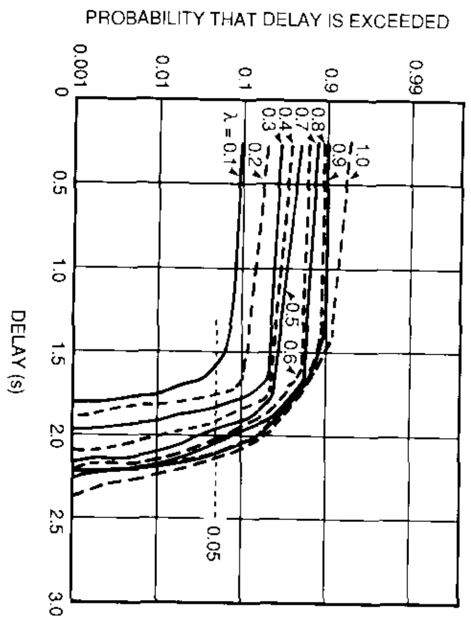

Figure 15. *Exceedance Probability vs Delay for Test Case 5 (10 frequency channels, inbound BER = 10^{-7})*

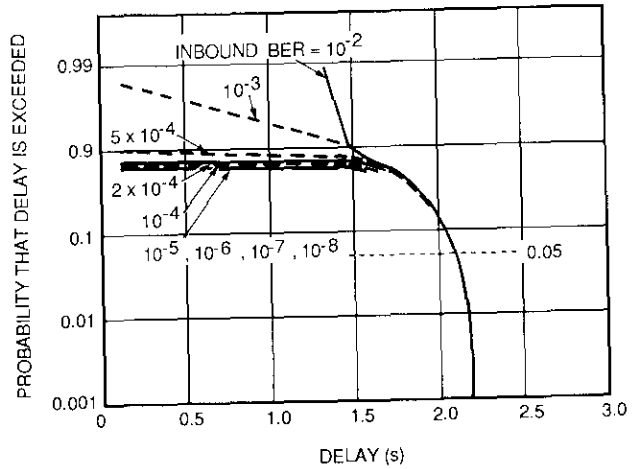

Figure 16. *Exceedance Probability vs Delay for Test Case 6 (λ = 0.6, BER is varied)*

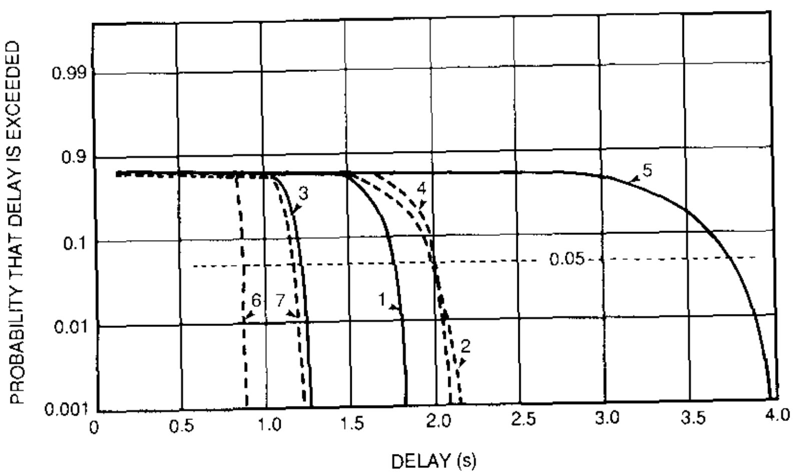

Figure 17. *Exceedance Probability vs Delay for the Seven System Configurations (λ = 0.6)*

TABLE 5. TEST CASE 5 SIMULATION RESULTS (200 USERS, 5 FREQUENCY CHANNELS, λ = 0.6 PACKET/PACKET SLOT, INBOUND BER = 10^{-7})

System Number	Data Channel: Bit Rate (kbit/s)	Data Channel: Packet Size (bytes)	Control Packet Size (bits)	Frame Length (s)	Total Data Slots/Frame	Packets Generated	Packets Repeated	Fraction Received on First Transmission (%)	Mean Delay (s)	Delay Exceeded x% of Time (s): 5%	1%	0.1%	Average Fraction Reserved Slots/Frame	Maximum No. of Slots/Frame
1	56	48	96	0.3428	250	10,400	5,884	41.4	1.04	1.74	1.79	1.82	0.33	135
2	56	256	48	0.512	70	9,988	6,068	38.8	1.18	1.97	2.05	2.12	0.36	49
3	128	48	96	0.150	250	10,400	5,643	42.7	0.761	1.20	1.23	1.24	0.32	127
4	256	256	128	0.40	250	10,400	5,885	41.4	1.18	2.00	2.06	2.09	0.33	135
5	56	256	64	1.024	140	9,988	5,918	39.8	1.51	3.73	3.87	3.98	0.35	81
6	256	48	48	0.0375	125	10,400	5,316	44.9	0.579	0.864	0.87	0.874	0.30	77
7	56	48	48	0.171	125	10,400	6,071	40.29	0.755	1.16	1.19	1.21	0.34	77

Summary and conclusions

A flexible simulation of the RAN link access protocol has been described. With the RAN technique, VSATs initially send packets to a hub station in a slotted-ALOHA mode, thus minimizing delay for those packets that do not experience contention or bit errors. Reservation channels are used by the VSATs to retransmit the packets that were not delivered on the first attempt.

A computer program has been developed to model and simulate the RAN protocol, with emphasis on developing a flexible simulation tool for evaluating RAN performance. Major outputs of the program include statistics on such items as successful first transmissions, the distribution of packet delay times, and the fraction of the RAN resources (frequency channels and time slots within each of these channels) that must be devoted to reservations.

The RAN protocol was briefly reviewed, and some of the variables that apply to the system being simulated were defined. In particular, relationships were established between such variables as data channel bit rate and packet size, and control channel bit rate and packet size, which determine limitations on the transmission frame time. The duration of this frame has a direct effect on delay time.

The simulation concept and the elements of the Fortran program that implements the simulation were described, and representative results obtained with the program were given to illustrate its capabilities. Test cases were run with a single frequency channel and with 10 frequency channels, with both variable system load and variable inbound BER for a representative system load. A series of tests case were also run using various sets of system parameters (bit rates and packet sizes) to determine the effect of these variables on delay time statistics. The results showed the behavior of the RAN protocol as system load increases, particularly the distribution of packet delay time. As system load approaches $\lambda = 1.0$, mean packet delay increases abruptly (as expected). Therefore, the statistics obtained from the simulation program tend to be erratic in that delays continue to increase as run length is increased.

The simulation program has been shown to provide a flexible and realistic tool for investigating the detailed behavior of the RAN protocol. The program can also be used to evaluate the performance of refinements and extensions to the protocol in VSAT networks.

Acknowledgments

The authors wish to acknowledge the assistance of F. Faris in implementing the statistics collection routines. The contribution of P. Chitre, who pointed out inconsistencies in early test results, is also acknowledged.

References

[1] I. Jacobs *et al.*, "General Purpose Satellite Networks," *Proc. IEEE*, Vol. 66, No. 11, November 1978, pp. 1448–1467.

[2] L. Palmer, J. Kaiser, S. Rothschild, and D. Mills, "SATNET Packet Data Transmission," *COMSAT Technical Review*, Vol. 12, No. 1, Spring 1982, pp. 181–212.

[3] S. S. Lam, "Satellite Packet Communication—Multiple Access Protocols and Performance," *IEEE Transactions on Communications*, Vol. COM-27, No. 10, October 1979, pp. 1456–1466.

[4] F. A. Tobagi, "Multiaccess Protocols in Packet Communication Systems," *IEEE Transactions on Communications*, Vol. COM-28, No. 4, April 1980, pp. 468–488.

[5] C. J. Wolejsza, D. Taylor, M. Grossman, and W. P. Osborne, "Multiple Access Protocols for Data Communications via VSAT Networks," *IEEE Communications Magazine*, Vol. 25, No. 7, July 1986, pp. 30–39.

[6] N. Abramson, "The ALOHA System: Another Alternative for Computer Communications," *AFIPS Conference Proceedings*, Vol. 37, 1970, pp. 281–285.

[7] L. Kleinrock and S. S. Lam, "Packet-Switching in a Slotted Satellite Channel," *AFIPS Conference Proceedings*, Vol. 42, 1973, pp. 703–710.

[8] J. I. Capetanakis, "Generalized TDMA: The Multi-Accessing Tree Protocol," *IEEE Transactions on Communications*, Vol. COM-27, No. 10, October 1979, pp. 1476–1484.

[9] S. Tasaka, "Multiple Access Protocols for Satellite Packet Communication Networks: A Performance Comparison," *Proc. IEEE*, Vol. 72, No. 11, November 1984, pp. 1573–1582.

[10] F. Borzonova and L. Fratta, "SRUC, A Technique for Packet Transmission on Multiple Access Channels," 4th International Conference on Computer Communications, Kyoto, Japan, September 1978, *Proc.*, pp. 601–607.

[11] H. W. Lee and J. W. Mark, "Combined Random/Reservation Access for Packet Switched Transmission Over a Satellite With On-Board Processing: Part I—Global Beam Satellite," *IEEE Transactions on Communications*, Vol. COM-31, No. 10, October 1983, pp. 1161–1171.

[12] Y. Ishibashi and S. Tasaka, "Performance Evaluation of the Split Reservation Upon Collision (SRUC) Protocol for Satellite Packet Communication" (in Japanese), *Transactions of the IECE Japan*, Vol. J65-B, September 1982, pp. 1077–1084.

[13] T. P. Yum, "The Design and Analysis of the Scheduled-Retransmission Multiaccess Protocol for Packet Satellite Communications," IEEE International Conference on Communications, Seattle, Washington, 1987, *Proc.*, pp. 278–283.

[14] S. Tasaka and K. Ishida, "The SRUC Protocol for Satellite Packet Communication—A Performance Analysis," *IEEE Transactions on Communications*, Vol. COM-34, No. 9, September 1986, pp. 937–945.

[15] D. Raychaudhuri, "Announced Retransmission Random Access Protocols," *IEEE Transactions on Communications*, Vol. COM-33, No. 11, November 1985, pp. 1183–1190.
[16] I. Jacobs *et al.*, "CPODA—A Demand Assignment Protocol for SATNET," ACM/IEEE 5th Data Communications Symposium, Snowbird, Utah, September 1977, *Proc.*, pp. 2-5 to 2-9.
[17] D. M. Chitre and J. S. McCoskey, "VSAT Networks: Architectures, Protocols, and Management," *IEEE Communications Magazine*, Vol. 26, No. 7, pp. 28–38.
[18] D. Taylor, Private communication, September 24, 1987.
[19] K. Joseph and D. Raychaudhuri, "Simulation Models for Performance Evaluation of Satellite Multiple Access Protocols," *IEEE Journal on Selected Areas in Communications*, Vol. SAC-6, No. 1, January 1988, pp. 210–222.

Larry C. Palmer received a B.S. from Washington and Lee University and a B.E.E. from Rensselaer Polytechnic Institute, both in 1955, and an M.S. and Ph.D. in electrical engineering from the University of Maryland in 1963 and 1970, respectively. From 1955 to 1957, he served in the U.S. Army Signal Corps as an Electronics Officer. Following this, he spent 6 years with the Radcom–Emertron Division of Litton Systems, where he was engaged in the design and development of airborne electronics systems. In 1963, he joined ITT INTELCOM and worked on the military communications satellite system. After the acquisition of INTELCOM by Computer Sciences Corporation in 1965, he was involved in systems analysis, modeling, and simulation related to communications and navigation satellite systems.

Dr. Palmer joined COMSAT Laboratories in 1974 and is currently Principal Scientist in the Communications Technology Division. He served as Program Manager for COMSAT's participation in the DARPA SATNET program, and was Systems Engineering Project Manager for the NASA Advanced Communications Technology Satellite (ACTS) program under subcontract to RCA. He is a Senior Member of IEEE, and a member of the IEEE Communications Society, the IEEE Information Theory Group, Tau Beta Pi, and Eta Kappa Nu.

Peter Y. Chang received a B.S.E.E. in 1966 from Cheng Kung University, Taiwan, China, and an M.S.E.E., M.Ph., and Ph.D. from Columbia University in 1969, 1972, and 1975, respectively. He joined COMSAT Laboratories in 1976 and is currently a Staff Scientist in the Systems Modeling and Analysis Department of the Communications Technology Division. His work at COMSAT has included TDMA and FDMA modulation, digital signal transmission, intermodulation analysis involving the nonlinear effect of transponders, direct-broadcast (TV, video, and audio) satellite transmission systems, intersatellite links, simulation of satellite marine and mobile communications systems with fading channels, and simulation of digital signal performance in satellite channels involving various modulation and coding schemes. Recently, he was involved in the NASA ACTS project, including low-bit-rate system study analysis and simulation, and the analysis, modeling, and simulation of rain fade effects. He has also worked on the modeling and simulation of a TDMA random-access-with-notification network for the VSAT system. He is currently involved in the study, simulation, and analysis of spread spectrum techniques. Prior to joining COMSAT, Dr. Chang was with the Satellite Communications Division of Computer Sciences Corporation. He is a member of IEEE, Eta Kappa Nu, and Sigma Xi.

CTR Notes

Dependence of mean opinion scores on differences in lingual interpretation

H. G. SUYDERHOUD

(Manuscript received November 24, 1987)

Introduction

The quality of speech received through telephone connections has for many years been quantified by a numeric called the mean opinion score (MOS). In English, the MOS is derived by averaging the numerical equivalents of the subjective judgment qualifiers *excellent* (5), *good* (4), *fair* (3), *poor* (2), and *bad* (1), obtained from a large number of persons after they have listened to a sample of telephone speech. This method of rating the quality of telephone speech has been standardized by the International Telegraph and Telephone Consultative Committee (CCITT) [1] and is used extensively by administrations and organizations around the world. The five words for expressing subjective judgment have been translated into various languages using, as closely as possible, words of equivalent meaning. The methodology of testing has also been standardized, including the use of equivalent test sentences, specified test circuits and telephone handsets, and specified listening levels.

Despite this effort, technically identical systems will not yield the same MOS value when evaluated in different languages. This is probably due to residual semantic differences resulting from translation; that is, the opinion equivalents of the subjective judgment qualifiers (*excellent*, *good*, *fair*, *poor*, and *bad*) are different in different languages. Minor semantic differences also exist between individuals speaking the same language.

It is desirable to define a method that reconciles existing semantic differences to enable meaningful comparison of results. This note describes a numerical method which reduces the observed spread of subjective ratings to the extent that an MOS value resulting from testing in one country with language A

Henri G. Suyderhoud, formerly with COMSAT, is the Washington representative of OKI America, Inc. (New York office), and also works as a consultant.

(obtained through a technically specified system) can be converted to an estimated MOS value in another country with language B.

As with all prediction techniques, the accuracy of this method of "cross-language prediction" is limited. Its level of accuracy is demonstrated by applying standard statistical measures of confidence, which are basically a ratio of variances.

Reasons for the investigation

In an effort to standardize a 32-kbit/s adaptive differential pulse-code modulation (ADPCM) algorithm (presently known as CCITT Recommendation G.721), the CCITT assembled an international team to obtain the quality of the algorithm under various operating conditions and in seven languages. The same ADPCM hardware was used as part of a test bed to process prerecorded tapes with test sentences in each language. The format, level, and language content (*i.e.*, meaning) of the source tapes were carefully controlled, and speech samples were prepared by engineers in China, France, West Germany (F.R.G.), the U.K., Italy, Japan, and the U.S. After the test sentences were processed and recorded in a common test bed, the test material was returned to the various countries and evaluated over prescribed systems to ensure uniformity of conditions.

The results of these tests showed two aspects quite clearly. One was that a fair degree of consistency existed within each country and its language, in that higher MOS values were obtained for less distorted speech, while lower values resulted for more distorted speech. However, the absolute ratings between countries for equally distorted speech varied significantly. This result was an engineering dilemma, which was resolved by applying some standard statistical tools.

To provide a basis for relative evaluation, certain test conditions were included as "anchor" or reference conditions. These consisted of speech processed with carefully specified (and equal) noise conditions for all languages. These conditions are known as *injected noise* (I-noise) and *speech-correlated noise* (Q-noise). I-noise is the well-known additive Gaussian noise inserted at a specified constant level, while Q-noise is added proportional to the short-term power content of the speech, in approximately 20-ms increments. As expected, Q-noise proved to be much less disturbing than I-noise for the same signal-to-noise ratio (S/N). Q-noise is also more representative of quantizing noise produced by digital codecs [2], as has been demonstrated in many experiments since the concept was first proposed by Law and Seymour [3] about 15 years ago. Consequently, it will be used here as the underlying database for developing the comparison methodology.

Comparison methodology

As mentioned above, each country obtained a set of data by means of a subjective test, relating Q-noise to MOS, in their native language. The results of these tests are given in Figure 1 in the form of smoothed curves of MOS as a function of Q (the ratio of speech power to speech-correlated noise power, in dB). By averaging the MOS values of this set of curves, a single "world average" MOS *vs* Q curve is obtained and serves as a universal norm. Subsequently, the average deviation of the individual national MOS *vs* Q values from the norm is calculated, forming a set of national correction values.

In order to express the subjective test results for any country in terms of another country, the difference between correction values is applied to translate, or predict, such results.

Database and methodology

Sixty-four test conditions were presented to subjects in seven countries for evaluation in order to assess the subjective performance of the 32-kbit/s ADPCM algorithm specified in CCITT Recommendation G.721. The test conditions having speech-correlated noise were selected as the basis for developing the comparison methodology [4].

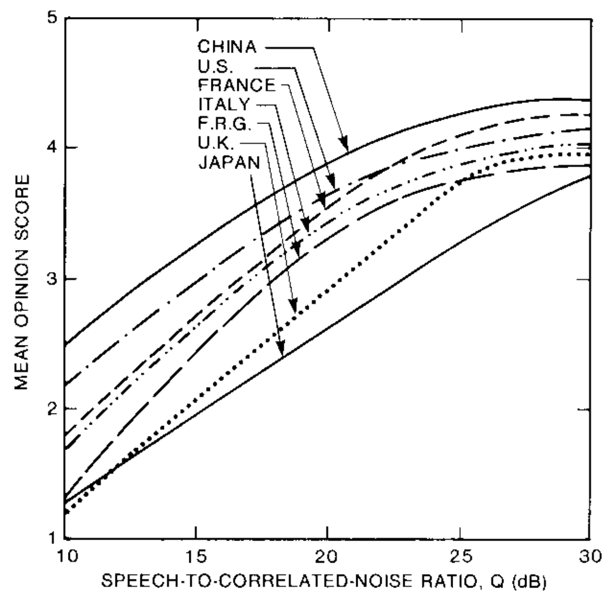

Figure 1. *Assessment of Q-Noise by Seven Nations*

Figure 1 shows smoothed curves of MOS obtained in seven countries as a function of Q, over the range of Q-values between 10 and 30 dB. The wide spread between the curves demonstrates the fundamental problem being addressed. The spread between countries is as much as 52 percent of the range of obtained MOS scores over the entire Q interval; however, the curves are very similar in shape (*i.e.*, positive slopes and general curvature toward a horizontal asymptote). Four curves intersect, but mostly near the extreme ends of the range.

It is possible to formally calculate the MOS values, averaged over the seven countries, as a function of Q. This function, shown in Figure 2, fits the following equation over the range of Q:

$$f_{wa}(Q) = -1.1744 + 0.32697\,Q - 0.00508\,Q^2 \quad ; \quad 10 \leq Q \leq 30 \text{ dB} \tag{1}$$

and will be called the *world average function of Q*. Similarly, equations have been fitted through test results for each individual country, j, using the generalized expression

$$f_j(Q) = a_o + a_1 Q + a_2 Q^2 \quad . \tag{2}$$

For the data of the seven countries used here, the coefficients a_i of this expression are given in Table 1.

It is useful to express the inverse functional relationship also [*i.e.*, letting $f_j(Q) = M$], as

$$Q = -\frac{a_1}{2a_2} + \frac{1}{2a_2}\left[a_1^2 + 4a_2(M - a_0)\right]^{1/2} \quad . \tag{3}$$

In general, let $M = f(Q)$ and $Q = f^{-1}(M)$.

The MOS correction term $\Delta_j(Q_i)$ has been defined for country j (= 1, . . . , 7) as

$$\Delta_j(Q_i) = f_{wa}(Q_i) - f_j(Q_i) \quad , \tag{4}$$

which is the difference between the world average of equation (1) and the national $f_j(Q)$ curve of country j at a value of Q_i, as determined by equation (2), for an MOS value scored when subjectively testing condition i. This is illustrated in Figure 3 for the case of a U.S. MOS value, M, of 3.87 for ADPCM (condition i), which translates to 3.68 after the correction of equation (4) is applied. Corrections were calculated for the same test condition i (ADPCM single link) evaluated in six other countries, resulting in the data given in Table 2.

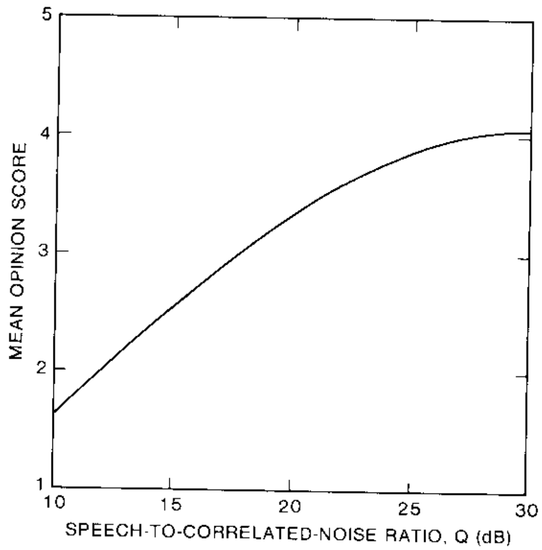

Figure 2. *World Average of MOS as a Function of Q*

The variance of the original MOS values is 0.1102. After correction, the variance was reduced to 0.0076, while the average value as given in Table 2 remained unchanged. The reduction in spread can be measured statistically or by calculating prediction gain. Statistically, the ratio of these two variances (F-distribution) has the value 15.26, which is highly significant (<0.005), implying that the correction was meaningful.

TABLE 1. a_0, a_1, a_2 COEFFICIENTS OF MOS $= a_0 + a_1 Q + a_2 Q^2$

COUNTRY	a_0	a_1	a_2
China	0.17530	0.27768	−0.00460
U.S.	0.08020	0.24514	−0.00357
France	−1.18465	0.34975	−0.00562
Italy	−1.17090	0.34552	−0.00570
F.R.G.	−2.67870	0.40820	−0.00703
U.K.	−1.00000	0.24604	−0.00254
Japan	0.26999	0.16587	−0.00103

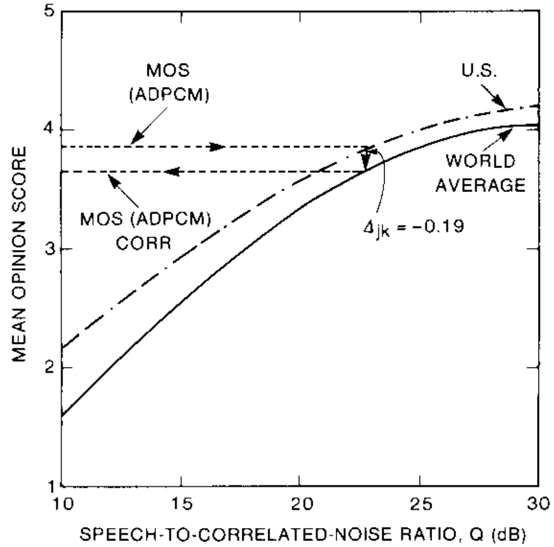

Figure 3. *Defining the Correction Δ_{jk} of the U.S. National Average to the World Average*

TABLE 2. MOS CORRECTIONS APPLIED TO ADPCM SINGLE LINK (Q_i = 23 dB)

COUNTRY	ORIGINAL SCORE	CORRECTED SCORE
China	4.27	3.82
U.S.	3.87	3.68
France	3.90	3.65
Italy	3.70	3.65
F.R.G.	3.46	3.62
U.K.	3.51	3.75
Japan	3.28	3.82
Average	3.71	3.71
Standard Deviation	0.332	0.084

As a further step in this development, the following average MOS correction factor relative to the world average has been defined for each country, j, as

$$\Delta_j = \frac{1}{Q_{\max} - Q_{\min}} \int_{Q_{\min}}^{Q_{\max}} [f_{wa}(Q) - f_j(Q)]\, dQ \quad . \tag{5}$$

The resulting values of Δ_j have been calculated and are given in Table 3.

TABLE 3. AVERAGE MOS CORRECTION FACTORS (Δ_j) OF SEVEN COUNTRIES

COUNTRY	j	Δ_m
China	1	−0.572
U.S.	2	−0.272
France	3	−0.211
Italy	4	−0.106
F.R.G.	5	+0.111
U.K.	6	+0.344
Japan	7	+0.563

The values in Table 3 can be used to estimate the performance results of a processing technique in country j, after results from country k have been obtained by subjective tests. The following prediction equation is proposed. Designating the test condition, T_i (including ADPCM, PCM, and tandem connections) for which an MOS of $M_k(T_i)$ has been obtained by country k, the estimate for country j can simply be determined by

$$M_j(T_i) = M_k(T_i) + (\Delta_k - \Delta_j) \quad . \tag{6}$$

For example, knowing from Reference 4 that the resulting MOS score from France for two asynchronously tandem ADPCM links was 3.66, the estimated values for the other countries can be obtained from equation (6), as presented in Table 4. Since this condition was evaluated by each country, the actual MOS values are also given, from which the residual values in Table 4 were calculated.

TABLE 4. ESTIMATED MOS SCORES FOR TWO ASYNCHRONOUSLY TANDEM ADPCM LINKS FROM FRENCH SCORE (3.66)

COUNTRY	ESTIMATED MOS	ACTUAL VALUE*	RESIDUAL
China	4.02	3.92	0.10
U.S.	3.60	3.56	0.04
Italy	3.55	3.53	0.02
F.R.G.	3.34	3.44	−0.10
U.K.	3.11	3.38	−0.27
Japan	2.88	2.94	−0.06

* Reference 4, p. 781, condition 20.

A number of standards of prediction accuracy were applied. First, it can be argued that since there is an inherent spread in assessment between countries, that same spread should be reflected in the predicted values. Statistically, then, the variance of predicted values should not differ significantly from that of the actual values. This is demonstrated by observing that

$$\sigma_a^2/\sigma_p^2 = 0.79 \text{ (not significant)}$$

where σ_a^2 is the variance of actual scores and σ_p^2 is the variance of predicted scores. Second, the variance of the applied correction factors $(\Delta_k - \Delta_j)$ should be significantly larger than the variance of the residuals after prediction. This is demonstrated by observing that

$$\sigma_c^2/\sigma_r^2 = 5.16 \text{ (significant at 0.05)}$$
$$\sigma_c^2 = \text{variance of corrections}$$
$$\sigma_r^2 = \text{variance of residuals.}$$

For the latter test, the term "significant" is applied whenever the theoretical value of the 0.10 (1-in-10) probability is exceeded. This is reasonable* because the national correction factors are averages and include an inherent variation, exhibited by the fact that each national Q-curve is not equidistant from the world average.

A third measure of success in applying equation (6) is the prediction gain. It is defined as

$$G_p = 20 \log \frac{\Sigma|\text{deviation without prediction}|}{\Sigma|\text{deviation with prediction}|} \quad , \qquad (7)$$

giving a logarithmic improvement factor due to prediction, in terms of the ratio of mean deviations from actual values before and after prediction.

A random sample of conditions selected from Reference 4 was tested in this manner, and the results are given in Table 5. In general, the predicted results meet the statistical requirements of significance assumed here. This supports the confidence in using equation (6).

Conclusions

A method has been developed for estimating the MOS scores of test conditions for subjects in one country based on the MOS scores obtained

* It is customary to use the 1-in-20, or 0.05 significance level.

TABLE 5. STATISTICAL ANALYSIS AND PREDICTION GAIN RESULTING FROM EQUATIONS (6) AND (7)

CIRCUIT CONDITION EVALUATED	$\sigma^2_{act}/\sigma^2_{pred}$ [a]	$\sigma^2_{corr}/\sigma^2_{resid}$	G_{pred} (dB)	PREDICTED FROM RESULTS IN
PCM With BER = 10^{-3}	2.50	2.36[b]	8.0	Japan
ADPCM With Eight Tandem Links	0.96	5.99[c]	−3.5[d]	Italy
PCM With −15-dBm Input	1.02	3.47[c]	6.6	U.S.
ADPCM With BER = 10^{-4}	0.69	8.20[c]	5.6	U.K.
S/N = 45 dB, Carbon Microphone	1.64	3.76[c]	2.9	U.K.
ADPCM With Four Synchronous Tandem Links	0.71	3.45[c]	14.7	Japan
ADPCM	0.52	3.66[c]	15.6	China

[a] Statistical values in this column are not significant.
[b] Not significant.
[c] Significant (p = 0.10).
[d] Anomalous result. Statistical results indicate significance; however, a bias in the predicted values of about 0.4 MOS units resulted in negative prediction gain.

using subjects in another country. The difference in MOS values is attributed to differences in the perception of the language equivalents of the terms *excellent*, *good*, *fair*, *poor*, or *bad*. The estimate is based on a set of data consisting of MOS scores obtained by subjects in each country when testing with correlated noise at a ratio Q. Results obtained using a prediction equation are shown to produce statistically acceptable MOS values.

Of the seven countries for which data were analyzed, most provided generally stable and reliable results which can serve as a basis for meaningful prediction of performance in other countries. Some countries, perhaps two, simply exhibited greater variability, making prediction less accurate.

The average correction values given in Table 3 should be generally applicable to results obtained in other tests using digital speech processing techniques. It must be remembered that subjective testing always depends on the circumstances and people used to obtain the results. However, the general methodology given here could be valid in other tests if a Q database is collected as part of the experiments for such tests.

Acknowledgments

The author acknowledges with pleasure the review comments of S. J. Campanella and M. Onufry. In particular, Dr. Campanella provided changes and additions which clarified the subject of this note.

References

[1] CCITT, "Supplements to Series P Recommendations," Vth Plenary Assembly, Geneva, December 1972, Green Book, Volume V, Part II, Supp. 14.

[2] CCITT, "Modulated Noise Reference Unit (MNRU)," Recommendation P.70, VIIIth Plenary Assembly, Malaga-Torremolinos, October 1984, Red Book, Volume V, Part I, Sec. 6, 1984, pp. 111–114.

[3] H. B. Law and R. A. Seymour, "A Reference Distortion System Using Modulated Noise," *Proc. IEE*, Vol. 109, Part B, No. 48, November 1962, pp. 484–487.

[4] G. Williams and H. Suyderhoud, "Subjective Performance Evaluation of the 32-kbit/s ADPCM Algorithm," IEEE Global Telecommunications Conference, Atlanta, Georgia, November 1984, *Digest*, Vol. 2, pp. 778–785.

Geostationary satellite log for year end 1987

C. H. SCHMITT

(Manuscript received May 1988, revised July 11, 1988)

This note provides lists of current and planned geostationary satellites for the Fixed-Satellite Service (FSS), the Broadcasting-Satellite Service (BSS), the Radiodetermination-Satellite Service (RDSS), the Aeronautical Mobile-Satellite Service (AMSS), the Maritime Mobile-Satellite Service (MMSS), the Land Mobile-Satellite Service (LMSS), and the Space Research Service (SRS). The lists are ordered by increasing East longitude orbit position and update the previously published material [1] through December 1987.

Table 1 lists the satellites that are operating as of late December 1987, or satellites that are in orbit and are capable of operating. Satellites being moved to new orbital positions are shown at their planned final positions for 1988, unless another satellite using the same frequencies occupies the position, or the final planned position is not known. Refer to the Remarks column for further information.

Table 2 lists newly proposed and replacement satellites at their currently planned orbital positions. Planned satellites are listed when information has been published by the International Frequency Registration Board (IFRB), or when it has been learned that satellite construction has commenced. Additional technical characteristics may be obtained from the author, the country or organization listed in the table, or the referenced IFRB Circulars, as published weekly in the circulars' special sections [2].

Table 3 gives the codes used in Tables 1 and 2 that correspond to the frequency bands allocated to the space services listed above. Other space services, such as the Meteorological-Satellite (MetSat) Service and the Earth Exploration-Satellite Service, appear only when needed to document a satellite network shown in Tables 1 and 2.

Carl H. Schmitt, formerly with COMSAT, is Principal Engineer and President of Satellite Communications (SatCom) Consultants, Inc., 1629 K Street, N.W., Suite 600, Washington, DC 20006, (301) 654-5000.

The regions referred to in Table 3 are those defined in Article 8 of the *ITU Radio Regulations*, and are summarized as follows:

- *Region 1*: Africa, Europe, Mongolia, and the USSR
- *Region 2*: North and South America and Greenland
- *Region 3*: Asia (except for Mongolia and the USSR) and Australasia.

Information on exact frequencies, and additional information on technical parameters, is available and is updated regularly. The author invites inquiries and comments, and would appreciate receiving information on newly planned satellite networks as they become available.

Acknowledgments

Special thanks are due to E. Reinhart for his invaluable assistance in reviewing the author's work. The author also wishes to thank R. Groshan for his contributions to this research and for his dedication in the revision of data.

References

[1] C. H. Schmitt, "Geostationary Satellite Log for Year End 1986," *COMSAT Technical Review*, Vol. 17, No. 1, Spring 1987, pp. 201–265.

[2] *IFRB Circulars*, AR11/A/ . . . (refers to Article 11, Section 1, which contains advanced publication requirements) and AR11/C/ . . . (refers to Article 11, Section 2, which contains coordination requirements), and SPA/AA/ . . . or /AJ/ . . . These special sections may be obtained from the International Telecommunications Union, IFRB, CH 1211, Geneva 20, Switzerland.

TABLE 1. IN-ORBIT GEOSTATIONARY COMMUNICATIONS SATELLITES FOR YEAR END 1987

Subsatellite Longitude[a]	Launch Date Object/Catalog Number[b]	Satellite Designation[c]	Country or Organization	Service	Frequency Code Up/Down-Link (GHz)	Remarks
1.4E	19 Jun 1981 12544	METEOSAT 2 (METEOSAT S2)	ESA (F)	MetSat	UHF/UHF,2	IFRB: 10W AR11/A/415/1815
3.6E	11 May 1978 10855	OTS 2 (OTS)	ESA (F)	FSS,BSS	14a/11	Experimental IFRB: 5E Notified SPA-AA/90/1194
7.1E	04 Aug 1984 15158	ECS (EUTELSAT 2-7E)	EUTELSAT-ESA (F)	FSS,STS[d]	14a/11	IFRB: 7E In Coordination A/305/1732 C/1205/1809
9.9E	16 Sep 1987 13851	ECS 4	ESA			AR11/A/305/1732 Incl. 6.7° AR11/C/1205/1809
13.3E	16 Jun 1983 14128	ECS 1 (EUTELSAT 1)	EUTELSAT-ESA	FSS	14a,11	IFRB: 10E AR11/A/229/1370 AR11/C/444/1644 AR11/C/1077/1789
19.1E	08 Feb 1985 15560	ARABSAT 1 (ARABSAT 1-A)	Arab League	FSS,BASS	6/4,2.6b,2.6c	IFRB: 19E AR11/A/278 AR11/C/330 AR11/A/7/1347 AR11/C/1/1597

TABLE 1. IN-ORBIT GEOSTATIONARY COMMUNICATIONS SATELLITES FOR YEAR END 1987 (CONT'D)

Subsatellite Longitude[a]	Launch Date Object/Catalog Number[b]	Satellite Designation[c]	Country or Organization	Service	Frequency Code Up/Down-Link (GHz)	Remarks
21.4E	13 Dec 1973 6974	DSCS 1-B OPS 9434	US	FSS	UHF,8/UHF,7	Incl. 8.2° Drift 0.36°W/day
24.5E	19 Dec 1978 11158	GORIZONT 1	USSR	FSS	6/4a	
26.0E	18 Jun 1985 15825	ARABSAT 1-B (ARABSAT 1-B)	Arab League	FSS,BSS	6/4, 2.6b, 2.6c	IFRB: 26E AR11/A/211/1347 AR11/C/173/1388
34.4E	26 Nov 1982 13669	RADUGA 11 (STATSIONAR 2)	USSR	FSS	6/4	IFRB: 35E SPA-AA/76/1179 C/26/1251 Incl. 3.36°
35.5E	15 Sep 1985 16250	RADUGA 17 (STATSIONAR D3)	USSR	FSS	6/4	IFRB: 35E AR11/A/195/1625
40.5E	28 Dec 1979 11648	GORIZONT 3 (STATSIONAR 12)	USSR	FSS	6,8/4,7	IFRB: 40E SPA-AA/271/1425 AR11/C/878/1737 Incl. 6.18°
45.8E	25 Oct 1986 17046	RADUGA 19 (STATSIONAR D4)	USSR	FSS	6/4	IFRB: 45E AR11/A/196/1675
46.5E	20 Feb 1980 11708	RADUGA 6	USSR	FSS	6/4	Incl. 5.6°
47.5E	30 Sep 1983 14377	EKRAN 11 (STATSIONAR T2)	USSR	BSS	6/UHF	IFRB: 99E SPA 2-3-AA/10/1426 C/7 Incl. 3.5°
49.4E	26 Jun 1981 12564	EKRAN 7	USSR	BSS	6/UHF	AR11/A/151 AR11/C/86 Incl. 4.52°
52.7E	18 Jan 1985 15484	GORIZONT 11 (STATSIONAR 7)	USSR	FSS	6,8/4,7	IFRB: 140E Incl. 1.3 SPA-AJ/31/1251 AR11/C/1118/1793
58.6E	26 Oct 197 9503	EKRAN 1	USSR	BSS	6/UHF	
59.7E	30 Oct 1982 13636	DSCS II (USGCSS PH2 IND OC)	US-Govt.	FSS	UHF,8/UHF,7	IFRB: 60E Notified SPA-AA/1271353 Incl. 2.4°
61.7E	28 Sep 1985 16101	INTELSAT VA F-12 (INTELSAT VA IND 1)	INTELSAT	FSS	6,14a/4,11	IFRB: 60E AR11/A/67/1580 C/462 Final Registration
62.4E	14 Dec 1978 11145	OPS 9442 DSCS II-C	US Govt.	FSS,MMSS	UHF,8/7,UHF	IFRB: 60E Incl. 4.5° Drift 0.13°E/day
62.9E	28 Sept 1982 13595	INTELSAT V F-5 (INTELSAT V IND OC 1)	INTELSAT	FSS	6,14a/4,11	IFRB: 63E Notified SPA-AA/134/1250 C/59
		(INTELSAT MCS IND OC A)	INMARSAT Lease	MMSS	1.6b,6/4, 1.5a	IFRB: 63E Maritime Package SPA-AA/214/1348 AR11/C/1096/1791 Final Registration

TABLE 1. IN-ORBIT GEOSTATIONARY COMMUNICATIONS SATELLITES FOR YEAR END 1987 (CONT'D)

Subsatellite Longitude[a]	Launch Date Object/Catalog Number[b]	Satellite Designation[c]	Country or Organization	Service	Frequency Code Up/Down-Link (GHz)	Remarks
63.0E	26 Dec 1980 12120	EKRAN 6	USSR	BSS	6/UHF 2/20	Incl. 5°
65.9E	19 Oct 1983 14421	INTELSAT 5 F-7 (INTELSAT V IND 4)	INTELSAT	FSS	6,14a/4,11	IFRB: 66E SPA-AA/253/1419 SPA-AJ/375/1511 Notified
		(MCS IND OC D)	INMARSAT Lease	MMSS	1.6b,6/1.5a,4	IFRB: 66E SPA-AA/275/1425 AR11/C/857/1735
71.7E	23 Nov 1984 7547	SKYNET 2B	UK	FSS	6/4	AR11/C/182 Drift 0.4473°W/day Incl. 7.72
72.3E	May 1979 11353	OPS 6392 (FLTSATCOM IND OC)	US-Govt.	FSS	UHF,8/UHF,7	IFRB: 72E AR11/A/338/1762 Incl. 4.7°
72.5E	10 Jun 1976 8882	MARISAT F-2 (MARISAT 2)	US-COMSAT General	MMSS	UHF 1.6b,6/4 UHF 1.5a	Spare, but unused except for UHF transponder. AR11/A/208/1344
73.0E	25 Apr 1979 11343	RADUGA 5	USSR			
73.9E	03 Aug 1983 14318	INSAT 1B (INSAT 1B)	India	FSS	6/4	IFRB: 74E SPA-AA/208/1344 AR11/C/231/1429 Notified
74.4E	13 Mar 1977 9862	PALAPA 2 (PALAPA A-2)	Indonesia	FSS	6/4	IFRB: 77E SPA-AA/45/1160 Notified Backup for PALAPA B-1.
74.7E	15 Feb 1984 14725	RADUGA 14 (STATSIONAR 3)	USSR	FSS	6/4	IFRB: 85E Notified SPA-AA/77/1179 SPA-AJ/27/1251 Incl. 2.3°
76.0E	08 Apr 1983 13974	RADUGA 12	USSR	FSS	6/4	Incl. 2.28°
76.0E	24 Aug 1984 15219	EKRAN 13	USSR	BSS	6/UHF 1.5a,4	Incl. 3.94° INMARSAT Spare
79.6E	01 Aug 1984 15144	GORIZONT 10 (STATSIONAR 13)	USSR	FSS	6,8/4,7	IFRB: 80E SPA-AA/276/1426 AR11/C/598/1737 AR11/C/1124/1793 Incl. 1.7°
81.0E	03 Oct 1979 11561	EKRAN 4	USSR	BSS	6/UHF	
81.6E	09 Oct 1981 12897	RADUGA 10	USSR	FSS	6/4	
82.0E	08 Jul 1976 9009	PALAPA 1 (PALAPA A1)	Indonesia	FSS	6/4	Near Retirement IFRB: 83E AR11/45/1339 Notified Incl. 2.3°

TABLE 1. IN-ORBIT GEOSTATIONARY COMMUNICATIONS SATELLITES FOR YEAR END 1987 (CONT'D)

Subsatellite Longitude[a]	Launch Date Object/Catalog Number[b]	Satellite Designation[c]	Country or Organization	Service	Frequency Code Up/Down-Link (GHz)	Remarks
85.3E	19 Mar 1987 17611	RADUGA 20 (STATSIONAR D5)	USSR	FSS	6/4	IFRB: 85E AR11A/197/1675
86.2E	11 Sep 1976 9416	RADUGA 2 (STATSIONAR 3)	USSR	FSS	6/4	IFRB: 85E SPA-AJ/27/1251
88.0E	20 Sep 1977 10365	EKRAN 2	USSR	BSS	6/UHF	
89.0E	22 Mar 1985 15626	EKRAN 14	USSR	BSS	6/UHF	
89.2E	18 Nov 1986 17083	GORIZONT 13 (STATSIONAR 6)	USSR	FSS	6/4	IFRB: 90E A/108 SPA-AJ/30/1251
90.4E	05 Jul 1979 11440	GORIZONT 2 (STATSIONAR 6)	USSR	FSS	6/4	IFRB: 90E A/108 SPA-AJ/30/1251
95.8E	15 Mar 1982 13092	GORIZONT 5 (STATSIONAR 14)	USSR	FSS	6,8/4,7	AR11C/306 IFRB: 95E Then moves to IFRB: 96.5E AR11/C/1181/1002
97.0E	26 Jun 1984 14940	GORIZONT 9	USSR	FSS	6/4	
99.0E	16 Mar 1981 14821	EKRAN 12	USSR	BSS	6/UHF	
99.1E	04 Sep 1987 18328	EKRAN 16	USSR	BSS	6/UHF	
99.2E	24 May 1976 16729	EKRAN 15	USSR		6/UHF	
103.0E	01 Feb 1986 16526	PRC 18	China, Peoples' Republic of	FSS	6/4	AR11/A/245/1695 AR11/C/1023/1777
104.7E	12 April 1985 15643	(SYNCOM IV-3) LEASESAT F-3 (LEASAT 3)	US-Govt.	FSS		AR11/A/222 AR11/C/242
108.1E	18 Jun 1983 14134	PALAPA B-1 (PALAPA B-1)	Indonesia	FSS	6/4	Domestic and Regional. IFRB: 108E SPA-AA/197/1319
110.0E	12 Feb 1986 16597	BS-2B	Japan	FSS	2,14a/12a, 12b,2	IFRB: 110E (BS-2) AR11/A/305 AR11/A/334, ADD-1/1762
110.0E	23 Jan 1984 14659	YURI 2A (BS-2A)	Japan	BSS	2,14a/12a,2	IFRB: 110E AR11/A/197
113.0E	21 Mar 1987 17706	PALAPA B-2 (PALAPA 2B) PALAPA B-2P	Indonesia			AR11/A/305 AR11/C/10 Drift 0.0230°W/day IFRB: 113E

TABLE 1. IN-ORBIT GEOSTATIONARY COMMUNICATIONS SATELLITES FOR YEAR END 1987 (CONT'D)

Subsatellite Longitude[a]	Launch Date Object/Catalog Number[b]	Satellite Designation[c]	Country or Organization	Service	Frequency Code Up/Down-Link (GHz)	Remarks
115.3E	23 Feb 19778 9852	KIKU 2 (ETS 2) ETS II	Japan	Experi- mental		AA/91/1194 IFRB: 130E Notified SPA-AA/91/1194
117.6E	18 Mar 1981 12351	RADUGA 8	USSR			
125.0E	08 Apr 1984 14899	PRC 15 (STW 1)	China, Peoples' Republic of			IFRB: 125E SPA-AA/141/1255 SPA-AJ/239/1431
128.2E	22 Jun 1984 15057	RADUGA 15 (STATSIONAR 15)	USSR	FSS	6/4a	IFRB: 128E SPA-AJ/312/1469 APA-AJ/317/1473 AR11/A/307/1469 Incl. 2.03° Drift 0.0295°W/day Notified
132.0E	04 Feb 1983 13782	SAKURA 2A (CS-2A)	Japan	FSS	6,30a/4,20a	IFRB: 132E Drift 0.0190°W/day SPA-AA/256/1421 SPA-AJ/323/1490 Notified
135.0E	18 Feb 1987 18877	CS 3A (CS-3A)	Japan	FSS		AR11/A/212/1680 IFRB: 132E AR11/C/1128/1794
135.9E	05 Aug 1983 14248	CS 2B (SAKURA 2B)	Japan	FSS,STS[d]	6/4	IFRB: 136.0E Drift 0.0218°W/day SPA-AA/257/1421 SPA-AJ/325/1490
139.3E	11 May 1987 17969	GORIZONT 14	USSR	FSS	6/4	
139.7E	20 Oct 1982 13624	GORIZONT 6	USSR	FSS	6,8/4,7	Drift 0.0183°E/day
139.7E	30 Nov 1983 14532	GORIZONT 8 (STATSIONAR 6)	USSR	FSS	6,8/4,7	
140.2E	02 Aug 1984 15152	HIMAWARI 3 (GMS 3)	Japan		UHF,2/UHF,1	AR11/A/54/1563 AR11/C/474/1648 IFRB: 140E Drift 0.0201°W/day
141.0E	10 Aug 1977 12677	HIMAWARI 2 (GMS 2)	Japan			IFRB: 140E SPA-AA/242/1394 SPA-AJ/372/1510
150.0E	27 Aug 1987 18316	ETS 5	Japan			
155.0E	25 Aug 1983 14307	RADUGA 13	USSR	FSS	6/4	Drift 3.60°E/day
156.0E	28 Nov 1985 16275	AUSSAT 2 (AUSSAT 2) AUSSAT K2	Australia	FSS	14a,12b,12c	Incl. 0.02° SPA-AA/300/1456 AR11/C/296/1624 AR11/C/305/1624 Drift 0.0122°W/day Notified

TABLE 1. IN-ORBIT GEOSTATIONARY COMMUNICATIONS SATELLITES FOR YEAR END 1987 (CONT'D)

Subsatellite Longitude[a]	Launch Date Object/Catalog Number[b]	Satellite Designation[c]	Country or Organization	Service	Frequency Code Up/Down-Link (GHz)	Remarks
160.0E	27 Aug 1985 15993	AUSSAT 1 (AUSSAT 1) AUSSAT K-1	Australia	FSS	14a,12b,12c	Incl. 0.10° Drift 0.0124°W/day SPA-AA/299/1456 IFRB: 160E AR11C/296/1624 Notified
164.0E	01 Sep 1985 18350	AUSSAT III (AUSSAT 3) AUSSAT K-3	Australia (OTC)	FSS/BSS	14a,12b,12c	RES 33/C/5/1643 RES 33/C/5/1647 AR11/C/314/1624
169.6E	08 Aug 1985 15946	RADUGA 16 (STATSIONAR 9)	USSR	FSS	6/4	SPA-A5/51/1276
171.3E	31 Oct 1980 12046	FLTSATCOM 4 W PAC (FLTSATCOM W PAC)	US-Govt.	FSS	UHF,8/UHF,7	IFRB: 172E SPA-AA/86/1186 SPA-AJ/167/1382
174.0E	23 May 1981 12474	INTELSAT 5 F-1 (INTELSAT V PAC 1)	INTELSAT	FSS	6,14a/4,11	SPA-AJ/376/1511 IFRB: 174E Incl. 1.22°
174.5E	21 Nov 1979 11621	DSCS II-D OPS 9443	US			AJ/369/1730 Leased by Hughes
176.1E	14 Oct 1976 9478	MARISAT F-3 (MARISAT PAC) MARISAT 3	US-COMSAT General	MMSS	UHF,1.6b,6/ UHF,1.5a,4	Spare, but unused except for UHF transponder. IFRB: 176.5E SPA-AA/6/1101 SPA-AJ/25/1244 Drift 0.0035°W/day Notified Incl. 7.09°
177.0E	Jan 1978 10557	INTELSAT 4-A F-3 (INTELSAT IVA PAC OC2)	INTELSAT	FSS	6/4	IFRB: 177.0E AR11/A/332 AR11/C/692 Incl. 2.08° Drift 0.015°W/day
178.0E	20 Dec 1981 13010	MARECS A (MARECS PAC OC 1) MARECS 1	ESA-INMARSAT	MMSS	1.6b/6 1.5a,4	Spare (MARECS PAC 1) AR11/D/3/1551 SPA-AJ/242/1432 IFRB: 178.0E Incl. 2.00° Drift 0.0203°W/day
179.3E	21 Nov 1979 11622	DSCS II-E OPS 9444	US			Incl. 4.15°
180.0E (180.0W)	20 Dec 1985 14786	INTELSAT V F-8 (INTELSAT V PAC 3)	INTELSAT	FSS	6,14a/4,11	IFRB: 180E SPA-AA/225/1419 Drift 0.015°W/day AR11/C/682/1668 Incl. 0.0043°E/day
		MCS D (MCS PAC A)	INMARSAT Lease	MMSS	1.6b,6/1.5a,4	IFRB: 180E AR11/C/692/1669
180.8E (177.2W)	31 Aug 1984 15236	LEASAT 2 (LEASESAT F-2) SYNCOM IV-2	US-Govt.	FSS		AR11/A/222 AR11/C/242 A11/C/682
183.5E (176.5W)	09 Feb 1978 10669	FLTSATCOM 1 (FLTSATCOM-A W PAC) OPS 6391	US			IFRB: 177W AR11/A/335/1762 Incl. 6.25° Drift 0.0393°E/day

TABLE 1. IN-ORBIT GEOSTATIONARY COMMUNICATIONS SATELLITES FOR YEAR END 1987 (CONT'D)

Subsatellite Longitude[a]	Launch Date Object/Catalog Number[b]	Satellite Designation[c]	Country or Organization	Service	Frequency Code Up/Down-Link (GHz)	Remarks
185.0E (175.0W)	12 Apr 1985 15643	LEASAT 3 (LEASESAT F-3) SYNCOM IV-3	US-Govt.	FSS		In place of LEASESAT F-2 now at 175.5W.
190.6E (169.4W)	08 Aug 1985 15946	RADUGA 16	USSR			
197.3E (162.7W)	29 Aug 1985 15995	LEASAT 4 (LEASESAT F-4) SYNCOM IV-4	US			
211.0E (149.0W)	07 Dec 1966 2608	ATS 1	US	FSS	6/4	Incl. 12.3 Notified Experimental
217.1E (142.9W)	26 Oct 1982 13631	SATCOM V (SATCOM 5) ALASCOM AURORA SATCOM V F5	US-Alascom, Inc.	FSS	6/4	AR11/A/7 AR11/C/414/1630 Formerly RCA SATCOM F-5. IFRB: 143.0W Notified
221.0E (139.0W)	11 Apr 1983 13984	SATCOM VI RCA SATCOM VI GE SATCOM 1R RCA SATCOM 6	US-RCA	FSS	6/4	AR11/4/6
		(SATCOM I-R)	US-RCA	FSS	6/4	AR11/A/7 IFRB: 139W AR11/C/337
224.0E (136.0W)	16 Jun 1978 10953	GOES 3 (GOES WEST)	US-Govt.	FSS		SPA-AA/28/1147 Incl. 4.86° Drift 0.0322°W/day IFRB: 135W
225.1E (134.9W)	30 Oct 1982 13637	DSCS III PSCS 16 (USGCSS PH3 E PAC)	US-Govt.	FSS	UHF,8/UHF,7	AR11/A/139 IFRB: 135W
		PSCS 16 (USGCSS PH2 E PAC)	US-Govt.	FSS	--	SPA-AA/127/1353 Notified IFRB: 135W
		LEASESAT (USGCSS PH 3W PAC)	US-Hughes	FSS,STS[d]	7a,8/7b	Drift 0.0168°W/day SPA-AJ/344/1499 IFRB: 135W
226.0E (134.0W)	28 Jun 1983 14158	GALAXY 1 (USASAT 11-D) HUGHES GALAXY 1	US-Hughes Comm.	FSS	6/4	IFRB: 134W Notified AR11/A/120/1615 AR11/C/821/1696
229.0E (131.0W)	21 Nov 1981 12967	SATCOM III-R (US SATCOM 3-R) GE SATCOM 3R RCA SATCOM 3R	US-RCA	FSS	6/4	AR11/A/329 AR11/C/347/1625 IFRB: 131W Notified
229.1E (130.9W)	05 Oct 1980 12003	RADUGA 7	USSR	FSS		Drift 0.3505°W/day
230.6E (129.4W)	14 Dec 1978 11144	DSCS II-B OPS 9441	US-Govt.	FSS		AR11/C/347 Incl. 4.81 Drift 0.0336°E/day
232.2E (127.8W)	27 Aug 1985 15994	ASC 1 (ASC-1) CONTEL ASC-1	US-American Satellite Co.	FSS,STS[d]	6,14a/4,12a	AR11/A/202/1676 Incl. 0.01 IFRB: 128W

TABLE 1. IN-ORBIT GEOSTATIONARY COMMUNICATIONS SATELLITES FOR YEAR END 1987 (CONT'D)

Subsatellite Longitude[a]	Launch Date Object/Catalog Number[b]	Satellite Designation[c]	Country or Organization	Service	Frequency Code Up/Down-Link (GHz)	Remarks
235.0E (125.0W)	19 Jun 1985 15826	TELSTAR 3D (USASAT 20A) TELSTAR ATT 303	US-AT/T	FSS	6/4 (4/6)	Name changed to TELSTAR 3D. IFRB: 126W AR11/C/968/1769
237.5E (122.5W)	09 Jun 1982 13269	WESTAR 5 (WESTAR 5) WU WESTAR 5	US-Western Union	FSS	6/4	IFRB: 123W Notified AR11/A/5 AR11/C/284
240.0E (120.0W)	23 May 1984 14985	SPACENET I (GTE SPACENET 1)	US-GTE Spacenet	FSS	6/14a/4,12a	AR11/C/166, ADD-1/1682 IFRB: 120W In Coordination
242.5E (117.5W)	12 Nov 1982 13652	ANIK C3 (ANIK C3) TELESAT 5	Canada-TELESAT	FSS	14a/12a	AR11/C/69 AR11/A/138 IFRB: 117.5W Notified
243.5E (116.5W)	27 Nov 1985 16274	MORELOS-B (MORELOS 2)	Mexico	FSS	6,14a/4,12a	IFRB: 116.5W Notified AR11/C/387 Incl. 1.00°
246.5E (113.5W)	17 Jun 1985 15824	MORELOS-A (MORELOS 1)	Mexico	FSS	6,14a/4,12a	IFRB: 113.5W Notified AR11/A/28 AR11/C/386
246.8E (113.2W)	16 Jun 1977 10061	GOES 2	US			Not in Use Incl. 5.84°
249.6E (110.4W)	09 Nov 1984 15383	ANIK D2 (ANIK D-2)	Canada-TELESAT	FSS	14a/12a	AR11/A/358/1500 IFRB: 110.5W AR11/C/716/1673 Notified
250.0E (110.0W)	18 Jun 1983 14133	ANIK C2 (ANIK C-2) TELESAT 7	Canada-TELESAT	FSS	14a/12a	IFRB: 110W Notified AR11/A/137/1500 AR11/C/129/1533
251.7E (108.3W)	22 May 1981 12472	GOES 5 (GOES EAST)	US	FSS	6/4	IFRB: 75W AR11/A/28 Notified Incl. 1.17°
252.8E (107.2W)	15 Mar 1976 8747	LES 9	US Govt.	Experi-mental	6/UHF,7,4	Incl. 29.40°
253.6E (107.4W)	13 Apr 1985 15642	ANIK C1 (ANIK C-1)	Canada-TELESAT	FSS	14a/12a	IFRB: 107.5W Notified SPA-AA/357/1500 AR11/C/569/1649 AR11/C/728/1698

TABLE 1. IN-ORBIT GEOSTATIONARY COMMUNICATIONS SATELLITES FOR YEAR END 1987 (CONT'D)

Subsatellite Longitude[a]	Launch Date Object/Catalog Number[b]	Satellite Designation[c]	Country or Organization	Service	Frequency Code Up/Down-Link (GHz)	Remarks
254.7E (105.3W)	12 Aug 1969 4068	ATS 5 (ATS-5)	US-NASA	Experi- mental	UHF,6/UHF,7,4	IFRB: 105W Drift 7.001°W/day Incl. 9.45° Notified No Circulars
255.0E (105.0W)	28 Mar 1986 16649	GSTAR 2 (GSTAR 2) GTE GSTAR 2	US-GTE	FSS	14a/12a	IFRB: 105W Notified AR11/A/15/1525 AR11/C/1075/1784
255.3E (104.7W)	05 Nov 1967 3029	ATS 3 (ATS 3)	US-Govt.	Experi- mental		IFRB: 86W Notified No Circulars Incl. 12.06°
255.4E (104.6W)	12 Apr 1985 15643	LEASAT 3 SYNCOM IV-3	US			Incl. 1.38°
255.6E (104.4W)	26 Aug 1982 13431	ANIK D1 (ANIK D-1) TELESAT 6	Canada-TELESAT	FSS	6/4	IFRB: 104.5W AR11/A/297/1682 AR11/C/465/1724 Notified
256.2E (103.8W)	03 Nov 1971 5587	OPS 9431	US-Govt.	FSS	UHF,8/UHF,7	Drift 0.0371°W/day Incl. 9.72°
256.9E (103.1W)	08 May 1985 15677	GSTAR 1 (GSTAR 1) GTE G-STAR 1	US-GTE	FSS	14a/12a	IFRB: 103W AR11/A/15/1525 AR11/C/1073/1784
259.9E (100.1W)	05 Dec 1986 17181	USA 20	US			Incl. 4.31 Drift 0.0389°W/day
260.9E (99.1W)	15 Nov 1980 12065	SBS 1 (USASAT 6A) SBS 1 SBS F3	US-Satellite Business Systems	FSS	14a/12a	IFRB: 97W AR11/C/325/1624 AR11/A/34/1553 Notified
261.2E (98.8W)	26 Feb 1982 13069	WESTAR 4 (WESTAR 4) WU WESTAR 4	US-Western Union	FSS	6/4	IFRB: 99W AR11/C/272/1623 Notified
263.0E (97.0W)	24 Sep 1981 12855	SBS 2 (USASAT 6C) SBS 2	US-Satellite Business Systems	FSS	14a/12a	IFRB: 95W AR11/C/331/1624 Notified
264.1E (95.9W)	28 Jul 1983 14234	TELSTAR 301 (TELSTAR 3A) ATT TELSTAR 301	US-AT&T	FSS	6/4	IFRB: 97W AR11/A/8/1524 AR11/C/879/1738 AR11/C/332-336/1624
265.0E (95.0W)	11 Nov 1982 13651	SBS 3 (USASAT 6B) SBS 3 SBS F-2	US-Satellite Business Systems	FSS	14a/12a	IFRB: 99W SPA-A3/61/1280 Notified
266.5E (93.5W)	21 Sep 1984 15308	GALAXY III (USASAT 12B) HUGHES GALAXY 3 GALAXY 3	US-Hughes Comm.	FSS	6/4	IFRB: 93.5W AR11/A/22/1687 Notified
268.9E (91.1W)	30 Aug 1984 15235	SBS 4 (USASAT 9A) SBS 4	US-Satellite Business Systems	FSS	14a/12a	IFRB: 91W AR11/A/10/1609

TABLE 1. IN-ORBIT GEOSTATIONARY COMMUNICATIONS SATELLITES FOR YEAR END 1987 (CONT'D)

Subsatellite Longitude[a]	Launch Date Object/Catalog Number[b]	Satellite Designation[c]	Country or Organization	Service	Frequency Code Up/Down-Link (GHz)	Remarks
269.1E (90.9W)	10 Aug 1979 11484	WESTAR 3 (WESTAR 3) WU WESTAR 3	US-Western Union	FSS	6/4	IFRB: 91W AR11/A/37 AR11/C/197 To be replaced by WESTAR VI-5 in 1988. Notified
274.0E (85.0W)	01 Sep 1984 15237	TELSTAR 302 (USASAT 3C) TELSTAR 3C ATT TELSTAR 302	US-AT&T	FSS	6/4	IFRB: 86W AR11/C/246/1620 AR11/C/247-256/1620
274.9E (85.1W)	12 Jan 1986 16482	SATCOM-KU1 (USASAT 9C) GE K1	US		11/12	IFRB: 85W
277.0E (83.0W)	31 Dec 1986 NA	ASC 3 (USASAT 7-D) SATCOM KU2	US	FSS	6,14a/4,12a	IFRB: 81W AR11/A/12/1525 AR11/C/50/1568 AR11/C/257/1623 Notified
278.0E (82.0W)	16 Jan 1982 13035	SATCOM IV (USASAT 7B) RCA SATCOM IV GE SATCOM 4	US-RCA	FSS	6/4	IFRB: 83W AR11/C/188/1612 Drift 0.0355°W/day Notified
279.1E (80.9W)	28 Nov 1985 16276	SATCOM KU2 GE SATCOM K2	US			Drift 0.0121°E/day
279.4E (79.6W)	19 Dec 1974 7578	SYMPHONIE 1	West Germany			
281.0E (79.0W)	10 Oct 1974 NA	USASAT 12A (USASAT 12A)	US	FSS,STS[d]	6/4	AR11/C/892, ADD-1,ADD-2 1752 AR11/C/895,898 ADD-1/1762 IFRB: 29W
282.5E (77.5W)	09 Feb 1978 10669	FLTSATCOM (FLTSATCOM 1) OPS 6391	US-Govt.	FSS	UHF,8/UHF,7	SP4-AJ/163/1382 Incl. 6.06° Drift 0.0345°W/day
284.0E (76.0W)	Sep 1983 12309	COMSTAR D4 (USASAT 12C) COMSTAR 4 COMSAT COMSTAR 4	US-COMSAT General	FSS	6/4	IFRB: 76W Colocated with COMSTAR D-2. AR11/C/907/1748 AR11/C/907/ CORR-1/1785 Incl. 1.88° Drift 0.0243°W/day Notified
283.9E (76.1W)	22 Jul 1976 9047	COMSTAR D2 (USASAT 12C) COMSTAR 2	US-COMSAT General	FSS	6/4	IFRB: 76W AR11/C/907/1748 AR11/C/908-909/1748 Colocated with COMSTAR D-4. Drift 0.0171°W/day Incl. 3.48° Notified

TABLE 1. IN-ORBIT GEOSTATIONARY COMMUNICATIONS SATELLITES FOR YEAR END 1987 (CONT'D)

Subsatellite Longitude[a]	Launch Date Object/Catalog Number[b]	Satellite Designation[c]	Country or Organization	Service	Frequency Code Up/Down-Link (GHz)	Remarks
285.0E (75.0W)	26 Feb 1981 17561	GOES H (GOES EAST) GOES 7	US	FSS	6/4	IFRB: 75W Notified SPA-AA/28/1147 Drift 0.0398°W/day
286.1E (73.9W)	22 Sep 1983 14365	GALAXY 2 (USASAT 7A) HUGHES GALAXY 2	US-Hughes Comm.	FSS	6/4	IFRB: 74W Drift 0.0117°W/day SPA-AJ/166/1382 AR11/A/312 AR11/C/812
287.0E (73.0W)	26 Jan 1978 10637	IUE	USA			Incl. 30.94° Drift 0.0144°W/day
288.0E (72.0W)	08 Sep 1983 14328	SATCOM II-R (USASAT 8B) SATCOM VII GE SATCOM 2R Formerly RCA SATCOM 7	US-RCA	FSS	6/4	IFRB: 72W AR11/A/37 AR11/C/221
289.9E (70.1W)	28 Mar 1986 16650	SBTS 2 (SBTS A1)	Brazil	FSS	6/4	IFRB: 75.40W AR11/A/16 Notified
290.8E (69.2W)	12 Mar 1983 13878	EKRAN 10	USSR	BSS	6/UHF	Incl. 3.75° Drift 2.98°E/day
291.0E (69.0W)	10 Nov 1985 15385	SPACENET II (USASAT 7C) SPACENET 2	US-GTE Spacenet	FSS	6,14a/4,2a	IFRB: 69W In Coordination with USASAT 7C.
		(USASAT 7C) GTE SPACENET 2	US	FSS	6/4	AR11/A/1525 FCC: 69.0W IFRB: 69W
295.0E (65.0W)	08 Feb 1985 15561	SBTS 1 (SBTS A2)	Brazil	FSS	6/4	IFRB: 65W AR11/A/17 AR11/C/99 Notified
298.3E (61.7W)	15 Mar 1976 8746	LES 8	US			Incl. 21.45° Drift 0.0052°W/day
299.2E (60.7W)	28 Jan 1977 9785	NATO III-B	NATO			Incl. 5.1°
307.0E (53.0W)	15 Dec 1981 12994	INTELSAT V F-3 53W (INTELSAT 5 CONTINENTAL 1)	INTELSAT	FSS	6,14a/4,11	Maneuvered from 27W during Sep 1985. IFRB: 53W AR11/C/591 AR11/A/82/1588 AR11/C/674/1667 AR11/A/115/1609 Notified
307.5E (52.5W)	31 Dec 1986 NA	USGCSS PHASE 3 (USGCSS PH 3W ATL)	US	FSS	2/2	AR11/C/140/1596
316.8E (43.2W)	09 Sep 1980 11964	GOES 4	US	FSS	6/4	Incl. 1.25° Drift 0.0146°W/day AR11/A/75

TABLE 1. IN-ORBIT GEOSTATIONARY COMMUNICATIONS SATELLITES FOR YEAR END 1987 (CONT'D)

Subsatellite Longitude[a]	Launch Date Object/Catalog Number[b]	Satellite Designation[c]	Country or Organization	Service	Frequency Code Up/Down-Link (GHz)	Remarks
318.0E (42.0W)	05 Apr 1983 13969	TDRS EAST (TDRS EAST)	US-NASA US-Systematics Gen.	SRS,FSS	1,14d/2,13 6/4	IFRB: 41.0W Notified Incl. 2.30°
	05 Apr 1983 13969	TDRS 1 TDRS-A	US	FSS	6/4	IFRB: 41.0W AR11/A/231 AR11/C/46 AR11/A/158/1637 Same satellite, registered separately. Drift 0.0581°W/day
325.0E (35.0W)	7 Apr 1978 10792	YURI (BSE)	Japan			Incl. 1.25° Drift 1.0792°W/day
325.5E (34.5W)	5 Mar 1982 13083	INTELSAT 5 F-4 (INTELSAT V ATL 4)	INTELSAT	FSS	6,14a/4,11	IFRB: 34.5W Notified AR11/A/121
330.7E (29.3W)	22 Apr 1976 8808	NATO III-A (NATO 3A)	NATO	FSS	8/7	Incl. 6.19° AR11/A/1681 AR11/C/215
332.5E (27.5W)	29 Jun 1985 15873	INTELSAT V-A F-11 (INTELSAT 5A ATL 2)	INTELSAT	FSS	6,14a/4,11	IFRB: 27.5W Notified AR11/A/335 AR11/C/123
334.0E (26.0W)	10 Nov 1984 15386	MARECS B2 (MARECS ATL1)	ESA-leased to INMARSAT	MMSS	1.6b,6b/ 1.5a,4	Operational 1 Jan 1985 Pacific Ocean as Maritime Satellite. IFRB: 177.5E, 26W Notified Incl. 2.01°
335.0E (25.0W)	17 Jan 1986 16497	RADUGA 18	USSR	FSS	6/4	IFRB: 25.0W AR11/A/95 (STATSIONAR 8) AR11/C/50
335.0E (25.0W)	31 Dec 1987 NA	VOLNA 1-A	USSR	AMSS,LMSS		IFRB: 25W
335.0E[e] (25.0W)	Dec 1990 NA	VOLNA 1-M	USSR			IFRB: 25W
335.0E (25.0W)	30 Nov 1983 14532	GORIZONT 8 (STATSIONAR 8)	USSR	FSS		SPA-AJ/62/1280 IFRB: 25W
335.5E (24.5W)	22 Mar 1985 15629	INTELSAT 5A F-10 (INTELSAT 5-A ATL 1)	INTELSAT	FSS	6,14a/4,11	IFRB: 24.5W Notified
335.7E (24.3W)	05 Oct 1980 12003	RADUGA 7	USSR	FSS	5,6/3	Operates below INTELSAT V-A frequencies. Drift 0.3505°W/day
337.3E (22.7W)	18 Jan 1980 11669	FLTSATCOM 3 (FLTSATCOM-B E ATL) OPS 6393	US-Govt.	FSS	UHF,8/UHF,7	IFRB: 23.0W AR11/A/48/1561 ADD-1/1587 Incl. 4.30°

TABLE 1. IN-ORBIT GEOSTATIONARY COMMUNICATIONS SATELLITES FOR YEAR END 1987 (CONT'D)

Subsatellite Longitude[a]	Launch Date Object/Catalog Number[b]	Satellite Designation[c]	Country or Organization	Service	Frequency Code Up/Down-Link (GHz)	Remarks
338.5E (21.5W)	25 May 1977 10024	INTELSAT 4A F-4 (INTELSAT IV-A ATL 1)	INTELSAT	FSS	6/4	IFRB: 21.5W Notified Incl. 2.50°
339.4E (20.6W)	19 Nov 1978 15391	NATO III (NATO 3D)	NATO	FSS	20a,8/2.3,7	On 12/26/85 drifting at 0.04E. Incl. 3.23°
341.5E (18.5W)	19 May 1983 14077	INTELSAT V F-6 (INTELSAT 5 ATL 2)	INTELSAT	FSS	6,14a/4,11 1.5a,4	IFRB: 18.5W Notified
		INMARSAT Lease (MCS ATL A)	MMS	FSS	1,6b,6	IFRB: 18.5W MCA ATL A is a spare for MARECS B2.
342.3E (17.7W)	19 Nov 1978 11115	NATO I NATO III-C	NATO			Incl. 3.21°
344.6E (15.4W)	10 Nov 1984 15384	SYNCOM IV-1 LEASESAT 1 LEASAT F-1	US Govt.		UHF/UHF	
345.1E (15.3W)	19 Feb 1976 8697	MARISAT F-1 (MARISAT ATL) MARISAT A-1	US-COMSAT General	MMSS,FSS	UHF 1,6b,6/ UHF 1,5a,4	Spare, but only UHF transponder used. IFRB: 15W AR11/A/7/1101 AR11/C/33/1254 Notified
346.2E (13.8W)	10 Jun 1986 16769	GORIZONT 12	USSR	FSS	6/4	
348.8E (11.2W)	14 Jun 1980 11841	GORIZONT 4 (STATSIONAR 11)	USSR	FSS	6,8/4,7	IFRB: 11W In Coordination AR11/C/877/1737 Incl. 5.81°
344.0E (10.9W)	30 Jun 1983 14160	GORIZONT 7	USSR	FSS	6/4	
352.0E (8.0W)	04 Aug 1984 15159	TELECOM 1-A (TELECOM 1A)	France	FSS	2,6,8,14a/2,4, 7,12a,12b,12c	IFRB: 8W In Coordination AR11/A/268 AR11/C/84/1611 Notified
354.9E (5.1W)	08 May 1985 15678	TELECOM 1-B (TELECOM 1-B) TELECOM I-B	France	FSS	2,6,8,14a/ 2,4,7c, 12a,12b,12	IFRB: 5W AR11/C/472
358.8E (1.2W)	12 May 1977 10001	OPS 9438 DCSC II-A	US			AR11/C/121 Incl. 6.76°
359.0E (1.0W)	06 Dec 1980 12089	INTELSAT 5 F-2 (INTELSAT V CONT 4)	INTELSAT	FSS	6,14a/4,11	IFRB: 1W Notified AR11/A/83 AR11/C/593 Drift 0.0042°W/day

[a]The list of satellite longitudes was compiled from the best information available.
[b]Space objects that can be tracked are assigned an object/catalog number which is used by NASA and others.
[c]Satellite names in parentheses are IFRB satellite network names; common names appear above, alternate names appear below.
[d]Space tracking satellite.
[e]Longitude is as compiled in the NASA Synchronous Satellite Catalog for January 4, 1988.

NA: This information is not currently available; satellite network not confirmed as operational.

TABLE 2. PLANNED GEOSTATIONARY COMMUNICATIONS SATELLITES FOR YEAR END 1987

Subsatellite Longitude[a]	In-Use Date/ Period of Validity[b] (yr)	Satellite Designation[c]	Country or Organization	Service	Frequency Code Up/Down-Link (GHz)	Remarks
0.0E	30 Jun 1985/NA	SKYNET A	UK	FSS	8,0.3a,45/ 7,0.3a,#	AR11/C/183/1611 AR11/A/22/1531
1.0E	31 Dec 1992/20	STATSIONAR 22	USSR	FSS	6/4	AR11/A/410/1806
1.0E	31 Aug 1987/10	GDL 5	Luxembourg	FSS,BSS	6b,14a/11,12b	AR11/C/612/1657 AR11/C/612, CORR-1/1744
3.0E	198?/10	TELECOM 1C	France	FSS,BSS	6b,8,14/4,#,#	AR11/A/29/1339 AR11/C/116/ ADD-2 AR11/C/157/1598 AR11/C/131/1594 AR11/C/116/ ADD-2/1643
3.0E	30 Sep 1991/10	TELECOM 2C	France	FSS, MMSS	6,14/4,12b,12c 8/7 2/2.2	AR11/A/326/1745
5.0E	198?/7	TELE-X	Norway, Sweden	FSS,BSS	2,6,30a,17,20a/2, 12a,12b,20d	AR11/A/27/1535 AR11/C/446/1644 AR11/C/773/1674
6.0E	07 Jan 1990/10	SKYNET 4B	UK	FSS,MMSS	1,7,44/8	C/183/1661
6.0E	07 Jan 1990	SKYNET 4B	UK	FSS,MMSS	14c,17/12f,2,12b	AR14/C/82/1677 AR11/C/183/ ADD-1/1652 AR11/C/589/1652 AR11/C/183/1611 AR11/C/773/1674 AR11/D/121/ ADD-1/1811 AR11/D/121/1780
7.0E	1987/10	F-SAT 1	France	FSS	2,14a,12b,12c,20d	AR11/C/568/1648 AR11/A/79/1587 AR11/C/566-557/ 1648
7.0E	10 May 1985	EUTELSAT I-3	France/EUT	FSS,BSS	14a/11,12b	AR11/C/1709/ 1789
7.0E	31 Oct 1989/20	EUTELSAT II-7E	France/EUT	FSS,STS	14a/12f	AR11/A/342/ ADD-2/1782
8.0E	31 Dec 1987/20	STATSIONAR 18	USSR	FSS,BSS	6a,6b,6/4a	AR11/A/219/1686 AR11/C/911/1749 AR11/C/911/ CORR-1/1756 AR11/C/911/ ADD-1/1756
8.0E	31 Dec 1987/20	GALS 7	USSR	FSS	8/7	AR11/A/238/1693 AR11/C/913/1750 AR11/C/913/ ADD-1/A56

TABLE 2. PLANNED GEOSTATIONARY COMMUNICATIONS SATELLITES FOR YEAR END 1987 (CONT'D)

Subsatellite Longitude[a]	In-Use Date/ Period of Validity[b] (yr)	Satellite Designation[c]	Country or Organization	Service	Frequency Code Up/Down-Link (GHz)	Remarks
8.0E	31 Dec 1987/20	VOLNA 15	USSR	AMSS	UHF,1.6e/ UHF,1.5c	AR11/A/241/1693 AR11/C/983/1769
8.0E	08 Aug 1990/20	TOR 8	USSR	FSS,AMSS, LMSS,MMSS	43,45,20b	AR11/A/285/1710
10.0E	1986/10	APEX	France	BSS,FSS	6,30a/2,4,20b, 39,40	AR11/C/ 1583-584/1651 AR11/A/62/1578 AR11/C/79/1676
10.0E	31 Oct 1991/20	EUTELSAT II-10E	France/EUT	FSS,STS	13a,14a/11	AR11/A/349, ADD-1/1766 AR11/C/1286/1809
12.0E	1982/20	PROGNOZ 2	USSR	SRS	14a,2	SPA-AA/317/1471
13.0E	31 Dec 1987/7	ITALSAT	Italy	FSS	30a/2,20b,39,40	AR11/A/151/1633 AR11/C/827/1697
13.0E	01 Apr 1987/11	EUTELSAT I-2	EUTELSAT (F)	FSS,BSS	14a/11,12a,12b,12c	AR11/C/1078/1789
13.0E	31 Oct 1989/15	EUTELSAT II-13E	France/EUTELSAT	STS	2/2	AR11/A/306/1732 AR11/C/876/ ADD-2/1803 AR11/A/30/1732/ ADD-2/1782
14.0E	Jun 1981/NA	NIGERIAN NATIONAL SYSTEM	Nigeria	FSS	6/4	SPA-AA/209/1346 SPA-AA/227/1361
15.0E	1986/10	AMS 1	Israel	FSS,STS	6,14a/4,11	AR11/A/39/1554 AR11/B/30/1593 AR11/C/816, ADD-2/1803
15.0E	Dec 1990/20	STATSIONAR 23	USSR	FSS	6/4a	AR11/A/318/1740
15.0E	31 Dec 1990/20	TOR 12	USSR	FSS,AMSS, MMSS,LMSS	43, 45 20b	AR11/A/309/1736
15.0E	1986/10	AMS 2	Israel	FSS,STS	6,14a/4,11	AR11/A/39/1554 AR11/C/817/1695 AR11/C/817/ ADD-2/1803
15.0E	31 Dec 1990/20	GALS 12	USSR	FSS	8/7	AR11/A/313/1740 AR11/A/318/1760
15.0E	30 Apr 1992/10	ZENON-B	France	FSS,STS	2,6a#/1.5c,2	AR11/A/364/1781
16.0E	1987/NA	SICRAL 1-A	Italy	FSS,STS	8,14a,45/7,12b, 12c,20b,44	AR11/A/44/1588 AR11/A/44/ ADD-1/1652
16.0E	31 Jan 1986/11	EUTELSAT I-4	France/EUTELSAT	FSS/STS	14a/11,11,12b,12c	AR11/C/1080/ 1789 AR11/A/218/1685 AR11/C/874/ ADD-1/ CORR-1/1762/ 1737 AR11/C/10801789

TABLE 2. PLANNED GEOSTATIONARY COMMUNICATIONS SATELLITES FOR YEAR END 1987 (CONT'D)

Subsatellite Longitude[a]	In-Use Date/ Period of Validity[b] (yr)	Satellite Designation[c]	Country or Organization	Service	Frequency Code Up/Down-Link (GHz)	Remarks
17.0E	30 Apr 1992/20	SABS	Saudi Arabia	BSS,FSS	14a/12b,12c	SPA-AA/235/1387 AR11/C/171/1601 A/353/1768
17.0E	1988/20	SABS 1-2	Saudi Arabia	BSS,STS, FSS	14a,14a/12b,12a	AR11/A/125/1616
19.0E	Sep 1986/10	GDL 6	Luxembourg	FSS/BSS	6b,14a/11,12	AR11/A/94/1594/ ADD-1/1708 AR11/A/94/ ADD-2/1747
19.0E	30 Apr 1992	ZENON-C	France/MPT	FSS,STS	2,1.6d,14a/2,1.5c,11	AR11/A/365/1781
20.0E	06 Jun 1987/NA	NIGERIAN NATIONAL SYSTEM	Nigeria	FSS	6/4	SPA-AA/209/1346 SPA-AA/227/1361
22.0E	01 Jan 1987/8	SICRAL 1-B	Italy	MMSS/FSS	UHF,8,14a,45/7, 12b,12c,20b	AR11/A/45/1557 AR11/A/45/1588
23.0E	31 Dec 1987/20	STATSIONAR 19	USSR	FSS/BSS	6a,6b/4a	AR11/A/220/1686 AR11/C/916/1752 AR11/C/917/1952 AR11/C/1917 CORR-1/1756
23.0E	31 Dec 1987/20	GALS 8	USSR	FSS	8/7	AR11/A/239/ 16930 AR11/C/914/1750 AR11/C/914/ ADD-1/1756
23.0E	31 Dec 1987/20	VOLNA 17	USSR	AMSS,LMSS	UHF,1.6e/UHF,1.5c	AR11/A/242/1693 AR11/C/980/1769
23.0E	01 Aug 1990/20	TOR 7	USSR	FSS,MMSS LMSS,AMSS	43,45,20b	AR11/A/284/1710
23.5E	01 Jun 1987/10	DFS 1	Germany	FSS,STS	2,14,30/11,12b,12c, 20b	AR11/A/40/1556 AR11/C/696-697/ 1670 AR11/C/774/1681 AR11/C/779/1681
26.0E	30 Apr 1991/20	ZOHREH 2	Iran	FSS	14a/11	SPA-AA/164/1278 SPA-AJ/76/1303 AR11/C/5011/ 1776
28.5E	23 Mar 1988	DFS 2	Germany	FSS,STS	2,14/11,12b,12c, 20d,30	AR11/A/41/1556 AR11/C/117/1781
31.0E	01 Jan 1991	ARABSAT 1-C	Saudi Arabia	FSS	6/4	AR11/A/345/1764 AR11/B/ ADD-1/1800
32.0E	1987/10	VIDEOSAT 1	France	FSS	14a/2,12b,12c	AR11/A/80/1588 AR11/C/574/1650 AR11/C/580/1650 AR14/C/781/1676
34.0E	30 Apr 1991/20	ZOHREH 1	Iran	FSS	14a/11	SPA-AA/163/1278 AR11/A/296, ADD-1/1728 AR11/C/5000/ 1776

TABLE 2. PLANNED GEOSTATIONARY COMMUNICATIONS SATELLITES FOR YEAR END 1987 (CONT'D)

Subsatellite Longitude[a]	In-Use Date/ Period of Validity[b] (yr)	Satellite Designation[c]	Country or Organization	Service	Frequency Code Up/Down-Link (GHz)	Remarks
35.0E	01 Jan 1984/20	PROGNOZ 3	USSR	SRS	UHF/4a,2,#	SPA-AA/318/1471
35.0E	01 Aug 1990/20	TOR 2	USSR	FSS,AMSS, LMSS,MMSS	43,45/20b	AR11/A/279/1710
35.0E	31 Dec 1987/20	VOLNA 11	USSR	AMSS,LMSS	UHF,1.6d/UHF,1.5c	AR11/A/150/1631 AR11/C/977/1769
35.0E	31 Dec 1984/20	GALS 6	USSR	FSS	8/7	AR11/C/109/1578
36.0E	30 Jul 1990/20	EUTELSAT II-36E	France/EUTELSAT	STS,FSS	2/2	AR11/A/307/1732 AR11/A/75/1783
38.0E	31 Dec 1987	PAKSAT 1	Pakistan	FSS,STS	14a/11,12b,12c	AR11/A/90/1592 AR11/A/90, ADD-1/1779
40.0E	31 Dec 1988/20	LOUTCH 7	USSR	FSS,STS	14a/11	AR11/A/270/ CORR-1/1707 AR11/C/1046/1779
40.0E	10 Oct 1984/20	STATSIONAR 12	USSR	FSS	4a/#?	AR11/C/878/1737
41.0E	30 Jun 1992/20	ZOHREH 4	Iran	FSS	14a/11	SPA-AA/203/1330 AR11/A/394/1800
41.0E	31 Dec 1988/15	PAKSAT-II (PAKSAT-2)	Pakistan	FSS	14a/12b,12c	AR11/A/91/1592 AR11/A/91, ADD-1/1715
45.0E	30 Jun 1988/20	STATSIONAR-D4	USSR	FSS	6a#/4b	AR11/A/196/1675 AR11/C/1171/1796
45.0E	01 Dec 1990/20	VOLNA 3M	USSR	MMSS,AMSS, LMSS	#?,1.6b/1.5a	AR11/A/249/1697 SPA-AJ/98/1329
45.0E	01 Jan 1980/NA	GALS 2	USSR	FSS	8/7	SPA-AJ/112/1335
45.0E	NA	LOUTCH P2	USSR	FSS	14a/11	SPA-AA/178/1289
45.0E	01 Aug 1990/20	TOR 3	USSR	FSS,AMSS, MMSS,LMSS	43,45/20b	AR11/A/280/1710
47.0E	30 Apr 1991/20	ZOHREH 3	Iran	FSS	14a/11	SPA-AA/165/1278
49.0E	31 Dec 1990/20	STATSIONAR 24	USSR	AMSS,MMSS FSS	6#/4a#	AR11/A/319 CORR-1/1760 AR11/A/298, ADD-2/1776
53.0E	01 Jan 1981/NA	LOUTCH 2	USSR	FSS	14a/11	SPA-AJ/85/1318 Leased to Intersputnik. AR11/C/889/1743
53.0E	01 Aug 1987/10	SKYNET 4C	UK	FSS,MMSS	UHF,8,45/UHF	AR11/B/45/1626 AR11/A/84, ADD-1/1597 AR11/A/84/1588 AR11/C/870/ 1737/867 AR11/C/870, ADD-1/1767
53.0E	01 Mar 1989/15	MORE 53	USSR	MMSS,FSS	1.6b,6b/1.5a,4	AR11/A/185/1662 AR11/C/1088/1791
57.0E	01 Oct 1987/NA	INTELSAT VI 57E	INTELSAT	FSS,STS	6,6b/4,11	AR11/C/625, ADD-1/1713
57.0E	1988/NA	INTELSAT VI IND 2	INTELSAT	FSS	6a,6b,6,14/4a,4,11	AR11/A/72/1584

TABLE 2. PLANNED GEOSTATIONARY COMMUNICATIONS SATELLITES FOR YEAR END 1987 (CONT'D)

Subsatellite Longitude[a]	In-Use Date/ Period of Validity[b] (yr)	Satellite Designation[c]	Country or Organization	Service	Frequency Code Up/Down-Link (GHz)	Remarks
57.0E	01 Jan 1985	INTELSAT V-A IND 2	INTELSAT	FSS,STS	6,14a/4,11	AR11/A/68/1580
57.0E	31 Dec 1984	INTELSAT V IND 3	INTELSAT	FSS,STS	6,14/4,11	AJ/374/1511
58.0E	31 Dec 1986/20	TOR 13	USSR	TSS,LMSS, FSS,AMSS	43,45/20b,#	AR11/A/310/1736
58.0E	31 Dec 1990/20	STATSIONAR 24	USSR	AMSS,MMSS FSS	6/4a	AR11/A/319 CORR-1/1760
58.0E	31 Dec 1990/20	GALS 13	USSR	FSS	8/7	AR11/B/314/1740
58.0E	31 Dec 1990/20	VOLNA 4	USSR	MMSS,FSS, AMSS	1.6b/1.5a,#	SPA-AA/172/1286
60.0E	Oct 1987/15	INTELSAT VI 60E	INTELSAT	FSS,STS	6a,6b,6,14/4a,4,11	AR11/A/71/1584 AR11/C/626, ADD-1/1712
60.0E	01 Jul 1986/10	INTELSAT MCS IND B	INTELSAT	FSS,MMSS	#?/#?	AR11/C/1096/1791
63.0E	01 Jul 1986/NA	INTELSAT MCS IND A	INTELSAT	FSS,MMSS	1,6b,6/1.5a,4a	AR/11/C/1096/1791 AJ/177/1398
63.0E	01 Jan 1985/10	INTELSAT V-A IND 3	INTELSAT	FSS,STS	6,14a/11,4	AR11/C/673/1667
63.3E	01 Jan 1992/15	INTELSAT VI 63E	INTELSAT	FSS,STS	6/#	AR11/A/366/1782
64.5E	NA/NA	MARECS IND 1	INMARSAT (F)	MMSS	1.6b,6b/1.5a,4	SPA-AJ/243/1432
64.5E	01 Oct 1990	INMARSAT IOR	INMARSAT (G)	MMSS/AMSS	1.6b,1.6c,1.6d/ 6b,/4a	AR11/A/178/1644 AR11/C/846/1706 AR11/C/846/1706
64.5E	31 Jan 1990/15	INMARSAT IOR-11	INMARSAT	MMSS,AMSS, FSS,STS	1.6b,1.6c,1.6d/ 1.5b,1.5c 6b,4a,4	AR11/A/293/1713 AR11/A/293/ ADD-1/1760
65.0E	01 Apr 1983/1	SIRIO	Italy	FSS	1,11,12,17/18,#?	AR11/C/601/1655
66.0E	01 Jul 1986/10	INTELSAT MCS IND D (SPARE)	INTELSAT	MMSS,FSS	6b,1.6b/1.5a,4	SPA-AA/275/1425 AR11/C/857/1735
66.0E	01 Jan 1989/10	INTELSAT V-A 66E	INTELSAT	FSS,STS	6,14a/4,11	AR11/C/783/1682
69.0E	31 Dec 1990/20	GALS 14	USSR	FSS	8/7	AR11/A/315/1740 AR11/A/315/ CORR-1/1760
69.0E	31 Dec 1990/20	STATSIONAR 20	USSR	FSS	6/4a	AR11/A/316/1740
69.0E	31 Dec 1990/20	TOR 14	USSR	FSS,AMSS	43,45/20d,20b	AR11/A/311/1736
70.0E	11 Jan 1991/10	USASAT 13N	US	FSS,STS	14a,/11,12g	AR11/A/334/1763 AR11/A/68/1763 AR11/C/182/ ADD-1/1652
70.0E	1985-86/NA	STW 2	China, Peoples Republic of	FSS	6/4	SPA-AA/142/1255
72.0E	Dec 1984/10	FLTSATCOM A IND	US	FSS,MMSS	UHF,8/UHF,7	AR11/A/100/ ADD-1/1652 AR11/A/100/1605
72.0E	01 Jan 1988/10	FLTSATCOM B	US	FSS,MMSS	45/20d	AR11/A/52/1561 AR11/A/377, ADD-2/1802

TABLE 2. PLANNED GEOSTATIONARY COMMUNICATIONS SATELLITES FOR YEAR END 1987 (CONT'D)

Subsatellite Longitude (GHZ)[a]	In-Use Date/ Period of Validity[b] (yr)	Satellite Designation[c]	Country or Organization	Service	Frequency Code Up/Down-Link (GHz)	Remarks
72.0E	NA/10	FLTSATCOM IND	US	FSS,AMSS	0.3a,0.3b,8/#, 0.3b,7a	AR11/338/1762 AA/87/1186
72.5E	01 Jan 1977/NA	MARISAT-IND	US	FSS,AMSS	#/#	AJ/57/1277
73.0E	NA/NA	MARECS IND 2	INMARSAT (F)	MMSS	1.6b,6b,/1.5a,4	
74.0E	31 Jul 1990/20	INSAT II-C (INSAT METEO)	India	BSS,FSS Met Aids	UHF,6b/4b, 0.4c/-	AR11/A/262/1702 RES 33/A/7/1702
75.0E	01 Apr 1980/10	FLTSATCOM IND	US	MMSS,AMSS	0.3a,8/.3a,7a	AA/87/1186 AJ/169/1382 A/338/1762 AR/11/A/52/ ADD-1/1587
75.0E	31 Dec 1986/10	FLTSATCOM B IND	US	FSS,MMSS	45/20d	AR11/A/52/1561 AR11/A/52/ ADD-1/1587
76.0E	31 Dec 1986/15	GOMS	USSR	MMSS,FSS Met Aids	30a/7,1.6f, 20a,20b/#?	AR11/A/205/1678 AR11/205/ ADD-1/1712
77.0E	30 Nov 1986/NA	FLTSATCOM A IND	US	FSS,STS	8a,.3b/7a,3b	AA/336/ADD-1/1794 AA/336/ADD-2/1802
77.0E	17 Oct 1989/20	CSSRD 2	USSR	FSS,RSS	14c,15,14b/11, 13,12e	AR11/A/188/1672 AR11/A/188/1711 AR11/A/188/ CORR-1/1711
80.0E	01 Dec 1970/NA	STATSIONAR 1	USSR	FSS	6/4a	No SS #.
80.0E	11 Nov 1987/NA	PROGNOZ 4	USSR	FSS,SRS	4/2	AA/319/1471 AR14/D/165/1748
80.0E	30 Dec 1982/15	POTOK 2	USSR	FSS	6/4	AR11/A/179/1645 SPA-AA/345/1485 AR11/C/22/1558
80.0E	31 Dec 1987/20	LOUTCH 8	USSR	FSS	6,14a/4a,11	AR11/A/271/ CORR-1/1707 AR11/A/271, CORR-1/1728
81.5E	01 Jun 1990/10	FOTON 2	USSR	FSS	6b/4b	AR11/A/236/1692 AR11/C/1015/ CORR-1/1790
83.0E	31 Jan 1989/15	INSAT ID	India	FSS,STS, Met Aids	6b/4,UHF 0.4c/-	AR11/A/126/1617 RES 33/A/3/ ADD-1-10/ AR14/C/91/1682 AR11/C/860/1735
83.0E	Jan 1990/20	INSAT IIA	India	FSS,MMSS	6,6b/4,4b	AR11/A/260/1702 RES 33/A/5/1702
85.0E	01 Jan 1990/NA	LOUTCH P3	USSR	FSS	14a/11	SPA-AA/179/1289 SPA-AJ/123/1340
85.0E	NA/NA	VOLNA 5	USSR	LMSS,AMSS	UHF,1.6b/1.5a	SPA-AJ/100/1329 SPA-AA/173/1286

TABLE 2. PLANNED GEOSTATIONARY COMMUNICATIONS SATELLITES FOR YEAR END 1987 (CONT'D)

Subsatellite Longitude[a]	In-Use Date/ Period of Validity[b] (yr)	Satellite Designation[c]	Country or Organization	Service	Frequency Code Up/Down-Link (GHz)	Remarks
85.0E	01 Aug 1990/20	TOR 4	USSR	FSS,AMSS, MMSS,LMSS	43,45,20b	AR11/A/281/1210 AR11/A/28/1710
85.0E	01 Jan 1980/NA	GALS 3	USSR	FSS	8/7	SPA-AJ/112/1335 SPA-AA/154/1262 SPA-AJ/113/1335 SPA-AA/155/1262
85.0E	Jun 1988/20	STATSIONAR D5	USSR	FSS	6/4b	AR11/A/197/1675 AR11/C/1172/1796 SPA-AA/173/1286
85.0E	31 Dec 1990/20	VOLNA 5M	USSR	MMSS	1.6b/1.5a	AR11/A/250/1697 SPA-AJ-100/1329
85.0E	31 Dec 1989/10	NAHUEL II	Argentina	FSS	14a,6/12,4	AR11/C/204/1677 AR11/A/204/1677
87.5E	15 Mar 1988/10	CHINASAT 1	China, Peoples Republic of	FSS	6/4	AR11/A/255/1702 AR11/A/1027/1778
89.0E	30 Jun 1990/10	CONDOR B	Andean Countries	FSS	6/4	AR11/A/209/1679
90.0E	01 Mar 1989/15	MORE 90	USSR	MMSS	1.6b,6b/1.5a,1.5b,4	AR11/A/154/1562 AR11/C/1090/1791 AR11/C/15/1589
90.0E	01 Jan 1981/NA	LOUTCH 3	USSR	FSS	14a/11	SPA-AJ/86/1318
90.0E	NA/20	VOLNA 8	USSR	MMSS	UHF,1.6b/1.5a,UHF	SPA-AA/289/1445 SPA-AA/2/1153 SPA-AJ/316/1473
90.0E	09 Jan 1981/NA	STATSIONAR 6	USSR	FSS	6/4a	AR11/C/1116/1793
93.5E	03 Mar 1990/20	INSAT 2B (INSAT IIB)	India	FSS,BSS,STS Met Aids	6,6b/UHF 0.4c/-	AR11/A/261/1702 RES 33/A/6/ 261/1702 RES533/G/10/1799
93.5E	01 Jul 1988/18	INSAT 1C (INSAT-IC)	India	FSS,STS, Met Aids	UHF,6/4,6/4a 6b/4, 0.4c/-	SPA-AJ/231/1429 AR11/C/851/1708 AR11/C/852- 856/1708
95.0E	01 Aug 1989/20	STATSIONAR 14	USSR	FSS,BSS	6/4a	SPA-AJ/311/1469 SPA-AJ/306/1469 AR11/C/1811/1802
96.5E	31 Dec 1988/20	LOUTCH 9	USSR	FSS	14a/11	AR11/A/272/ CORR-1/1707 AR11/A/272/ CORR-1/1728
97.0E	30 Apr 1989/10	STSC 2	Cuba	FSS	6/4	AR11/A/268/1706 AR11/A/268/1723
98.0E	15 Mar 1989/10	CHINASAT 3	China, Peoples Republic of	FSS	6/4	AR11/A/257/1702 AR11/C/1039/1778
99.0E	20 Oct 1976/NA	STATSIONAR-T	USSR	FSS,BSS	6/UHF	RES-SPA2-3- AA10/1426
99.0E	30 Sep 1983/10	STATSIONAR-T2	USSR	FSS,BSS,MMSS	6/UHF#	SPA-AJ/316/1473
103.0E	31 Dec 1988/20	STATSIONAR 21	USSR	FSS,BSS	5a,6,6b/4a,4	AR11/A/244/1692 AR11/C/905/1748 AR11/C/906/1748 AR11/C/905/ ADD-1/1752

TABLE 2. PLANNED GEOSTATIONARY COMMUNICATIONS SATELLITES FOR YEAR END 1987 (CONT'D)

Subsatellite Longitude[a]	In-Use Date/ Period of Validity[b] (yr)	Satellite Designation[c]	Country or Organization	Service	Frequency Code Up/Down-Link (GHz)	Remarks
103.0E	30 Apr 1986/10	STW 2	China, Peoples Republic of	FSS	6/4	SPA-AA/142/1255 AR11/A/245/ ADD-1/1712
103.0E	31 Dec 1988/20	LOUTCH 5	USSR	FSS	14a/11	AR11/A/243/1694 AR11/C/966/1766 A/334/ADD-1/1762
110.0E	01 Aug 1990/NA	BS 3A	Japan	FSS	2,14a/2,12a,12b	AR11/A/334/1750 AR11/A/334/1762
110.5E	31 Dec 1988/10	CHINASAT 2 (CHINASAT 2B)	China, Peoples Republic of	FSS	6/4	AR11/A/25b/1702 AR11/C/1034/1778
118.0E	30 Jun 1980/10	PALAPA-B3	Indonesia	FSS	6/4	AR11/A/157/1637 AR11/C/654/1666
124.0E	31 Dec 1988/13	SCS 1B	Japan	FSS,STS	-/12c,30a,14a,20a, 20b, 12b, 12c	AR11/A/274/1708
128.0E	01 Jun 1990/20	GALS 10	USSR	FSS	8/7	AR11/A/247/1695 AR11/C/919/1753
128.0E	31 Dec 1986/NA	VOLNA 9	USSR	FSS,BSS MMSS	UHF,1.60b/1.5a,UHF 1,2,11,34	AR11/149/ ADD-1/1677 AR11/A/149/1631
128.0E	30 Jun 1988/13	SCS 1A	Japan	FSS,STS	14a/12c,30a,20a, 20b,12b,12c	AR11/A/273/1708 AP30/1/37
128.0E	01 Aug 1990/20	TOR 6	USSR	FSS,LMSS AMSS,MMSS	43,45,20b	AR11/A/283/1710
128.0E	30 Jun 1988/20	STATSIONAR-D6	USSR	FSS	6a/4b	AR11/A/198/1675 AR11/C/1173/1796
128.0E	31 Dec 1990/20	VOLNA 9M	USSR	MMSS/FSS	1.6b/1.5a	AR11/A/251/1697
130.0E	Jul 1990/20	PROGNOZ 5	USSR	SRS	2/4a	AR11/A/275/1709 AR11/C/938/1709
130.0E	20 Jun 1986/20	GALS 5	USSR	FSS	8/7	AR11/C/108/1578 AR11/C/28/1561 SPA-AA/339/1480
130.0E	01 Aug 1990/20	TOR 10	USSR	FSS,MMSS AMSS,LMSS	43,45,20d,20b/#?	AR11/A/290/1711
136.0E	30 Jun 1988/10	CS 3B	Japan	FSS,STS	6,30a,20a,20b/-?	AR11/A/213/1680 AR11/C/1145/1794 AR11/A/213/1794
140.0E	10 Aug 1984/7	GMS 3	Japan	FSS, Met Aids, STS	2,4a/UHF,1.6m,1.6n	AR11/C/474/1648 AR11/A/54/1563
140.0E	01 Mar 1989/15	MORE 140	USSR	MMSS	1.6b,6b/1.5a,4	AR11/A/186/1662
140.0E	29 May 1983/NA	LOUTCH 4	USSR	FSS	14a/11	AA/51/1261 SPA-AJ/87/1318
140.0E	20 Jun 1982/NA	VOLNA 6	USSR	FSS/BSS	1.6b,/1.5b	AR11/C/1092/1791

TABLE 2. PLANNED GEOSTATIONARY COMMUNICATIONS SATELLITES FOR YEAR END 1987 (CONT'D)

Subsatellite Longitude[a]	In-Use Date/ Period of Validity[b] (yr)	Satellite Designation[c]	Country or Organization	Service	Frequency Code Up/Down-Link (GHz)	Remarks
140.0E	Aug 1989/4 Per NASDA Japan	GMS (GMS 4)	Japan	FSS	0.4a,2/2#?	AR11/A/423/1821
140.0E	31 Dec 1990/NA	STATSIONAR 7	USSR	FSS,MMSS	6,1.5a/4a,#?	AJ/31/1251
145.0E	31 Dec 1987/20	STATSIONAR 16	USSR	FSS	6b,6,4a	AR11/A/76/1593 & 1586 AR11/C/850/ CORR-2/1728 AR11/C/849/ CORR-2/1728 AR11/C/849/1707 AR11/C/1126/1793
145.0E	24 Dec 1980/NA	ECS	Japan	STS	-/14	AJ/227/1427
150.0E	01 Aug 1987/5	ETS 5 (ETS-V)	Japan	MMSS,FSS, STS,AMSS, Experi- mental	6/5 6/-? 1.6d,1.6e/1.5c	AR11/A/217/1685 AR11/C/923/ 1754/920
150.0E	31 Dec 1987/12	JCSAT 1	Japan	FSS	14a/12b,12c	AR11/A/253/1700 AR11/C/946/1763
154.0E	01 Apr 1988/12	JCSAT 2	Japan	FSS	14a/12b,12c	AR11/A/254/1700 AR11/C/953/1763
156.0E	NA/NA	AUSSAT 2 (AUSSAT-II)	Australia (DC)	NA	#/#?	
156.0E	29 Feb 1992	AUSSAT B1-MOB	Australia (DC)	FSS	14,1.6d/12c	AR11/A/356/1772
156.0E	29 Feb 1992/15	AUSSAT B2	Australia (DC)	FSS,BSS	14a,12e#?	AP30/A/81 AR11/A/361/1779
156.0E	29 Feb 1992/15	AUSSAT B2-MOB	Australia (DC)	STS,AMSS	14a,1.6d/12e,1.5c	AR11/A/356/1772
158.0E	12 Jan 1988	SUPERBIRD-A	Japan	FSS,STS	8a,4a,3a/#?,7a, 12e,#?	AR11/A/340/1762
160.0E	01 Jan 1982/4	GMS-160E	Japan	FSS	2/2	AR11/C/8/1555
160.0E	NA/10	ANSCS 1	Australia (DC)	STS,FSS	14a,12e	AR11/A/1/1522
160.0E	01 Jan 1985/10	ANSCS 2 (ANSCS-II)	Australia (DC)	FSS,STS	-?/12e	A/2/1522
160.0E	29 Feb 1992/15	AUSSAT B1	Australia (DC)	FSS,STS	14a/12e	AP30/A/80/1796
160.0E	29 Feb 1992/NA	AUSSAT B1-MOB	Australia (DC)	FSS	14,1.6d/12c	AR11/A/356/1772
162.0E	01 Jun 1989/NA	SUPERBIRD 2	Japan	FSS,STS	8,14a,3a,#?/ 20a-20b#,7	AR11/A/341/1762
164.0E	1986/10	AUSSAT PAC3	Australia (OTC) South Pacific Region	FSS	14a/12b,12c	Adv. Publication AR11/A/215/1684 AR11/C/1008/ ADD-1/1791
164.0E	01 Jan 1985/10	ANSCS 3 (ANSCS-III)	Australia	FSS,STS	14a/12e	AR11/A/3/1522
166.0E	01 Jul 1990/20	PROGNOZ 6	USSR	FSS	2/4a	AR11/C/940/1763
166.0E	31 Dec 1988/15	GOMS 2	USSR	MMSS,FSS, Met AidS	3a/20d	AR11/A/207/1578 AR11/A/207/ ADD-1/1712

TABLE 2. PLANNED GEOSTATIONARY COMMUNICATIONS SATELLITES FOR YEAR END 1987 (CONT'D)

Subsatellite Longitude[a]	In-Use Date/ Period of Validity[b] (yr)	Satellite Designation[c]	Country or Organization	Service	Frequency Code Up/Down-Link (GHz)	Remarks
167.0E	17 Oct 1989/20	VSSRD 2	USSR	FSS,SRS	14c,15,14b/11, 13,12c	AR11/A/187/1672
167.0E	10 Sep 1990/15	PACSTAR-A1	Papua, New Guinea	AMSS,MMSS	1.6,1.6e/1.5c#?	AR11/A/331/1749
167.45E	31 Dec 1989/20	PACSTAR 1	Papua, New Guinea	FSS,STS	14a/#?	AR11/A/200/1676 AR11/A/331/1749
170.0E	10 Jan 1991/10	USASAT 13M	US	FSS,STS	14a/12a,12f-12g#	AR11/A/343/1763
172.0E	01 Dec 1986/10	FLTSAT B W PAC	US	FSS,MMSS	45/20d	AR11/A/51/1561
174.0E	01 Jan 1987/10	INTELSAT VA PAC 1	US-INTELSAT	FSS	6,14a/4,11	AR11/C/680/1668 AR11/C/680/ ADD-1/1802
174.0E	Dec 1984/10	INTELSAT V PAC 1	US-INTELSAT	FSS	6,14a/4,11	SPA-AJ/377/1511
176.0E	01 Dec 1986/10	FLTSATCOM B W PAC	US	FSS/MMSS	45/20d	SPA-AJ/872/1318 SPA-AJ/283/1446 AR11/A/51/ ADD-1/1587
177.0E	11 Feb 1976/NA	INTELSAT V PAC 2	US-INTELSAT	FSS	6,14a/4,11	AR11/A/81/1588/ See also 79E.
				FSS,STS	6,14a/4,11	AR11/A/81/1588 AR11/C/681/1668 SPA-AA/255/1419 AR11/C/681/ ADD-1/1802 66/1580 AR11/C/681/1668 SPA-AA/255/1419 AR11/C/590/1652 AR/11/C/681/ ADD-1/1802
177.0E	01 Jan 1987/10	INTELSAT V-A PAC 2	US-INTELSAT	FSS,STS	6/14a/4,11	AR11/A/66/1580 AR11/C/678/1668
179.5E	31 Oct 1990/15	INMARSAT POR-1	UK/INMARSAT	MMSS,AMSS, FSS,STS	1.6b,1.6c,1.6d/ 1.5b,1.5c,6g/ 4a,6,4	AR11/A/329/1747
180.0E (180.0W)	1991/10	INTELSAT V-A PAC 3	INTELSAT	FSS	6,14a/4,11	AR11/???
					6b/4a	AR11/C/859/1735
182.0E (178.0W)	01 Jul 1990/10	USASAT 13K	US	FSS	6/4	AR11/C/945/1763
185.0E (175.0W)	01 May 1990/20	PACSTAR 2	Papua, New Guinea	FSS,STS	14,6b,7,11/ 12a,12b,4a	AR11/A/201/1676
185.0E (175.0W)	10 Sep 1990/20	PACSTAR A-2	Papua, New Guinea	FSS,AMSS, MMSS	6b/5	AR11/A/332/1749 ADD-1/1783
188.0E (172.0W)	04 Jan 1981/NA	MARECS B PAC 1	France	MMSS,FSS	1,6/4a	SPA-AA/222/1351

TABLE 2. PLANNED GEOSTATIONARY COMMUNICATIONS SATELLITES FOR YEAR END 1987 (CONT'D)

Subsatellite Longitude[a]	In-Use Date/ Period of Validity[b] (yr)	Satellite Designation[c]	Country or Organization	Service	Frequency Code Up/Down-Link (GHz)	Remarks
189.0E (171.0W)	01 Apr 1984/10	TDRS WEST	US-NASA/ SPACECOM	SRS,STS	2,14d,14b/2,13	SPA-AA/232/1381 AR11/C/47/1568 AR11/C/47/ ADD-1(VIII)
190.0E (170.0W)	30 Jun 1988/20	STATSIONAR-D2	USSR	FSS	6/4b	AR11/A/194/675 AR11/C/1169/1796
190.0E (170.0W)	01 Jan 1981/NA	LOUTCH P4	USSR	FSS	14a/11	SPA-AA/180/1289 SPA-AJ/124/1340
190.0E (170.0W)	01 Aug 1990/20	TOR 5	USSR	FSS,AMSS, LMSS,MMSS	43,45,20b#?/#?	AR11/A/282/1710
190.0E (170.0W)	30 Jun 1982/NA	STATSIONAR 10	USSR	FSS	6/4	SPA-AJ/64/1280
190.0E (170.0W)	31 Dec 1985/NA	VOLNA 7	USSR	MMSS,AMSS, LMSS	UHF,1.6b/1.5a,UHF	SPA-AA/175/1286 SPA-AJ/102/1329
190.0E (170.0W)	01 Jan 1980/20	GALS 4	USSR	FSS	8/7	SPA-AJ/114/1335 SPA-AA/156/1262 SPA-AJ/124 CANCELLED
190.5E (169.5W)	01 Jun 1990/10	FOTON 3	USSR	FSS	6b/4b	AR11/A/237/1692 SPA-AA/346/1485
195.0E (165.0W)	09 Jan 1991/10	USASAT 13L	US	FSS,STS	14a/11	AR11/A/354/1770
192.0E (168.0W)	01 Dec 1983/10	POTOK 3	USSR	FSS	6/4	SPA-AA/346/1485
200.0E (160.0W)	06 Jan 1986/20	ESDRN	USSR	FSS,SRS	14d,14b,10,11,13	SPA-AA/343/1484 AR11/C/72/1570
201.0E (159.0W)	07 Jul 1990/20	PROGNOZ 7	USSR	SRS	2/4a	AR11/A/277/1709 AR11/C/942/1763
214.0E (146.0W)	Jun 1988/NA	AMIGO	Mexico			RES 33/A/1/1560
214.0E (146.0W)	01 Jan 1985/10	AMIGO 2	Mexico	BSS,STS	17,20a/12b,12a	RES 33/A/2/1560
214.0E (146.0W)	15 Nov 1990/10	USASAT 20C (AURORA 2)	US	FSS	6/4	AR11/A/259/1702 AR11/C/970/1769
215.0E (145.0W)	Dec 1984/10	FLTSATCOM A PAC	US	FSS,STS	UHF,8/UHF,7	AR11/A/181/1652
215.0E (145.0W)	31 Mar 1987/10	MORELOS 4 (ILHUICAHUA 4)	Mexico	FSS	6,14a/4,12a	AR11/A/25/1533 AR11/A/25/ ADD-1/1556
215.0E (145.0W)	01 Dec 1990/20	VOLNA 21M	USSR	AMSS,MMSS	1.6e,1.6d/1.5a, 1.5c	AR11/A/252/1697
218.0E (142.0W)	1987/10	USASAT 11C (WESTAR B)	US	FSS	14a/12a	AR11/111/1609
219.0E (141.0W)	31 Dec 1989/10	USASAT 17C (GALAXY 4)	US	FSS	6/4	AR11/A/228/1687 AR11/C/993/1761
219.0E (141.0W)	31 Dec 1986/10	MORELOS 3 (ILHUICAHUA 3)	Mexico	FSS,STS	6,14a/4,12a	AR11/A/24,1533 AR11/A/24/ ADD-1/1556

TABLE 2. PLANNED GEOSTATIONARY COMMUNICATIONS SATELLITES FOR YEAR END 1987 (CONT'D)

Subsatellite Longitude[a]	In-Use Date/ Period of Validity[b] (yr)	Satellite Designation[c]	Country or Organization	Service	Frequency Code Up/Down-Link (GHz)	Remarks
223.0E (137.0W)	Dec 1989/10	USASAT 17B (SPACENET 4)	US	FSS	6/4	AR11/A/227/1687
224.0E (136.0W)	NA/10	AMIGO 1	Mexico	FSS,STS	11/12,18a	AR11/A/1/1560
224.0E (136.0W)	22 Nov 1986/10	USASAT 16D (GSTAR 3)	US	FSS	14a/12a	AR11/A/225/1687
225.0E (135.0W)	10 Aug 1976/NA	US SATCOM 1	US	FSS	6/	AJ/42/1270
226.0E (134.0W)	Jan 1990/10	USASAT 16C	US	FSS	14/11	AR11/A/224/1687
226.0E (134.0W)	Jan 1990/10	USASAT 11D (HUGHES GALAXY)	US	FSS	14a/11	AR11/A/120/1615
228.0E (132.0W)	Jun 1990/10	USASAT 20B (WESTAR 7)	US	FSS,STS	6/4	AR11/A/258/1702
230.0E (130.0W)	Jun 1987/10	USASAT 10D (GALAXY B)	US	FSS	14a/12a	AR11/A/108/1609 AR11/C/1057/1781
230.0E (130.09W)	01 Oct 1991/15	ACS-3	US	AMSS	1.6d,1.6c/1.5c	AR11/A/303/1792
230.0E (130.0W)	31 Dec 1987/10	USRDSS West	US	FSS,STS	1.6a,6b/5,2	AR11/A/176/ ADD-2/1780
230.0E (130.0W)	NA/NA	USASAT 10D	US	FSS	14a/12a	AR11/A/1057/1781
234.0E (126.0W)	31 Oct 1985/10	USASAT 20A	US	FSS/STS	6/4	AR11/C/989/1769 AR11/C/1064/1783
234.0E (126.0W)	15 Sep 1987/10	USASAT 10C	US	FSS	14a/11	AR11/A/107/1609 AR11/C/989/1769
236.0E (124.0W)	30 May 1975/10	WESTAR 2 (WESTAR-II)	US	FSS	6/4	SPA-AJ/72/1302
236.0E (124.0W)	11 Jan 1988/10	USASAT 10B	US	FSS	14a/12a	AR11/A/106/1609
238.0E (122.0W)	15 Jan 1987/10	USASAT 10A (SBS-5)	US	FSS	14a/12a	AR11/A/105/1609 AR11/C/883/1741 AR11/A/10/1525 AR11/A/10/ ADD-1/1548 AR11/C/616 AR11/C/617- 624/1658 AR11/C/616/1658 AR11/A/4/1567
246.0E (114.0W)	NA/NA	TELESAT D2 (ANIK)	Canada-Telesat	FSS	6/4	SPA-AA/358/1500
249.5E (110.5W)	31 Mar 1991/12	TELESAT E-B (ANIK E-B)	Canada-Telesat	FSS	6b,14a/4,12a	AR11/A/323/1744 AR11/A/323/ CORR-1/1750
251.0E (109.0W)	01 Jan 1983/10	TELESAT C-3 (ANIK C-3)	Canada-Telesat	FSS	14a/12a	AR11/C/737- 738/1674 AR14/C/101/1686
252.5E (106.5W)	31 Mar 1991/12	TELESAT E-A	Canada-Telesat	FSS	6b,14a/4.12a	AR11/322/1744 AR11/A/322/ CORR-1/1750

TABLE 2. PLANNED GEOSTATIONARY COMMUNICATIONS SATELLITES FOR YEAR END 1987 (CONT'D)

Subsatellite Longitude[a]	In-Use Date/ Period of Validity[b] (yr)	Satellite Designation[c]	Country or Organization	Service	Frequency Code Up/Down-Link (GHz)	Remarks
253.5E (106.5W)	05 Apr 1988/10	MSAT	Canada	FSS,MMSS AMSS	UHF/UHF-EHF 1.6d/1.5c	AR11/A/55/1563 AR14/C/32/1663 AR11/C/797-811/1689 AR11/A/56/1563 AR14/C/33/1663 AR11/A/56/ADD-1/1678 AR14/C/37/1664 AR11/C/797-811/1689
255.0E (105.0W)	31 Dec 1984/10	FLTSATCOM A E PAC	US	FSS,MMSS LMSS	0.3a,8/UHF,7	AR11/A/98/ADD-1/1652 AR11/A/98/1605
259.0E (101.0W)	07 Jan 1990/10	USASAT 17A	US	FSS	6/4	AR11/A/226/1687
259.0E (101.0W)	07 Jan 1990/10	USASAT 16B	US	FSS	14a/12a	AR11/A/223/1687 AR11/C/999/1772
260.0E (100.0W)	10 Sep 1990/15	ACS 1	US	AMSS,FSS, STS	1.6d,1.6e/1.5c	AR11/4/301/1723 AR11/4/301/ADD-1/1780
260.0E (100.0W)	31 Dec 1986/10	FLTSATCOM B E PAC	US	FSS,LMSS	45/20d	A/50/ADD-1/1587 A/150/1561
260.0E (100.0W)	15 Jul 1990/10	USRDSS Central	US	FSS/RDSS STS	1.6a,6b/2,5	AR11/A/175/1641 AR11/A/175/ADD-2/1780
260.0E (100.0W)	10 Aug 1989/10	ACTS	US-NASA	FSS	30a/20b	AR11/A/321/1944 AR11/A/321/ADD-1/1753
263.0E (97.0W)	30 Apr 1989/10	STSC 2	Cuba	FSS	6/4	AR11/A/268/1706 AR11/A/26/ADD-1/1723
267.0E (93.0W)	04 Oct 1989/10	USASAT 16A	US	FSS	14a/12a	AR11/A/222/1687 AR11/C/998/1772 AR11/C/962/1765 AR11/C/229/1722
269.0E (91.0W)	15 Apr 1989/10	WESTAR 6-S (WESTAR VI-S)	US-Western Union	FSS	6/4	AR11/C/962/1765 AR11/C/963/1765
269.0E (91.0W)	01 Jul 1985/10	ADVANCED WESTAR I	US	FSS,STS	16,14a/4,12a	A/13/ADD-1/1708
271.0E (89.0W)	30 Jun 1990/10	CONDOR-B	Andean Countries	FSS	6/4	AR11/A/209/1679
271.5E (88.5W)	01 Sep 1985/10	USASAT 12D	US	FSS	6/4	AR11/A/124/1615 AR11/A/13, ADD-1/1708
271.5E (88.5W)	01 Feb 1984/10	SPACENET 3 (SPACENET-III)	US	FSS	14a,6/4,1a	AR11/C/834/1699
273.0E (87.0W)	14 Oct 1985/NA 15 Jun 1985/10	USASAT 9B	US-RCA US	FSS	14a/12a	Under Construction. AR11/A/102
274.0E (86.0W)	01 Mar 1988/10	STSC 2	Cuba	FSS	6/4	AR11/A/268/1706

TABLE 2. PLANNED GEOSTATIONARY COMMUNICATIONS SATELLITES FOR YEAR END 1987 (CONT'D)

Subsatellite Longitude[a]	In-Use Date/ Period of Validity[b] (yr)	Satellite Designation[c]	Country or Organization	Service	Frequency Code Up/Down-Link (GHz)	Remarks
275.0E (85.0W)	15 Mar 87/10	USASAT 9C	US	FSS	14a/12a	AR11/A/103/1609
275.0E (85.0W)	31 Dec 1989/10	NAHUEL-II	Argentina	FSS,BSS	6/4 14a/11	AR11/C/204/1677
277.0E (83.0W)	01 Mar 1988/NA	STSC 1	Cuba	FSS	6/4	AR11/A/58/1578, Note: 83.0W occupied by USASAT 7B or SATCOM IV.
277.0E (83.0W)	31 Dec 1985/10	USASAT 9D (RCA-B)	US	FSS	14a/11	AR11/A/104/1609 AR11/C/1053/1780
280.0E (80.0W)	30 Jun 1989/10	NAHUEL-I	Argentina	FSS,STS	14a,6/12,4	AR11/A/203/1677
281.0E (79.0W)	01 Apr 1984/10	TDRS CENTRAL	US-NASA/Spacecom	SRS,STS	2,14d,14b/2,13a	SPA-AA/233/1381
			US-Systemat. Gen.	FSS	6/4	AR11/D/94/1724
281.0E (79.0W)	31 Jan 1987/15	TDRS-C2	US-NASA/Spacecom	SRS,STS	2,14d,14b/2,13	AR11/B/166/1750 AR11/A/265/1704
281.0E (79.0W)	15 Mar 1987/10	USASAT 11A	US	FSS	14a/12a	AR11/A/109/1609 AR11/C/991/1769
282.5E (77.5W)	30 Jun 1990/10	CONDOR-A	Andean Countries	FSS	6/4	AR11/A/208/1679
283.0E (77.0W)	02 Jan 1989/10 27 Nov 1985/10	USASAT 11B (FEDEX-A)	US RCA	FSS	14a/12a	AR11/A/110/1609 AR11/C/1060/1782 Under Construction.
284.6E (75.4W)	31 Jul 1986/10	SATCOL 1A (SATCOL 1B)	Colombia	FSS	6/4	SPA-AA/322, 323/1474 AR11/C/79/1573 AR11/C/907/ CORR-1/1785
285.0E (75.0W)	31 Jul 1986	SATCOL 2	Colombia	FSS	6/4	SPA-AJ/128/1343 SPA-AA/324/1474 AR11/C/81/1573
285.0E (75.0W)	Jan 1990/10	USASAT 18A	US	FSS	14a/11	AR11/A/230/1687
287.0E (73.0W)	01 Jan 1990/10	USASAT 18B	US	FSS	14a/11	AR11/A/231/1687 AR11/C/1004/1773
288.0E (72.0W)	10 Sep 1990/15	ACS 2	US	AMSS,STS	1.6d,4/1.5c	AR11/C/1108/1792
288.0E (72.0W)	30 Jun 1990/10	CONDOR-C	Andean Countries	FSS,STS	6/4	AR11/A/210/1679
289.0E (71.0W)	31 Jan 1990/7	USASAT 18C	US	FSS	14a/11	AP30/A/60/1748 AR11/C/1005/1773
290.0E (70.0W)	15 Jul 1991/10	USRDSS East	US	FSS,RDS STS	1.6a,6b/-? 5.1a/-?	AR11/A/174/1641 AR11/A/174/ ADD-1/1780
290.0E (70.0W)	31 Dec 1986/10	FLTSATCOM B W ATL	US-Govt.	FSS,MMSS	UHF,8/UHF,7	AR11/A/41/ ADD-1/1587 AR11/A/49/ ADD-1/1587

TABLE 2. PLANNED GEOSTATIONARY COMMUNICATIONS SATELLITES FOR YEAR END 1987 (CONT'D)

Subsatellite Longitude[a]	In-Use Date/ Period of Validity[b] (yr)	Satellite Designation[c]	Country or Organization	Service	Frequency Code Up/Down-Link (GHz)	Remarks
293.0E (67.0W)	01 Jan 1986/10	USASAT 8A (SATCOM 6)	US (RCA)	FSS	6/4	AR11/C/394/1629 A/36/1553/1629
293.0E (67.0W)	04 Mar 1987/10	USASAT 15D	US	FSS	14a/12a	AR11/A/165/1637 FCC: 67.0W AR11/C/997/1770
296.0E (64.0W)	30 Nov 1990/10	USASAT 15C	US	FSS	14a/12a	AR11/C/990/1770 AR11/C/930/1755
296.0E (64.0W)	30 Nov 1990/10	USASAT 14D	US	FSS	6/4	AR11/C/99/1576 AR11/C/930/1755
298.0E (62.0W)	09 Sep 1989/10	USASAT 15B (SBS 6)	US	FSS,STS	14a/11,12a	AR11/A/163/1637 AR11/C/993/1770
298.0E (62.0W)	30 Jun 1989/10	USASAT 14C	US	FSS	6/4	AR11/A/160/1637 AR11/C/929/1755
300.0E (60.0W)	01 Jan 1986/10	INTELSAT IBS 300E	INTELSAT	FSS,STS	6b,14a/4a, 11a,12b,12c	AR11/A/167/1638 AR11/C/752/ ADD-1/1731
300.0E (60.0W)	31 Dec 1988/10	USASAT 15A	US	FSS	14a/12a	AR11/A/162/1637 AR11/A/162/ ADD-1/1673
300.0E (60.0W)	31 Dec 1989/10	USASAT 17D	US	FSS	6/4	AR11/A/229/1687
300.0E (60.0W)	01 Aug 1988/8	SATCOM PHASE 3B (SATCOM PHASE IIIB)	US			AR11/A/358/1773 SPA-AJ/342
300.0E (60.0W)	Jan 1986/10	INTELSAT VA	US-INTELSAT	FSS	6,14a/4,11	AR11/A/166/1638
302.0E (58.0W)	31 Jan 1987/10	USASAT 8C	US	FSS	6/4	AR11/A/38/1553
302.0E (58.0W)	30 Jul 1988/10	USASAT 13E (ISI SERIES)	US	FSS-INT'L	14a/11,12a,12b	AR11/A/136/1620 AR11/C/702/1670
303.0E (57.0W)	30 Sep 1987/10	USASAT 13H (PANAMSAT I)	US	FSS,STS	6b/4,11	AR11/A/177/1643
304.0E (56.0W)	01 Apr 1986/10	INTELSAT 5A 304E (INTELSAT VA 304E)	INTELSAT	FSS,STS	6,14a/4,11	AR11/A/168/1638 AR11/C/750/1676
304.0E (56.0W)	01 Apr 1986/10	INTELSAT IBS 304E	INTELSAT	FSS,STS	6b,14a/4a, 11,12b,12c	AR11/A/169/1638 AP/A/125/ ADD-1/1801
304.0E (56.0W)	30 Jul 1988/10	USASAT 13-D (ISI SERIES)	US	FSS	6/4	AR11/C/246/1620 AR11/C/701/1670
305.0E (55.0W)	31 Dec 1988/10	USASAT 14B	US	FSS	6/4	AR11/A/159/1637
305.0E (55.0W)	31 Mar 1989/15	INMARSAT AOR WEST	INMARSAT	MMSS,AMSS	1.6b,1.6c,1.6d/ 1.5b,1.5c	AR11/A/328/1747
307.0E (53.0W)	01 Jan 1986/10	INTELSAT IBS 307E	INTELSAT	FSS	6b,14a/4,11,12a	Under construction. AR/11/C/704/ ADD-1/1731
310.0E (50.0W)	1986/NA	INTELSAT VA CONTINENTAL 2	INTELSAT	FSS	6,14a/4,11	AR11/A/74/1586 AR11/C/594/1573

TABLE 2. PLANNED GEOSTATIONARY COMMUNICATIONS SATELLITES FOR YEAR END 1987 (CONT'D)

Subsatellite Longitude[a]	In-Use Date/ Period of Validity[b] (yr)	Satellite Designation[c]	Country or Organization	Service	Frequeny Code Up/Down-Link (GHz)	Remarks
310.0E (50.0W)	01 Jan 1986/10	INTELSAT IBS 310E	INTELSAT	FSS,STS	6b,14a/4,11,12	AR11/A/129/1617 ADD-1/1628 AR11/C/706/1673 AP30/A/14/ ADD-1/1801 AR11/C/706/ ADD-1/1731
310.0E (50.0W)	01 Jun 1986/10	INTELSAT V CONTINENTAL 2	US-INTELSAT	FSS,STS	6,14a/4,11	AR11/A/74/1586 AR11/C/594/1660
310.0E (50.0W)	30 Jun 1987/10	USASAT 13C (ORION SERIES)	US	FSS-INT'L	14a/11	AR11/A/134/1618 AR11/C/748/1675
310.0E (50.0W)	01 Jul 1989/15	INTELSAT VI 310E	INTELSAT	FSS	6b/4, 6,6b,14a/4a,4,11	AR11/A/287/1711 AR11/A/287/ ADD-1/1724
313.0E (47.0W)	01 Aug 1990/10	USASAT 13J	US	FSS	6/4	AR11/A/263/1703 AR11/C/944/1763
313.0E (47.0W)	03 Jun 1987/10	USASAT 13B (ORION SERIES)	US	FSS,STS	14a/11	AR11/A/133/1618 AR11/A/133/ ADD-1/1716 AR11/A/36/1722
315.0E (45.0W)	01 Jan 1988/10	USASAT 13F (CYGNUS SERIES)	US	FSS-INT'L, STS	14a,12a/11,12b,12c	AR11/A/154/1635 ADD-1/1714 AR11/C/795/1722
315.0E (45.0W)	01 Jan 1989/10	USASAT 13I (PANAMSAT II)	US	FSS	6/4,11	AR11/A/199/1675 AR11/C/866/1736
316.5E (43.5W)	01 Jan 1988/10	VIDEOSAT 3	France	FSS	14a,2/11,12b,12c	AR11/A/148/1631 AR11/C/766/1678 AR14/C/110/1698
317.0E (43.0W)	01 Jun 1988/10	USASAT 13G (CYGNUS SERIES)	US	FSS-INT'L, STS	14a/12a,11,12b,12c	AR11/A/155/1635 AR11/C/756/1676
317.5E (42.5W)	31 Dec 1986/10	USGCSS PH3 MID-ATL	US	FSS,MMSS, LMSS,STS	8/7 2/7	AR11/A/140/1622 AR11/A/42/ ADD-1/1730
319.5E (40.5W)	01 Apr 1986/10	INTELSAT VA 319.5E	INTELSAT	FSS	6,14a/4,11	AR11/A/127/1617
319.5E (40.5W)	01 Apr 1986/10	INTELSAT IBS 319.5E	INTELSAT	FSS,STS	6a,14a/4a,5,11, 12b,1	AR11/A/130/1617 AR11/A/130/ ADD-1/1628 AR11/C/707/1673 AP30/A/16/ ADD-1/1801
322.5E (37.5W)	30 Dec 1987/10	VIDEOSAT 2	France	FSS	14a/2,12b,12c	AR11/A/86/1589 AR11/C/727/1673 AR14/C/76/1676 AR11/C/746/1675
322.5E (37.5W)	30 Jun 1988/10	USASAT 13A (ORION SERIES)	US	FSS	14a/11,4a	AR11/132/1618 AR11/C/746/1675
325.5E (34.5W)	10 Jun 1987/10	INTELSAT VA ATL 3	INTELSAT	FSS,STS	6,14a/4,11	AR11/A/63/1580 AR11/A/288/ ADD-1/1724
325.5E (34.5W)	01 Aug 1989/15	INTELSAT VI 324.5E	INTELSAT	FSS,STS	6b/4b 6/6b,14a,4,4a,11	AR11/A/288/1724 AR11/A/288/1711

TABLE 2. PLANNED GEOSTATIONARY COMMUNICATIONS SATELLITES FOR YEAR END 1987 (CONT'D)

Subsatellite Longitude[a]	In-Use Date/ Period of Validity[b] (yr)	Satellite Designation[c]	Country or Organization	Service	Frequency Code Up/Down-Link (GHz)	Remarks
326.0E (34.0W)	30 Nov 1989/15	INMARSAT AOR-CENT 1A	UK/DT	FSS,AMSS	1.6a,1.6b,6aa,6a/ 4,1.5a,1,5b	AR11/A/351/1767
327.0E (33.0W)	30 Nov 1991/NA	SKYNET 4D	UK	FSS,MMSS,BSS	0.3a,8/45,7,0.3a	AR11/A/333/1749 AR11/A/393/1749
328.0E (32.0W)	Dec 1988/15	INMARSAT AOR- CENT 2A	UK/DT	AMSS,MMSS	1.6c,6/1.5a,2.6e#	AR11/A/352/1767
329.0E (31.0W)	30 Jun 1986/10	BSB 1	UK	FSS		AR11/C/731/ADD-1
329.0E (31.0W)	30 Jun 1986/10	UNISAT 1 ATL	UK-British Telecom	FSS	14/12d,12f	AR11/A/26/1534 AR11/C/424/1639
329.0E (31.0W)	30 Jun 1986/10	UNISAT 1	UK	FSS/BSS	17,20a,14a,14b/12b, 12c,2,4,12d,12e	AR11/C/576/1650 AR11/A/23/1532
329.0E (31.0W)	01 Jan 1987/10	INTELSAT VA ATL 6	INTELSAT	FSS	6,14a/4,11	AR11/A/119/1611 AR11/A/119/ ADD-1/1628 AR11/A/119/ ADD-2/1638
329.0E (31.0W)	31 Dec 1987/12	EIRESAT 1	Ireland	FSS/BSS	13/11,#	AR11/A/182/1656 AR11/A/182/ ADD-1/1803
329.0E (31.0W)	01 Jan 1987/10	INTELSAT V ATL 6	INTELSAT	FSS	6,14/4,11	AR11/A/118/1611
332.5E (27.5W)	Oct 1987/15	INTELSAT VI 332.5E	INTELSAT	FSS	6a,6b,14a/4a,4,11	AR11/A/70/1584 AR11/C/628/1658, ADD-1/1713
332.5E (26.5W)	31 Dec 1987/20	STATSIONAR 17	USSR	FSS,BSS	6b,5e,6/4a,4	AR11/A/219/1686 AR11/C/910/1749
333.5E (26.5W)	01 Jan 1980/20	GALS 1	USSR	FSS	8/7	SPA-AJ/365/1508 SPA-AJ/111/1335 SPA-AA/153/1262
333.5E (26.5W)	31 Dec 1987/20	VOLNA 13	USSR	AMSS,LMSS	UHF,1.6c,1.6e/ UHF,0.3a,1.5c	AR11/A/240/1693 AR11/C/910/ ADD-1/1756
333.5E (26.5W)	Jun 1988/20	STATSIONAR-D1	USSR	FSS	6a/4b	AR11/A/193/1675
333.5E (26.5W)	01 Aug 1990/20	TOR 1	USSR	FSS,AMSS, MMSS,LMSS	43,45/20b	AR11/A/278/1710
334.0E (26.0W)	01 Aug 1989/15	INMARSAT AOR-CENT	UK	AMSS,MMSS, FSS,STS	1.6b,1.6c,1.6d/1.5b, 1.5c,6.4,6b,4a	AR11/A/152/1634 AR11/C/843/1706
335.0E (25.0W)	01 Jan 1981/NA	LOUTCH P1	USSR	FSS	14a/11	SPA-AA/177/1289 SPA-AJ/121/1340
335.0E (25.0W)	01 Aug 1990/20	TOR 9	USSR	FSS,LMSS, AMSS,MMSS	43,45,20b/#	AR11/A/289/1711
335.0E (25.0W)	01 Jun 1990/20	GALS 9	USSR	FSS,AMSS, LMSS	8/7	AR11/A/246/1695 AR11/A/291/1712 AR11/C/918/1752 AR11/C/918/ CORR-1/1756

TABLE 2. PLANNED GEOSTATIONARY COMMUNICATIONS SATELLITES FOR YEAR END 1987 (CONT'D)

Subsatellite Longitude[a]	In-Use Date/ Period of Validity[b] (yr)	Satellite Designation[c]	Country or Organization	Service	Frequency Code Up/Down-Link (GHz)	Remarks
335.0E (25.0W)	30 Sep 1991/10	TELECOM 2B	France	FSS,STS	2,4/6,7	AR11/A/325/1745 AR11/A/325/ ADD-2/1998
335.5E (24.5W)	01 Oct 1987/15	INTELSAT VI	INTELSAT	FSS	6,6a,14a/4,11	AR11/A/69/1584 AR11/C/627/1658
336.0E (24.0W)	31 Dec 1984/20	PROGNOZ 1	USSR	FSS,SRS	3/2	SPA-AA/316/1471 AR14/C/95/1685
336.0E (24.0W)	31 Dec 1989/15	INMARSAT AOR-CENT 2	INMARSAT	MMSS,AMSS, FSS,STS	1.6b,1.6c,1.6d/ 1.5b,1.5c	AR11/A/292/1713 AR11/A/292/ ADD-1/1760
				FSS	6/4	
				STS	6b/4a	
337.0E (23.0W)	NA/NA	MARECS ATL 2	France	FSS/MMSS	1.6b,6,UHF/ 1.5a,4a,UHF	SPA-AJ/241/1432 SPA-AA/219/1351
338.5E (21.5W)	01 Jun 1986/10	INTELSAT MCS ATL C	US	MMSS,FSS	1.6b,6/1.5a,4	AR11/C/858/1735
338.5E (21.5W)	31 Dec 1984/10	INTELSAT V ATL 5	INTELSAT	FSS	6,14a/4,11	SPA-AA/252/1419 SPA-AJ/378/1511
338.5E (21.5W)	01 Jan 1989/10	INTELSAT VA 338.5E	INTELSAT	FSS,STS	6,14a/4,11	AR11/A/781/1682 AR11/A/180/1645 SPA-AA/48/1161 SPA-AA/65/1170 AR11/A/92/ ADD-1/1802
340.0E (20.0W)	31 Jan 1989/10	GDL 4	Luxembourg	FSS,BSS	6b,12a,14/11, 12b,12c	AR11/A/92/1594/ ADD-1/1708 AR11/C/610/ CORR-1/1744 AR11/C/611/ CORR-1/1744
341.0E (19.0W)	31 Dec 1988/10	TDF 2	France	BSS,FSS	2/2	AR11/A/216/1684
341.0E (19.0W)	30 Jun 87/10	TDF 1	France	BSS,FSS	20a/12e	AR11/A/57/1570 AR11/C/107/1578 AR11/C/741/1674
341.0E (19.0W)	01 Oct 1985/7	TV-SAT 1	Federal Republic of Germany	BSS,STS	17a,20a,17/20a, 2,12a,12e,2	SPA-AA/311/1464 SPA-AA/325/1474 SPA-AA/366/1526 AR14/C/4/1550 AR11/C/608/1656 AR11/C/609/1656
341.0E (19.0W)	31 Dec 1988/10	TV-SAT 2	Federal Republic of Germany	FSS,STS	20a,20b/2,12a	AR11/A/350/1767
341.0E (19.0W)	01 Jan 1986/NA	L-SAT	ESA (France)	BSS/FSS	14a,30a/12b,12a 20b	SPA-AA/308/1463 AR11/A/33/1544 AR11/A/88/1590 AR11/A/57/1570 AR11/C/124/1592
	01 Jul 1986/10	L-SAT	France	BSS	17/20a	AR11/C/6/1554 AR11/A/308/1463 AR11/C/782/1682 AR14/D/23/1707

TABLE 2. PLANNED GEOSTATIONARY COMMUNICATIONS SATELLITES FOR YEAR END 1987 (CONT'D)

Subsatellite Longitude (GHZ)[a]	In-Use Date/ Period of Validity[b] (yr)	Satellite Designation[c]	Country or Organization	Service	Frequency Code Up/Down-Link (GHz)	Remarks
	01 Jul 1986/10	L-SAT (30/20 GHz)	France	FSS/FSS	30a/20a	AR11/C/232/1619 AR11/A/32/1544 AR11/A/32 ADD-1/1716
	01 Jul 1986/10	L-SAT (14,13g/12 GHz)	France	BSS/FSS	14a,13,12b,12c	AR11/C/174/1605 AR11/C/174/ ADD-1/1643 SPA-AA/337/1479 AR11/A/88/1590
	01 Jul 1986/10	L-SAT	France	BSS/FSS	2/2	AR11/C/176/1605 AR11/A/33/1544
341.0E (19.0W)	1986/10	HELVESAT 1	Switzerland	FSS,BSS	17,20a,18/2,12b,12a	SPA-AA/365/1512
341.0E (19.0W)	1986/07	SARIT	Italy	BSS,FSS,STS	13,30b/20c	SPA-AA/360/1505 SPA-AA/371/1547 AR11/294/1716
341.0E (19.0W)	1986/10	LUX-SAT	Luxembourg	FSS,BSS,STS	17a/12a,12b, 12e,20a	AR11/A/20/1529 AR11/C/459/1789
341.5E (18.5E)	01 Jul 1986/NA	INTELSAT MCS ATL A	INTELSAT	FSS,MMSS	1.6b,6b/1.5a,4a	AR11/C/1096/1791
341.5E (18.5W)	Jul 1986/10	INTELSAT IBS 341.5E	INTELSAT	FSS	6,14a/4,11,12a, 12b,12c	Under construction by Ford Aerospace; replaces INTELSAT VA above.
342.0E (18.0W)	01 Jan 1987/10	INTELSAT VA ATL 4	INTELSAT	FSS,STS	6,14a/4,11	AR11/A/64/1580
342.0E (18.0W)	01 Jul 1986/10	INTELSAT IBS 342E	INTELSAT	FSS,STS	6,6b,14a/3,4a,12a	AP30/A/7/ ADD-1/1801
342.0E (18.0W)	12 Sep 1990/20	SATCOM III	Belgium	FSS,MMSS	#/#	AR11/A/1762
342.0E (18.0W)	20 Mar 1970/NA	SATCOM 2	Belgium	FSS	8/7	AR11/A/342 ADD-1/1787
342.0E (18.0W)	15 Oct 1979/NA	SATCOM PHASE-3	Belgium	FSS	8/7	SPA-AJ/137/1355 SPA-AA/144/1257
342.0E (18.0W)	01 Sep 1990/20	SATCOM 4	Belgium	FSS,MMSS	20a,20b/2,12a	AR11/A/342/1762
343.5E (16.5W)	01 Jan 1986/10	INTELSAT V 343.5E	INTELSAT	FSS,STS	6,14a/4,11	AR11/A/172/1639 AR11/C/758/1677 AP30/A/25/ ADD-1/1801
343.5E (16.5W)	01 Jul 1986/10 CANCELLED	INTELSAT VA 343.5E	INTELSAT	FSS,STS	6,14a/4,11	AR11/A/170/1638 AR11/A/751/1676
343.5E (16.5W)	01 Jul 1986/10	INTELSAT IBS 343.5E	INTELSAT	FSS	6a,14a/4a,11d,11, 12d	AR11/A/171/1638 AR11/C/754/ ADD-1/1731
344.0E (16.0W)	01 Jun 1987/20	WSDRN	USSR	FSS,SRS	14d,14b,11,13	AR11/C/67/1570 SPA-AA/341/1484 AR11/C/68/1570
344.0E (16.0W)	17 Jan 1989/20	ZSSRD 2	USSR	FSS,STS,SRS	11,12b,12c/13d 14b,14d	AR11/A/189/1672 AR11/C/850/ 1740/880 AR11/C/880/ ADD-1/1765

TABLE 2. PLANNED GEOSTATIONARY COMMUNICATIONS SATELLITES FOR YEAR END 1987 (CONT'D)

Subsatellite Longitude[a]	In-Use Date/ Period of Validity[b] (yr)	Satellite Designation[c]	Country or Organization	Service	Frequency Code Up/Down-Link (GHz)	Remarks
345.0E (15.0W)	31 Dec 1984/10	FLTSATCOM A ATL	US-Govt.	FSS,MMSS, LMSS	UHF,8/UHF,7	AR11/A/97/ ADD-1/1652 AR11/97/1605: 23W
345.0E (15.0W)	02 Aug 1989/15	INMARSAT AOR-EAST	UK	MMSS,FSS, AMSS	1.6b,1.6c, 1.6d,1.5c,6/ 1.51,4,4a,6b	AR11/A/153/1634 AR11/A/153/ ADD-1/1760
345.0E (15.0W)	01 Jun 1990/10	FOTON 1	USSR	FSS	6b/4b	AR11/A/235/1692
345.0E (14.0W)	31 Dec 1987/15	GOMS 1	USSR	MMSS,FSS, Met Aids	30a/20b	AR11/A/206/1578 AR11/A/206/ ADD-1/1712
345.0E (14.0W)	01 Mar 1989/15	MORE 14	USSR	MMSS,FSS	1.6b,6b/1.5a,4a	AR11/A/183/1662 AR11/C/1086/1797
346.0E (14.0W)	01 Jan 1981/NA	LOUTCH 1	USSR	FSS	14a/11	SPA-AA/157/1262 SPA-AJ/84/1318
346.0E (14.0W)	01 Jan 1980/10	VOLNA 2	USSR	MMSS	1.6b/1.5a	SPA-AJ/97/1329 SPA-AA/170/1286: 14W
346.5E (13.5W)	30 Dec 1982/15	POTOK 1	USSR	FSS	4a-4b#/4	SPA-AA/344/1485
347.5E (12.5W)	NA/NA	MAROTS-B	France	MMSS	1.6b,UHF/1.5a,UHF	SPA-AA/204/133
348.0E (12.0W)	30 Sep 1988/10	HIPPARCOS	France	FSS,SRS,STS	2/2	AR11/A/138/1621 AR11/A/138/ ADD-1/1636 AR14/C/64/1673 AR11/C/902/1746
349.0E (11.0W)	31 Dec 1987/10	F-SAT 2	France	FSS,STS	14a,30a/12b-12c	AR11/A/73/1586 AR11/C/466/1647 AR11/C/467-468/1647 AR14/C/71/1675
349.0E (11.0W)	31 Dec 1988/20	LOUTCH 6	USSR	FSS	14a/11	AR11/A/269/1728 AR11/C/964/1769
352.0E (8.0W)	30 Sep 1991/10	TELECOM 2A	France	FSS,BSS STS	2,6,8/2,4,7,12b,4a	AR11/A/324/1745 AR11/A/325, ADD-2/1798
352.0E (8.0W)	30 Apr 1992/20	ZENON-A	France	FSS,STS	1.6d,2,14a/1.5e,2,11	AR11/A/363/1781
355.0E (5.0W)	01 Oct 1987/15	INTELSAT VI 335.5E	INTELSAT	FSS	6,6a,14a/4,11	AR11/A/69/1584
356.0E (4.0W)	01 Jul 1987/10	INTELSAT V-CONT 3	INTELSAT	FSS	6,14a/4,11	AR11/A/112/1609
356.0E (4.0W)	01 Jul 1986/10	INTELSAT VA CONT 3	INTELSAT	FSS	6,14a/4,11	AR11/A/116/1609 AR11/A/116/ ADD-1/1628 AR11/C/675/1667
357.0E (3.0W)	31 Dec 1990/20	TOR 11	USSR	FSS,LMSS, AMSS,MSS MMSS	43,45/20b	AR11/A/308/1736 AR11/A/317/ CORR-1/1760

TABLE 2. PLANNED GEOSTATIONARY COMMUNICATIONS SATELLITES FOR YEAR END 1987 (CONT'D)

Subsatellite Longitude[a]	In-Use Date/ Period of Validity[b] (yr)	Satellite Designation[c]	Country or Organization	Service	Frequency Code Up/Down-Link (GHz)	Remarks
357.0E (3.0W)	31 Dec 1990/20	STATSIONAR 22	USSR	FSS	6/4	AR11/A/317/1740 AR11/A/317/ CORR-1/1760
357.0E (3.0W)	31 Dec 1990/20	GALS 11	USSR	FSS	8/7	AR11/A/312/1740
359.0E (1.0W)	01 Jan 1985/10	INTELSAT V CONT 4	INTELSAT	FSS,STS	6,14a/4,11	AR11/A/83/1588 AR11/C/593/1652
359.0E (1.0W)	01 Jan 1987/10	INTELSAT VA CONT 4	INTELSAT	FSS,STS	6,14a/4,11	AR11/A/117/1609 AR11/117/ ADD-1/1628 AR11/117/ ADD-2/1638 AR11/A/117/ ADD-2/1638 AR11/C/677/1668
359.0E (1.0W)	01 Nov 1985/10	SKYNET 4A	UK	FSS/MMSS	UHF,44/UHF,7	AR11/C/182/1611 AR11/C/588/1652

[a]The list of satellite longitudes was compiled from the best information available.
[b]The period of validity is the number of years over which the frequency assignments of the space station are to be used.
[c]Satellite names in parentheses are alternate names not filed with the IFRB.

#: Satellite network is operating outside allocated satellite frequency bands.
NA: Information is not available at this time.
STS: Space tracking satellite.

TABLE 3. FREQUENCY CODES FOR ALLOCATED BANDS, SERVICES, AND ITU REGIONS

Code	Service	Link Direction, ITU Region[1]		Allocated Frequency Band (GHz)
0.1	MSS[2]	Up[3]		0.12145-0.12155
0.2	MSS	Up[3]		0.24295-0.24305
0.3a	MSS	Up	Down	0.235-0.322
0.3b	MSS	Up	Down	0.3354-0.3999
0.4a	LMSS,MMSS	Up[4]		0.4055-0.406
0.4b	MSS	Up[3]		0.406-0.4061
0.4c	Met Aids	Up		0.402-0.403
0.6	LMSS,MSS (sec[5])	Up (sec) 2		0.608-0.614
0.7	BSS (CR[6,7])			
0.8	LMSS,MMSS	Up	Down 2,3[8]	0.806-0.89
0.9	LMSS,MMSS	Up	MSS Down 3[8]	0.942-0.96
1.5a	MMSS		Down	1.530-1.544
1.5b	MMSS,AMSS		Down[9]	1.544-1.545
1.5c	AMSS		Down	1.545-1.559
1.6a	AMSS	Up	Down	1.610-1.6265
1.6b	MMSS	Up		1.6265-1.6455
1.6c	MSS	Up[9]		1.6455-1.6465
1.6d	AMSS	Up		1.6465-1.660
1.6e	AMSS	Up		1.660-1.6605
1.6f	SRS	Passive (No direction given)		1.6605-1.6684
2		(See Tables 1 and 2)		Various frequencies in the 2.0 to 2.99-GHz range
2.6a	FSS		Down 2,3	2.5-2.535
2.6b	FSS		Down 2	2.535-2.655
2.6c	FSS	Up 2,3	Down 2	2.655-2.69
2.6d	BSS (CR)		Down	2.5-2.69
4	FSS		Down	3.7-4.2
4a	FSS		Down	3.4-4.2
4b	FSS		Down	4.5-4.8
5	AMSS	Up	Down	5.0-5.25
6	FSS	Up		5.925-6.425
6a	FSS	Up 1		5.725-5.85
6b	FSS	Up		5.85-7.075
7	FSS		Down	7.25-7.75
7a	MSS		Down	7.25-7.375
8	FSS	Up		7.9-8.4
8a	MSS	Up		7.9-8.025
11	FSS	Up 1	Down	10.7-11.7
12a	FSS		Down 2	11.7-12.2
12b	FSS	Up 1	Down 1,3	12.5-12.7
12c	FSS	Up 1,2	Down 1,3	12.7-12.75
12d	BSS		Down 1,3	11.7-12.2
12e	BSS		Down 1,2	12.2-12.5
12f	BSS (CR)		Down 2,3	12.5-12.7
12g	BSS (CR)		Down 3	12.7-12.75
13	FSS	Up		12.75-13.25
13a	SRS	Up		13.25-14.0
14a	FSS	Up		14.0-14.5

TABLE 3. FREQUENCY CODES FOR ALLOCATED BANDS, SERVICES, AND ITU REGIONS (CONT'D)

Code	Service	Link Direction, ITU Region[1]		Allocated Frequency Band (GHz)
14b	FSS	Up		14.5-14.8
14c	LMSS[7] (sec)	Up		14.0-14.5
14d	SRSS (sec)	Up		14.8-15.35
15	AMSS	Up	Down	15.4-15.7
17	FSS	Up		17.3-17.7
20a	FSS	Up	Down	17.7-18.1
20b	FSS		Down	18.1-21.2
20c	MSS (sec)		Down	19.7-20.2
20d	MSS		Down	20.2-21.2
23	BSS		Down 2,3	22.5-23.0
27	FSS	Up 2,3		27.0-27.5
30a	FSS	Up		27.5-31.0
30b	MSS (sec)	Up		29.5-30.0
30c	MSS	Up		30.0-31.0
39	FSS		Down	37.5-40.5
40	MSS		Down	39.5-40.5
42	BSS		Down	40.5-42.5
43	FSS	Up		42.5-43.5
45	MSS	Up	Down	43.5-47.0
48	FSS	Up		47.2-49.2
50a	FSS	Up		49.2-50.2
50b	FSS	Up		50.4-51.4
50c	MSS (sec)	Up		50.4-51.4
84	BSS		Down	84.0-86.0

[1]If the allocation to the service is confined to one or more ITU Regions, the regions are identified by numbers placed after the link direction.
[2]In all cases, MSS includes LMSS, MMSS, and AMSS.
[3]Emergency positioning indicator beam only.
[4]Canada only.
[5]sec = secondary allocation.
[6]CR = community reception, TV only.
[7]This allocation is covered by footnote 693 in the allocation tables.
[8]Norway, Sweden.
[9]Distress/safety.

Translations of Abstracts

Diodes varactors hyperabruptes à implantation ionique pour circuits intégrés hyperfréquence monolithiques (MMIC) au GaAs

P. J. MCNALLY ET B. B. CREGGER

Sommaire

On décrit la conception, la fabrication et la caractérisation de diodes varactors à l'arséniure de gallium (GaAs) compatibles avec les dispositifs monolithiques. On a utilisé un processus d'implantation entièrement ionique pour fabriquer des diodes varactors hyperabruptes avec de grands rapports d'accord (>10:1). On a fait appel à une implantation à grande énergie (4 et 6 MeV) pour former une couche n^+ enfouie au-dessous de la partie active du dispositif. On a procédé à d'autres implantations pour établir le contact entre la surface et la couche enfouie et former le profil de condensateur hyperabrupt. On a fabriqué des barrières de Schottky presque parfaites avec un anneau de garde intégral à résistivité élevée pour l'épuisement du profil hyperabrupt. Ces barrières de Schottky montrent un facteur de perfection de 1.0, un faible courant de fuite inversé et une forte tension de claquage avalanche inversée (>30 V). Les diodes varactors ont été caractérisées à des fréquences situées entre 2 et 10 GHz. On présente des données de performance mesurée dans cette gamme de fréquences, et leur corrélation avec la structure du dispositif. On analyse en détail la conception du dispositif, les données expérimentales de l'implantation ionique et la caractérisation électrique des diodes.

paquetes a una estación central, empleando el protocolo ALOHA a intervalos de tiempo iguales para los primeros intentos, y segmentos de reservación para las retransmisiones que sea preciso hacer bien sea debido a los canales libres o a los errores en los bitios en el primer intento. Esta técnica de acceso ha sido modelada y simulada para compilar estadísticas sobre el tiempo de propagación y el rendimiento de los paquetes en función de la carga del sistema, haciéndose hincapié en la transición entre los protocolos de acceso aleatorio y de reservación. Se muestran los resultados de los parámetros de una red típica y las condiciones de la proporción de errores en los bitios de los enlaces.

Author Index, CTR 1987

The following is a cross-referenced index of articles that appeared in the *COMSAT Technical Review* in 1987. The code number at the end of each entry is to be used for ordering reprints from Corporate Records, COMSAT Corporation, 22300 Comsat Drive, Clarksburg, MD 20871-9475.

ASSAL, F. T., see Egri, R. G. [CTR87/314].
BHASKAR, U., see Dimolitsas, S. [CTR87/317].
BHASKAR, U., see Fang, R. J. F. [CTR87/328].
CHANG, P. Y., see White, L. W. [CTR87/326].
CORCORAN, F. L., see Dimolitsas, S. [CTR87/324].
deBETTENCOURT, J. T., see Suryadevara, O. [CTR87/325].
DIMOLITSAS, S., and Bhaskar, U., "Hurwitz Stability Analysis of an ADPCM System," *COMSAT Techincal Review*, Vol. 17, No. 1, Spring, pp. 105–125 [CTR87/317].
DIMOLITSAS, S., Corcoran, F. L., Onufry, M., and Suyderhoud, H. G., "Evaluation of ADPCM Coders for Digital Circuit Multiplication Equipment," *COMSAT Technical Review*, Vol. 17, No. 2, Fall, pp. 323–345 [CTR87/324].
EGRI, R. G., Karimullah, K., and Assal, F. T., "A 120-Mbit/s TDMA QPSK Modem for On-Board Applications," *COMSAT Technical Review*, Vol. 17, No. 1, Spring, pp. 23–54 [CTR87/314].
FANG, R. J. F., Bhaskar, U., Hemmati, F., Mackenthun, K. M., and Shenoy, A., "Design of an MSAT-X Mobile Transceiver and Related Base and Gateway Stations," *COMSAT Technical Review*, Vol. 17, No. 2, Fall, pp. 421–466 [CTR87/328].
FU, M. C., see Gupta, R. K. [CTR87/313].
GUPTA, R. K., Reynolds, J. H., Fu, M. C., and Heikkila, T., "Design and Modeling of a GaAs Monolithic 2- to 6-GHz Feedback Amplifier," *COMSAT Technical Review*, Vol. 17, No. 1, Spring, pp. 1–22 [CTR87/313].
HEIKKILA, T., see Gupta, R. K. [CTR87/313].
HEMMATI, F., "Decoding the Eight-State Partial Unit-Memory Code," *COMSAT Technical Review*, Vol. 17, No. 2, Fall, pp. 311–322 [CTR87/323].
HEMMATI, F., see Fang, R. J. F. [CTR87/328].
KAPPES, J. M., "An Adaptive Equalizer for 120-Mbit/s QPSK Transmission," *COMSAT Technical Review*, Vol. 17, No. 1, Spring, pp. 55–86 [CTR87/315].
KARIMULLAH, K., see Egri, R. G. [CTR87/314].
LYONS, J. W. III, and Ozkul, A.,* "In-Orbit Performance of INTELSAT IV-A Spacecraft Solar Arrays," *COMSAT Technical Review*, Vol. 17, No. 2, Fall, pp. 403–419 [CTR87/327].

* INTELSAT author.

MACKENTHUN, K. M., "Modulation Selection for the Mobile Satellite Experiment (MSAT-X)," *COMSAT Technical Review*, Vol. 17, No. 2, Spring, pp. 87–103 [CTR87/316].
MACKENTHUN, K. M., see Fang, R. J. F. [CTR87/328].
MASS, J.,* "A Simulation Study of Rain Attenuation and Diversity Effects on Satellite Links," *COMSAT Technical Review*, Vol. 17, No. 1, Spring, pp. 159–188 [CTR87/319].
ONUFRY, M., see Dimolitsas, S. [CTR87/324].
OZKUL, A.,† see Lyons, J. W. [CTR87/327].
PALMER, L. C., see White, L. W. [CTR87/326].
POKLEMBA, J. J., "Pole-Zero Approximations for the Raised Cosine Filter Family," *COMSAT Technical Review*, Vol. 17, No. 1, Spring, pp. 127–157 [CTR87/318].
POKLEMBA, J. J., "An All-Pole Approximation for the Reciprocal sin $(x)/(x)$ Frequency Response," *COMSAT Technical Review*, Vol. 17, No. 2, Fall, pp. 467–479 [CTR87/329].
REYNOLDS, J. H., see Gupta, R. K. [CTR87/313].
RHODES, S. A., "Differentially Coherent FEC Block Coding," *COMSAT Technical Review*, Vol. 17, No. 2, Fall, pp. 283–310 [CTR87/322].
SCHMITT, C. H., "Geostationary Satellite Log for Year End 1986," *COMSAT Technical Review*, Vol. 17, No. 1, Spring, pp. 201–265 [CTR87/321].
SHENOY, A., see Fang, R. J. F. [CTR87/328].
SHENOY, A., see White, L. W. [CTR87/326].
SHULMAN, R. B., see Suryadevara, O. [CTR87/325].
SNYDER, J. S., "Programmable Convolutional Encoder and Threshold Decoder," *COMSAT Technical Review*, Vol. 17, No. 1, Spring, pp. 189–200 [CTR87/320].
SURYADEVARA, O., deBettencourt, J. T., and Shulman, R. B., "Network Control Processor for a TDMA System," *COMSAT Technical Review*, Vol. 17, No. 2, Fall, pp. 347–365 [CTR87/325].
SUYDERHOUD, H. G., see Dimolitsas, S. [CTR87/324].
WHITE, L. W., Palmer, L. C., Chang, P. Y., and Shenoy, A., "Application of Software Simulation to DBS Transmission Design and Evaluation," *COMSAT Technical Review*, Vol. 17, No. 2, Fall, pp. 367–401 [CTR87/326].

* Non-COMSAT author.
†INTELSAT author.

Index of 1987 Publications by COMSAT Authors

The following is a cross-referenced index of publications by COMSAT authors for 1987, not including papers published in the *COMSAT Technical Review*. Copies of these publications may be obtained by contacting the COMSAT authors at COMSAT Corporation, 22300 Comsat Drive, Clarksburg, MD 20871-9475.

ALLISON, J. F., see Hung, H-L. A.
ANDERSON, S., see Gupta, R. (two papers).
ASSAL, F. T., and Zaghloul, A. I., "Efficient Combined Global/Spot Beam Configurations for Satellite Communications," IEEE International Symposium on Antennas and Propagation, Blacksburg, VA, June 1987, *Digest*, pp. 564–567.
ASSAL, F. T., see Gupta, R.; Zaghloul, A. I.
ATIA, A. E., "RF and Microwave Filters Technology: Past, Present and Future," RF Expo East '87, Boston, MA, November 1987, *Proc.*, pp. 364–365.
ATIA, A. E., see Zaki, K. A.* (four papers).
BAKER, W., see Gupta, R.
BASS, J. F., see Hung, H-L. A. (two papers).
BONETTI, R. R., and Williams, A. E., "Quadruple-Mode Filters," IEEE MTT-S International Microwave Symposium, Las Vegas, NV, June 1987, *Digest*, pp. 145–148.
BONETTI, R. R., and Williams, A. E., "A Review of Dielectric Resonator Filter Design," International Microwave Symposium, Rio de Janeiro, Brazil, July 1987, *Digest*, pp. 673–680.
BONETTI, R. R., "Potential Impact of High T_c Superconductors in Satellite Communications Components," RF Expo East '87, Boston, MA, November 1987, *Proc.*, p. 362.
BONETTI, R. R., and Williams, A. E., "Advances in Dielectric Resonator Filter Design," RF Expo East '87, Boston, MA, November 1987 *Proc.*, pp. 231–237.
BONETTI, R. R., and Williams, A. E., "Application of Dual TM Modes to Triple- and Quadruple-Mode Filters," *IEEE Transactions on Microwave Theory and Techniques*, Vol. MTT-35, No. 12, December 1987, pp. 1143–1149.
BUTLER, D.,* Chauchard, E. A.,* Webb, K. J.,* Zaki, K. A.,* Lee, C. H.,* Polak-Dingels, P.,* Hung, H-L. A., and Huang, H. C., "A New Optoelectronic Continuous Wave Millimeter-Wave Source," 12th International Conference on Infrared and Millimeter Waves, Orlando, FL, December 1987, *Digest*, pp. 140–141.
CAMPANELLA, S. J., "Satellite Communications," *Space*, Vol. 3, No. 4, September–October 1987, pp. 40–47.

* Non-COMSAT author.

CLARK, C. J.,* Chauchard, E. A.,* Webb, K. J.,* Zaki, K. A.,* Lee, C. H.,* Polak-Dingels, P.,* Hung, H-L. A., and Huang, H. C., "Optoelectronics CW Microwave Source," Topical Meeting on Picosecond Electronics and Optoelectronics, Lake Tahoe, NV, January 1987, *Digest*, pp. 269–271.

CLARK, C. J.,* Chauchard, E. A.,* Webb, K. J.,* Zaki, K. A.,* Lee, C. H.,* Polak-Dingels, P.,* Hung, H-L. A., and Huang, H. C., "Monolithic Microwave and Millimeter Wave Phased Array Application of a New Optoelectronics Source," IEEE 6th Annual Benjamin Franklin Symposium on Advances in Antenna and Microwave Technology, Cherry Hills, NJ, March 1987, *Digest* pp. 74–76.

CLARK, C. J.* Chauchard, E. A.,* Webb, K. J.,* Zaki, K. A.,* Lee, C. H.,* Polak-Dingels, P.,* Hung, H-L. A., and Huang, H. C., 'Studies of a New Optoelectronic Microwave Source," *Lightwave Technology*, Vol. LT-5, No. 3, November 1987, pp. 388–397.

CORNFELD, A. B., see Hung, H-L. A. (two papers).

DIMOLITSAS, S., and Gunn, J. E.,* "A Length Adaptive Trasversal Data Echo Canceller," *Signal Processing*, Vol. 12, No. 3, April 1987, pp. 321–324.

DUNLOP, J. D., see Vaidyanathan, H.

EDWARDS, R., see Gupta, R.

EKELMAN, E. P., "Antenna Diagnosis Using Microwave Holographic Techniques on a Far-Field Range," Meeting of the Antenna Measurement Techniques Association, Seattle, WA, September–October 1987, *Proc.*, pp. 180–186.

EZZEDDINE, A., see Hung, H-L. A. (four papers).

FU, M., see Gupta, R.

GELLER, B., and Goettle, P., "Miniaturized High-Efficiency Push-Pull and Single-Ended Power Amplifiers for Active Aperture Systems," Government Microcircuits Applications Conference (GOMAC), October 1987, Orlando, FL, *Digest*, pp. 425–426.

GELLER, B., see Gupta, R.

GOETTLE, P., see Geller, B.

GUPTA, R., Anderson, S., and Getsinger.W.,* "Impedance Transforming 3-dB 90° Hybrids," IEEE MTT-S International Microwave Symposium, Las Vegas, NV, June 1987, *Digest*, pp. 203–206.

GUPTA, R., Smith T., and Reynolds, J., "GaAs MMICs: CAD, Modeling, and Process Monitoring," *Microwave Journal*, Vol. 30, No. 8, August 1987, pp. 95–114.

GUPTA R., Fu, M., Baker, W., and Edwards, R., "A Broadband MMIC Dual-Gate FET Switch Module With On-Chip TTL Control Interface," 17th European Microwave Conference, Rome, Italy, Septembr 1987, *Proc.*, pp. 243–248.

GUPTA, R., Holdeman, L., Potukuchi, J., Geller, B., and Assal, F., "A 0.05- to 14-GHz MMIC 5-bit Digital Attenuator," IEEE GaAs IC Symposium, Portland, OR, October 1987, *Digest*, pp. 231–234.

* Non-COMSAT author.

GUPTA, R., Anderson, S., and Getsinger, W.,* "Impedance Transforming 3-dB 90° Hybrids," *IEEE Transactions on Microwave Theory and Techniques*, Vol. MTT-35, No. 12, December 1987, pp. 1303–1307.

GUPTA, R., see Potukuchi, J.

HOLDEMAN, L. B., see Gupta, R.; Hung, H-L. A.; Jach, T.

HUANG, H. C., see Butler, D.;* Clark, C. J.* (three papers); Hung, H-L. A. (five papers).

HUNG, H-L. A., Ezzeddine, A., McNally, P. J., and Huang, H. C., "A GaAs MMIC Broadband Distributed Amplifier," IEEE 6th Annual Benjamin Franklin Symposium on Advances in Antenna and Microwave Technology, Cherry Hills, NJ, March 1987, *Digest*, pp. 54–57.

HUNG, H-L. A., Ezzeddine, A., Holdeman, L. B., Phelleps, F. R., Allison, J. F., Cornfeld, A. B., Smith, T., and Huang, H. C., "K_a-Band Monolithic GaAs Power FET Amplifiers," IEEE Microwave and Millimeter-Wave Monolithic Circuits Symposium, Las Vegas, NV, June 1987, *Digest*, pp. 97–100.

HUNG, H-L. A., Ezzeddine, A., Phelleps, F. R., Bass, J. F., and Huang, H. C., "GaAs MMIC Power FET Amplifiers at K-Band," 17th European Microwave Conference, Rome, Italy, September 1987, *Proc.*, pp. 255–260.

HUNG, H-L. A., Phelleps, F., Bass, J., Cornfeld, A., Ezzeddine, A., and Huang, H., "A 2-W Multistage K-Band GaAs Monolithic FET Amplifier," IEEE GaAs IC Symposium, Portland, OR, October 1987, *Digest*, pp. 239–242.

HUNG, H-L. A., Smith, T., Huang, H. C., Polak-Dingels, P.,* Webb, K. J.,* Lee, C. H.,* "Optical Electronic Characterization of Monolithic Millimeter-Wave Integrated Circuits," 12th International Conference on Infrared and Millimeter Waves, Orlando, FL, December 1987, *Digest*, pp. 87–88.

HUNG, H-L. A., see Butler, D.;* Clark, C. J.* (three papers); Meulenberg, A.

HYDE, G., Guest Associate Editor, *IEEE Journal on Selected Areas in Communications*, Special Issue on Satellite Communications Towards the Year 2000, Vol. SAC-5, No. 4, May 1987.

HYDE, G., see Mahle, C.

INUKAI, T., see Mahle, C.

JACH, T.,* Hembree, G.,* and Holdeman, L. B., "Observation of Whisker Growth on Gold Thin Films Using Reflection Electron Microscopy," (Abstract), *Bulletin of the American Physical Society*, Vol. 32, No. 3, 1987, p. 770.

KAO, Y. S., and Lee, L-N., "Time-Mulitplexed Analog Transmission of Three Broadcast-Quality Television Channels Through One Satellite Transponder," *IEEE Journal on Selected Areas in Communications*, Vol. SAC-5, No. 4, May 1987, pp. 676–684.

LEE, L-N., see Kao, Y. S.

MAHLE, C., Hyde, G., and Inukai, T., "Satellite Scenarios and Technology for the 1990s," *IEEE Journal on Selected Areas in Communications*, Vol. SAC-5, No. 4, May 1987, pp. 556–570.

* Non-COMSAT author.

MAIN, E. L. "Learning to Fly a Satellite," *Space*, Vol. 3, No. 3, July–August 1987, pp. 25–27.

McNALLY, P. J., see Hung, H-L. A.

MEULENBERG, A., and Hung, H-L. A., "Degradation Mechanisms in Irradiated GaAs MMICs," GaAs Reliability Workshop, Portland, OR, October 1987, *Program and Abstracts*, pp. 25–26.

MEULENBERG, A., Dozier, C. M.,* Anderson, W. T.,* Mittleman, S. D.,* Zugoch, M. H.,* and Caefer, C. E.,* "Dosimetry and Total Dose Radiation Testing of GaAs Devices," *IEEE Transactions on Nuclear Science*, Vol. NS-34, No. 6, December 1987, pp. 1745–1750.

MOTT, R., "A GaAs Monolithic 6-GHz Low-Noise Amplifier for Satellite Receivers," IEEE MTT-S International Microwave Symposium, Las Vegas, NV, June 1987, *Digest*, pp. 561–564.

MOTT, R., see Potukuchi, J.

PALMER, L., "Space Communications: Systems and Technology," Symposium on NASA Space Communications Research, Development, and Applications, *Proc.*, pp. 78–97, Space Applications Board, National Research Council, 2101 Constitution Avenue, N.W., Washington, DC 20418.

PAUL, D. K., "High-Power Semiconductor Diode Lasers: Reliability Data and Lifetest Methodology," Fiber/Lase '87—Conference on Fiber Optics Reliability: Benign and Adverse Environments, San Diego, CA, August 1987, *Proc. SPIE*, Vol. 842, D. K. Paul, ed., pp. 86–94.

POTUKUCHI, J., Gupta, R., and Mott, R., "Design and Development of Monolithic Subsystems for Satellite Applications," IEEE Military Communications (MILCOM) Conference, Washington, DC, October 1987, *Conf. Rec.*, pp. 661–665.

POTUKUCHI, J., see Gupta, R.

PHELLEPS, F. R., see Hung, H-L. A. (three papers).

REYNOLDS, J., see Gupta, R.

ROGERS, D. V., "Rain Effects on Slant Propagation Paths," International Microwave Symposium, Rio de Janeiro, Brazil, July 1987, *Proc.*, Vol. 2, pp. 1279–1286.

ROGERS, D. V., and Allnutt, J. E.,† "A Practical Tropospheric Scintillation Model for Low Elevation Angle Satellite Systems," 5th International Conference on Antennas and Propagation, York, U.K., 1987, IEEE Conference Publication 274, pp. 273–276.

SAYEGH, S. I., Kok, Y-L.,* and Hong, J-H.,* "An Algorithm to Find Two-Dimensional Signals With Specified Zero Crossings," *IEEE Transactions on Acoustics, Speech, and Signal Processing*, Vol. ASSP-35, No. 1, January 1987, pp. 107–111.

SIDDIQI, S., see Zaghloul, A. I.

SMITH, T., see Gupta, R.; Hung, H-L. A. (two papers).

* Non-COMSAT author.
†INTELSAT author.

SORBELLO, R. M., see Tulintseff, A. N.;* Zaghloul, A. I.

TULINTSEFF, A.,* and Sorbello, R. M., "Currents and Radiation Fields of Electromagnetically Coupled Microstrip Antennas," IEEE International Symposium on Antennas and Propagation, Blacksburg, VA, June 1987, *Digest*, Vol. 2, pp. 928–931.

VAIDYANATHAN, H., "Long-Term Storage of Nickel-Hydrogen Cells," Space Electrochemical Research and Technology Conference, Cleveland, OH, April 1987, *Proc.*, pp. 41–48, NASA Conference Publication 2484.

VAIDYANATHAN, H., and Dunlop, J. D., "Performance of Nickel-Hydrogen Cells for Battery-Powered Electric Propulsion Operation in GEO," 22nd Intersociety Energy Conversion Engineering Conference, Philadelphia, PA, August 1987, *Proc.*, pp. 882–884. Available from AIAA, Washington, D.C.

WILLIAMS, A. E., see Bonetti, R. R. (four papers).

ZAGHLOUL, A. I., Siddiqi, S., and Bornemann, W.,† "Phased Arrays Versus Reflector Systems for Multibeam Satellite Applications," URSI Radio Science Meeting, Blacksburg, VA, June 1987, *Program and Abstracts*, p. 141.

ZAGHLOUL, A. I., and Mailloux, R. J.,* "MMIC Phased Arrays," Antenna Applications Symposium, Allerton Park, IL, September 1987, *Proc.*, pp. 1–29.

ZAGHLOUL, A. I., Assal, F. T., and Sorbello, R. M., "Multibeam Active Phased Array System Configurations for Communications Satellites," IEEE Military Communications (MILCOM) Conference, Washington, DC, October 1987, *Conf. Rec.*, pp. 289–293.

ZAGHLOUL, A. I., and Mailloux, R. J.,* "Report From 1987 AP-S Workshop on MMIC Phased Arrays," *IEEE Antennas and Propagation Society Newsletter*, December 1987, pp. 14–19.

ZAGHLOUL, A. I., see Assal, F. T.

ZAKI, K. A.,* Chen, C.,* and Atia, A. E., "Dual-Mode Dielectric Resonator Filters Without Iris," IEEE MTT-S International Microwave Symposium, Las Vegas, NV, June 1987, *Digest*, pp. 141–144.

ZAKI, K. A.,* Chen, C.,* and Atia, A. E., "Improved Selectivity Dual-Mode Dielectric Resonator Filters," International Microwave Symposium, Rio de Janeiro, Brazil, July 1987, *Digest*, pp. 627–632.

ZAKI, K. A.,* Chen, C.,* and Atia, A. E., "New Realization of Dual-Mode Dielectric Resonator Filters," 17th European Microwave Conference, Rome, Italy, September 1987, *Proc.*, pp. 169–174.

ZAKI, K. A.,* Chen, C.,* and Atia, A. E., "Canonical and Longitudinal Dual-Mode Dielectric Resonator Filters Without Iris," *IEE Transactions on Microwave Theory and Techniques*, Vol. MTT-35, No. 12, December 1987, pp. 1130–1135.

* Non-COMSAT author.